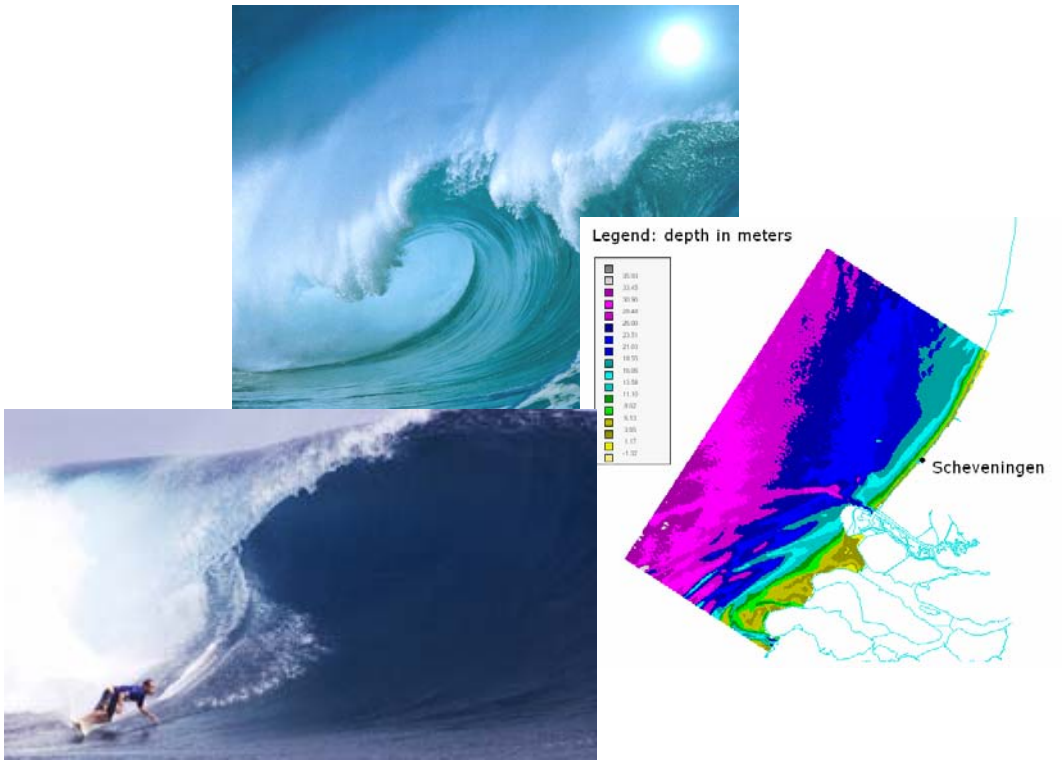
Surfability of an ASR in irregular waves

A study after the surfability of an existing Artificial Surf Reef design in wave conditions typically found at Scheveningen, the Netherlands



Surfability of an ASR in irregular waves
by
Rutger Over

A study after the surfability of an existing Artificial Surf Reef design of wave conditions typically found at Scheveningen, the Netherlands

June 2006

Graduation committee

prof.dr.ir. M.J.F. Stive	(Chairman, Coastal engineering)
dr.ir. A.J.H.M. Reniers	(Coastal engineering)
dr.ir. H.L. Fontijn	(Environmental fluid mechanics)
dr.ir. W.S.J. Uijttewaal	(Environmental fluid mechanics)
ir. M. Henriquez	(Coastal engineering)

Preface

This thesis is written as part of the master thesis of the study Civil Engineering at the Faculty of Civil Engineering and Geosciences at Delft University of Technology. The thesis is one of the last subjects in the study and all knowledge from previous courses can be used.

The subject of this thesis is an Artificial Surf Reef (ASR), and is part of a series of studies with the intention to optimize the design and gain knowledge about processes up and around it. In previous studies the aim was to determine the relation between the reef shape, surfability and currents around the reef using regular and bichromatic waves. This research aims to study the surfability of irregular waves.

I would like to thank all members of my graduation committee, prof.dr.ir. M.J.F. Stive, dr.ir. A.J.H.M. Reniers, dr.ir. H.L. Fontijn, dr.ir. W.S.J. Uijttewaal and ir. M. Henriquez for their supportive advice and remarks. In particular Ad for his almost weekly advice and practical solutions towards unforeseen problems and Martijn for his time and advice towards this report. Furthermore I would like to thank all staff of the Laboratory for Fluid Mechanics at the Faculty of Civil Engineering and Geosciences for their help and advice in solving practical problems during the experimental study.

Delft, June 2006

R.W.J. Over

Abstract

Wave surfing is a popular sport all around the world where the conditions allow for it. Waves preferred by surfers are higher than 1 meter, have a certain hollow breaker shape (plunger) and the angle under which a wave breaks, the peel angle, is within 30-70 degrees. Also in the Netherlands surfing becomes increasingly popular but Dutch wave conditions are far from ideal because firstly the breaker shape is almost always spilling which is not a desirable breaker shape, and secondly peel angles are in the range 60-90 degrees most of the time. To alter the breaking characteristics of a wave a submerged structure can be built: a so called Artificial Surf Reef (ASR).

An ASR has been designed by van Ettinger (2005) to reduce the rip currents around the sides of the structure. The wave conditions that the ASR was tested for, namely bichromatic waves, are not representative for the south of the North Sea where most of the coast line of the Netherlands is located. Therefore physical model tests are done with irregular wave conditions, typical found in this part of the North Sea, to determine the effectiveness of the ASR on the surfability of Dutch irregular waves.

One of the locations for an ASR in the Netherlands is Scheveningen and wave conditions typical found in this area are determined with a numerical simulation in the wave model in SWAN. From wave buoy data it is found what the common surfable wave conditions are and these are used for boundary conditions of the wave model. The direction the waves come from most often in a sector of 30° is found to be from direction 240°-270° (Nautical). Only waves with a chance of occurrence of more than 24 hours a year and a wave height of more than 1 meter are taken into account. The output data of the numerical model are used as test conditions in the experimental study (scale 1:15) in the Laboratory for Fluid Mechanics at the Faculty of Civil Engineering and Geosciences. The experimental study is carried out with constant water depth, representing a situation without tides. Three tests with different water levels are recorded to analyze the influence of tidal water level fluctuations on the surfability.

The parameters that determine the surfability of a wave are:

- Peel angle
- Length of ride
- Breaker type

These surfability parameters are estimated from recordings of the behavior of waves on the reef (taken from above) in the physical

model. From each second of recording five images are extracted and in these images the location of the break point of a wave is tracked. From the location of the break point in each image the peel angle and the length of a ride is estimated. The breaker type is determined by looking at the foam intensity created by the breaking wave: it is found that the foam intensity becomes higher for larger Irribarren numbers (for ξ_b<3). This is explained by the fact that more air is enclosed due to intense wave breaking.

With the algorithms developed to determine the surfability of individual waves, the recordings of the experimental study are analyzed. From the results an estimate is made for the total number of surfable waves for waves coming from direction 240°-270°, which is 7180 a year if no tides would be present.

The influence of the tides is found to be twofold: more waves have desirable breaker shapes, but the possible lengths of ride are shorter. Tides will reduce the number of surfable waves with approximately 40%, which brings the number of surfable waves to 4300 a year with tides present.

Index

1 INTRODUCTION 1

1.1 GENERAL 1
1.2 OBJECTIVE AND OUTLINE OF THE PRESENT STUDY 7

2 MODELING WAVE CONDITIONS FOR SCHEVENINGEN WITH SWAN 9

2.1 INTRODUCTION 9
2.2 MODEL DESCRIPTION 9
2.3 BOUNDARY CONDITIONS 10
2.4 COMPUTATIONAL GRIDS AND TOPOGRAPHY 15
2.5 PARAMETER SENSITIVITY AND VERIFICATION 16
2.6 TYPICAL WAVE CONDITIONS FOR SCHEVENINGEN 19

3 EXPERIMENTAL STUDY 21

3.1 INTRODUCTION 21
3.2 EXPERIMENTAL SETUP 21
3.3 TESTS CONDITIONS 23
3.4 INSTRUMENTS 25
3.5 TEST PROCEDURE 25

4 RESULTS OF EXPERIMENTAL STUDY 27

4.1 INTRODUCTION 27
4.2 METHOD OF ANALYSIS OF VIDEO DATA 27
4.2.1 Locating the break point 28
4.2.2 Estimating the peel angle and length of a ride 30
4.2.3 Determining the breaker type 33
4.3 ANALYSIS OF THE WATER SURFACE ELEVATION 40
4.4 ANALYSIS OF THE VIDEO DATA 42
4.4.1 Number of surfable waves 42
4.4.2 Influence of tidal water level fluctuations on surfability 46

5 CONCLUSIONS AND RECOMMENDATIONS 51

6 BIBLIOGRAPHY 55

APPENDICES 2

List of figures

FIGURE 1: PERFECT WAVE FOR EXPERIENCED SURFERS (SOURCE: MAVSURFER.COM) 1
FIGURE 2: SPILLING WAVES 2
FIGURE 3: PLUNGING WAVE (SOURCE: MAVSURFER.COM) 2
FIGURE 4: DEFINITION OF PEEL ANGLE α (SOURCE: SURFERMAG.COM) 4
FIGURE 5: OPTIMAL REEF SHAPE ACCORDING TO HENRIQUEZ (2004) 5
FIGURE 6: REEF SHAPE DESIGN BY VAN ETTINGER (2005) 6
FIGURE 7: THE MODEL AREA (RED SURFACE) AND THE WAVE MEASURE LOCATIONS 11
FIGURE 8: WAVE HEIGHT IN GRID 3 FOR INPUT WITH WAVES FROM DIRECTION 210°-240° 12
FIGURE 9: WAVE HEIGHT DISTRIBUTION IN GRID 3 FOR THE SITUATION WHEN MV2 WILL HAVE BEEN CONSTRUCTED 13
FIGURE 10: LOCATIONS OF THE THREE COMPUTATIONAL GRIDS 15
FIGURE 11: BATHYMETRY OF THE MODEL AREA 16
FIGURE 12: LAY OUT OF THE PHYSICAL MODEL 21
FIGURE 13: SHAPE OF THE REEF 22
FIGURE 14: EXAMPLE IMAGE CAPTURED WITH DIGITAL CAMERA 23
FIGURE 15: THE COORDINATES OF BREAK POINTS FOUND WITH THE ALGORITHM AND BY VISUAL LOCATING OF IN TOTAL 5 SEPARATE WAVES IS FOLLOWED IN TIME: THE TIME INTERVAL IN BETWEEN TWO IMAGES IS 0.2 SECONDS. 29
FIGURE 16: MOVEMENT OF A BREAK POINT IN TIME 30
FIGURE 17: PEEL ANGLE, LENGTH OF RIDE S AND SPEED OF A SURFER FROM THE MOVEMENT OF A BREAK POINT IN IMAGES IN TIME (ZOOM IN AREA OF FIGURE 16) 30
FIGURE 18: THE DOWN-LINE VELOCITIES ALONG THE REEF FOR A TEST WITH BICHROMATIC WAVES AS FOUND WITH THE METHOD DEVELOPED 32
FIGURE 19: THE CHANGE OF THE DOWN-LINE VELOCITY ALONG THE REEF FOR A TEST WITH BICHROMATIC WAVES AS FOUND BY VAN ETTINGER (2005) 33
FIGURE 20: HISTOGRAM OF THE PIXEL BRIGHTNESS IN THE RANGE 150-250 FOR AN IMAGE OF A SPILLING WAVE 34
FIGURE 21: HISTOGRAM OF THE PIXEL BRIGHTNESS IN THE RANGE 150-250 FOR AN IMAGE OF A PLUNGING WAVE 35
FIGURE 22: AREA USED FOR SELECTION OF HIGHEST INTENSITY PIXELS 35
FIGURE 23: NUMBER OF FALSE POSITIVES VERSUS THE NUMBER OF PIXELS SELECTED 36
FIGURE 24: CHANGE OF FOAM BRIGHTNESS IN TIME (ALONG THE BREAKER LINE) FOR A SPILLING, INTERMEDIATE AND PLUNGING WAVE 38
FIGURE 25: THE NUMBER OF WAVES GIVEN FOR THE FOAM BRIGHTNESS FOR ALL WAVES OF THE RECORDING WITH 2834 IMAGES, FOR EACH OF THE THREE BREAKER TYPES. 39
FIGURE 26: POWER DENSITY SPECTRUM FOR TEST 4 FROM THE MEASUREMENTS AND THE INPUT SPECTRUM 41
FIGURE 27: POWER DENSITY SPECTRUM FOR TEST 7 AND 8 42
FIGURE 28: THE POSSIBLE LENGTH OF RIDE *S* FOR ALL PLUNGING AND INTERMEDIATE WAVES IN TEST 1 TO 8 44
FIGURE 29: THE WHITE RECTANGLE SHOWS THE AREA DEPICTED IN THE NEXT FIGURE 44
FIGURE 30: LOCAL PEEL ANGLES FOR BREAK POINT OF ALL PLUNGING AND INTERMEDIATE WAVES IN TEST 1 TO 8. IN THE TWO SUBFIGURES THE AVERAGE PEEL ANGLE OVER THE X- AND Y-AXIS IS PLOTTED. THIS IS DONE BY TAKING THE AVERAGE OF THE PEEL ANGLE OF ALL BREAK POINTS WITH A CERTAIN X- OR Y-COORDINATE. 45
FIGURE 31: HISTOGRAM FOR S FOR TEST 5 COMPARED TO TESTS 36 AND 32 47
FIGURE 32: HISTOGRAM FOR S FOR TEST 4 COMPARED TO TESTS 28 47
FIGURE 33: LOCATIONS OF ALL BREAK POINTS OF PLUNGING AND INTERMEDIATE WAVES FOR TEST 36, 32 AND 28 48

List of tables

TABLE 1: WAVE DATA FOR EUROGEUL (SOURCE: GOLFKLIMAAT.NL) 13
TABLE 2: INPUT FOR SCHEVENINGEN MODEL 14
TABLE 3: CHANCE OF OCCURRENCE OF TEST CONDITIONS 14
TABLE 4: SPECIFICATIONS OF THE THREE COMPUTATIONAL GRIDS 15
TABLE 5: WAVE AND WIND INPUT FOR TEST WITH SWAN WITH H_S = 1.5 M 17
TABLE 6: RESULTS OF TESTS WITH SWAN FOR H_S = 1.5 M 17
TABLE 7: INFLUENCE OF DIRECTIONAL SPREADING ON RESULTS FOR THE WAVE HEIGHT AT SCHEVENINGEN 18
TABLE 8: WAVE INPUT FOR TEST WITH SWAN FOR H_S = 1.95 M 18
TABLE 9: RESULTS FOR TEST WITH SWAN FOR H_S = 1.95 M 18
TABLE 10: INPUT AND OUTPUT FOR THE 8 RUNS OF SWAN FOR SCHEVENINGEN 19
TABLE 11: TEST CONDITIONS 24
TABLE 12: THE WAVE SPECTRUM PARAMETERS H_S AND T_P FROM THE MEASUREMENTS COMPARED TO THE INPUT 40
TABLE 13: DIFFERENCE IN BRIGHTNESS FOR EACH TEST COMPARED TO REFERENCE TEST 37
TABLE 14: NUMBER OF PLUNGING AND INTERMEDIATE WAVES FOR TESTS 1-8 43
TABLE 15: NUMBER OF SURFABLE WAVES FOR TESTS 1-8 43
TABLE 16: NUMBER OF SURFABLE WAVES TO BE EXPECTED FOR EACH TEST A YEAR 45
TABLE 17: NUMBER OF PLUNGING AND INTERMEDIATE WAVES FOR TESTS 36, 32 AND 28 46
TABLE 18: NUMBER OF SURFABLE WAVES FOR TESTS 36, 32 AND 28 49
TABLE 19: NUMBER OF SURFABLE WAVES FOR TEST 36, 32 AND 28 IN PROTOTYPE 49
TABLE 20: RESULTS FOR REGULAR WAVE TESTS WITH DIFFERENT LIGHTING 11
TABLE 21: RESULTS FOR IRREGULAR WAVE TESTS WITH DIFFERENT LIGHTING 11
TABLE 22: DIFFERENCES IN RESULTS OF SIMILAR TESTS 12

1 Introduction

1.1 General

Wave surfing is a fast growing sport in the Netherlands and is becoming more popular and well known every day. Where ten years ago a dozen people were surfing you will find hundreds today.
This despite of the fact that Dutch wave conditions are far from ideal: large hollow waves (Figure 1) as preferred by surfers are never observed in the Netherlands.



Figure 1: perfect wave for experienced surfers (source: mavsurfer.com)

These hollow waves are formed when waves with a long wave period, called swell, reach the shore. Swell consists of waves which are formed in storms hundreds kilometers or more away of which the waves with longest wave period are able to travel thousands of kilometers. The North Sea hardly shows swell because of the sheltered position it has lying to the east of England, which blocks almost all waves formed on the Atlantic Ocean. The waves that do occur on the North Sea are formed by local winds, which cause the wave climate to be irregular and the waves to have short wave periods.

Two types of breaking waves are important for this study, which are characterized by Galvin (1968) as follows:

- Spilling waves occur if the wave crest becomes unstable and flows down the front face of the wave producing a foamy water surface (see Figure 2).



Figure 2: spilling waves

- Plunging waves occur if the crest curls over the front face and falls into the base of the wave, resulting in a high splash (see Figure 3).



Figure 3: plunging wave (source: mavsurfer.com)

A measure to classify the type of breaking wave is the Irribarren parameter (Battjes, 1974):

$$\xi_b = \tan\alpha / \sqrt{H_b / L_0} \qquad (1.1)$$

Where tan (α) is the slope of the sea bottom, H_b is the wave height at breakpoint and L_0 is the wave length, where $L_0 = gT^2/2\pi$ with *g* the gravitational acceleration and *T* the wave period. The wave steepness s is given by $s = H_b / L_0$. Therefore the Irribarren parameter can physically be seen as the ratio between the steepness of the sea bottom and the steepness of the water surface. Spilling waves are found when $\xi < 0.5$ while plunging waves are found when $0.5 > \xi > 3$.

Typical values of s for locally generated waves are in the order of 0.04 for the southern part of the North Sea. This means that the main parameter which determines the breaker type in the Netherlands is tan (α) representing the slope of the sea bottom. Typical values for tan (α) near the shore of the Netherlands are in the range of 1:50 to 1:100. A slope of 1:50 gives for the Irribarren parameter $\xi = 0.02/\sqrt{0.04} = 0.10 < 0.5$ which means almost every wave in the Netherlands breaks spilling. A wave will break plunging if the Irribarren

parameter $\xi > 0.5$. This means it is required for the bottom steepness to be in the order of 1:10. An artificial submerged structure with a slope of 1:10 can be used to make waves break plunging in the Netherlands: an artificial surf reef (ASR).

It should be noted that locally the bottom slope can be steeper in the Netherlands (naturally formed sand banks for instance) which causes waves to break as plungers. These conditions are always very local and temporary: sediment transport tends to cause the bottom slope to become more gradual after time.

Waves that reach the shore are subject to shoaling and also to refraction if the wave front is at an angle with the depth contours. Shoaling is the process that makes waves slow down and higher (thus steeper) when the water depth decreases and is dependent on the wave length and local water depth. The change in wave height due to shoaling is calculated with the dispersion relation:

$$\omega^2 = g * k * \tanh(k * h) \qquad (1.2)$$

where $k = \frac{2*\pi}{L}$ and $\omega = \frac{2*\pi}{T}$, with L the wave length and T the wave period.
Refraction is the process by which the direction of propagation of a wave front changes due to non-uniform depths in the direction of propagation (which is the case when waves reach a shore with parallel depth contours under an angle). The decrease in wave height due to refraction can be calculated with Snell's law.

Due to shoaling the wave gets higher and just before breaking the wave front gets steep enough to be ridden by surfers. Surfers develop speed by constantly riding down the wave. Ideal for surfing is a plunging wave that breaks gradually and constant toward one side. This way surfers can ride in the so called pocket of the wave: the pocket is the place where the wave is just about to break and therefore at its steepest; this is where surfers reach highest speeds.

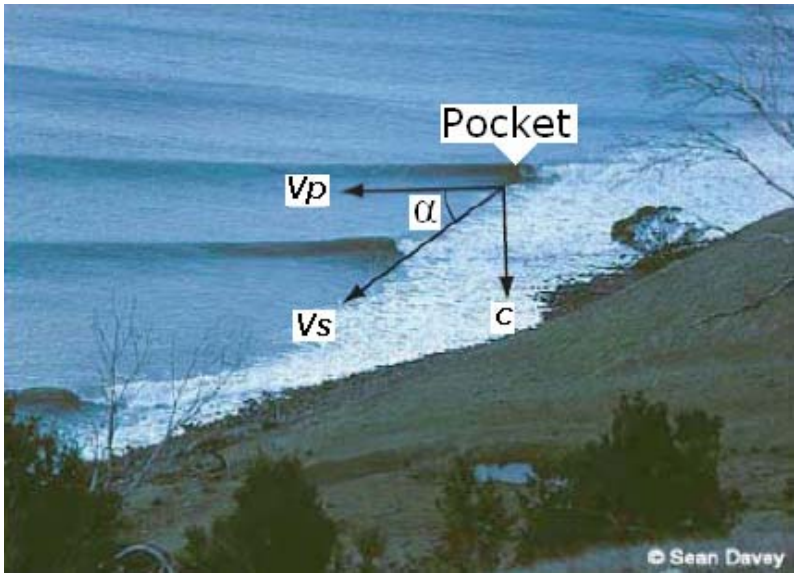


Figure 4: definition of peel angle α (source: surfermag.com)

The wave itself travels towards the shore at a speed *c* and at the same time breaks ('peels') at a speed V_p: the peel rate. A surfer in the pocket travels at an angle α (the peel angle) towards the coast with speed V_s. The peel angle is defined as the angle between the tangent of the wave front at the pocket of the wave and the direction of the breaker line (the direction of the vector V_s). A peel angle of 0° means the wave breaks over the length of the entire crest at once. Surfers say the wave is closing out. The consequence is that there is no pocket left and the ride of the wave is over. A large peel angle ($80 < \alpha < 90$) means the wave breaks really slowly to a side and a surfer can not develop high speeds. A lot depends therefore on the peel angle because it determines the difficulty for the surfer and consequently the speed a surfer can develop (which depends on the skill of the surfer and the wave height). For most surfers in the Netherlands a peel angle of in between 40 and 70 degrees is desirable.

The surfability of waves is altogether determined by:

- The peel angle
- The breaker shape
- The down-line velocity
- The length of a ride for a surfer

The down-line velocity is the velocity a surfer develops when riding the wave in the pocket. The peel angle is determined by the peel rate and the speed of wave propagation, which means that mostly the peel rate determines the peel angle, and the peel rate also determines the down-line velocity. The down-line velocity is therefore related to the

peel angle which means that only restrictions for the peel angle are given, not for the down-line velocity.

For the length of a ride for a surfer it is decided that rides longer than 20 meters are desirable.
It is concluded that a surfable wave meets the following requirements:

- The wave breaks plunging
- The peel angle is in between 30 and 70 degrees
- The length of a ride is longer than 20 meters.

Over the past few years research has been done to optimize (the design of) ASRs. Henriquez (2004) determined how the surfability is influenced by the design of an ASR through both numerical and experimental models. The reef was tested for regular waves because the (numerical) modeling of the surfability of irregular waves is complex.

This resulted in the design of an ASR with a shape as can be seen in Figure 5 (the lines are depth contours). Henriquez (2004) also concluded that about 20% of the wave ride was influenced negatively by rip currents.

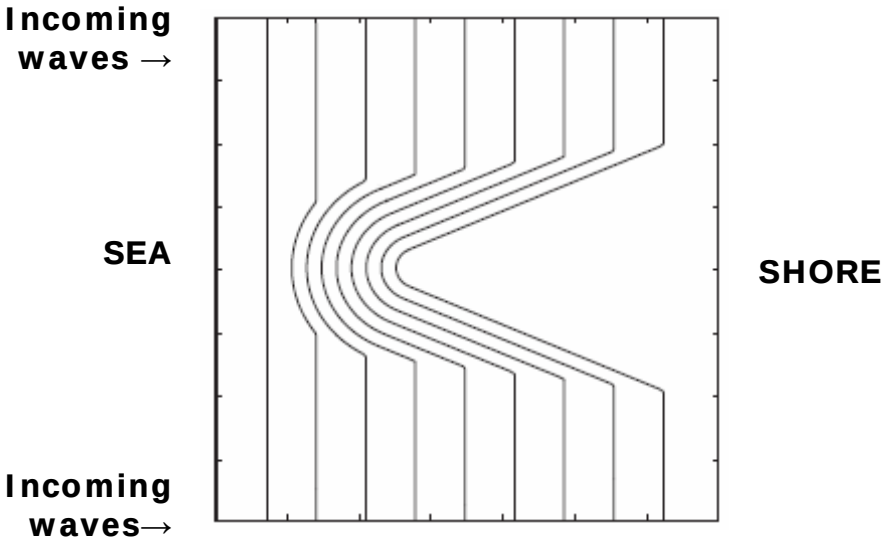


Figure 5: optimal reef shape according to Henriquez (2004)

Rip currents are currents that are directed seaward and are driven by breaking waves. Strong rip currents can be dangerous for swimmers: the main cause of death for swimmers is drowning after getting caught in a strong rip current.
Van Ettinger (2005) designed a reef with aim to reduce rip currents around the tips of the reef. This is achieved by constructing a channel in the middle of the reef over the main axis, see Figure 6. About 40%

of the rip current around the tips of the reef will go through this channel. The main advantages are:

- Because the currents through the surf area are less strong surf conditions are improved.
- A rip current through the channel in the reef will allow surfers to easily paddle out from the shore to the point where waves start breaking.

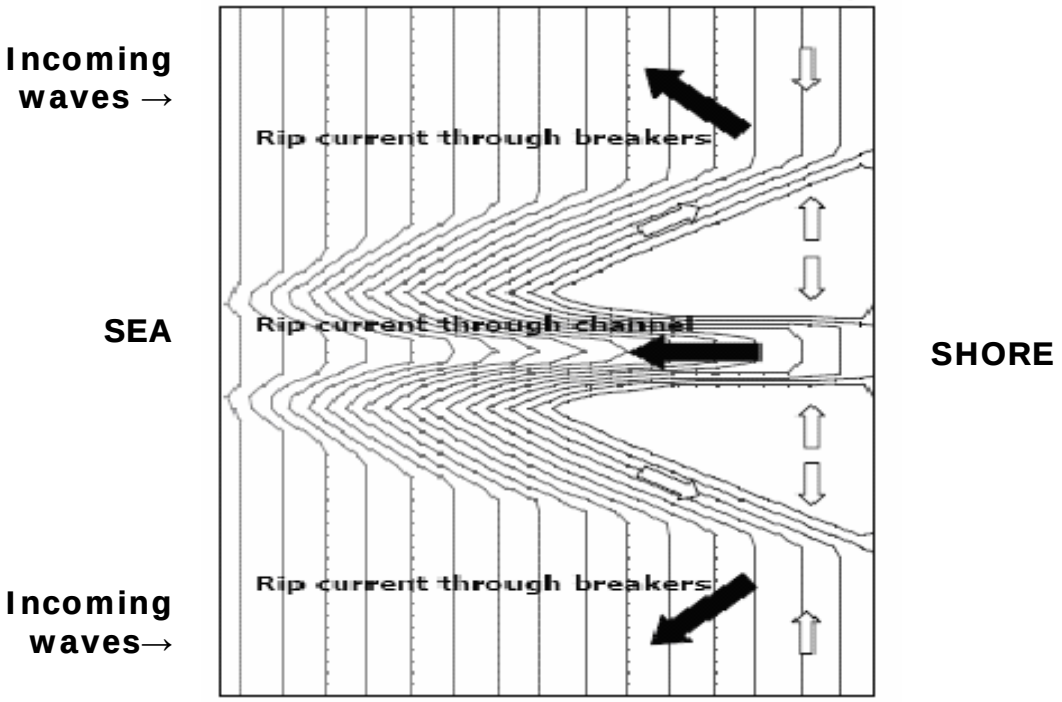


Figure 6: reef shape design by van Ettinger (2005)

The reef as it was designed by van Ettinger (2005) was built on scale 1:15 in a wave basin at the Laboratory for Fluid Mechanics at the Faculty of Civil Engineering and Geosciences. The reef was tested for Dutch swell conditions (bichromatic waves: wave groups) to be able to look at the rip currents for a wave climate more representative of reality than regular waves.

For an ASR to be successful in the Netherlands it is necessary that it is tested for typical Dutch wave conditions; irregular waves. It will be interesting to see how the existing ASR designed by van Ettinger (2005) influences the surfability of an irregular wave field which has not been done before because of its complexity. It will improve understanding on the performance of this ASR for conditions that represent real conditions. Physical experiments are used in the study because of the complexity of determining the surfability of irregular wave conditions with a numerical model.

Because the ambition is to built an ASR in prototype in the end the focus of this study will be on a realistic location in the Netherlands for an ASR. There are several spots in the Netherlands where wave surfing is practiced and all these spots are easily accessible. One of the main spots nowadays is at Scheveningen because the town is located directly at the shore and the breakwaters of the harbor provide relatively good surf conditions. This study focuses therefore on an ASR near Scheveningen.

1.2 Objective and outline of the present study

The main objective of the present study is to determine the number of surfable waves a year on an existing surf reef design under irregular waves typically found at Scheveningen, the Netherlands.

The subject of this thesis is therefore:
"Surfability of an ASR in irregular waves"

The main objective can be divided in a number of sub-objectives:

- Determine the wave conditions typically found at Scheveningen close to the shore.
- Develop a method to determine the surfability of irregular waves in the breaker zone.
- Determine the surfability of typical Dutch irregular waves breaking on an existing surf reef design.
- Determine the influence of Dutch tidal water level fluctuations on the surfability of irregular waves.

The study starts with the estimation of the typical wave conditions found at Scheveningen with SWAN in chapter 2. The setup of the experimental study, the instruments used and the analysis method of the video data will be the subject of chapter 3.

The results of the experimental study will be the subject of chapter 4 and the conclusions on the main objective and the sub-objectives are given in chapter 5. Recommendations for further research are given in chapter 0.

2 Modeling wave conditions for Scheveningen with SWAN

2.1 Introduction

In order to be able to determine the performance of an ASR near Scheveningen the local wave climate needs to be known. Because no wave buoy is located close to the coast at Scheveningen the local wave climate is estimated with the numerical wave model SWAN.
To start with the theoretical background of SWAN is discussed in paragraph 2.2 and the setup of the model for Scheveningen with its boundary conditions is the subject of paragraph 2.3. The grids which are used in the model and the local depths that are provided to these grids are described in paragraph 2.4. In paragraph 2.5 the sensitivity of the parameters used in the input of the model are discussed and the validity of the model to estimate the wave conditions for Scheveningen is verified. Finally in paragraph 2.6 the output of the model, namely the typical wave conditions for Scheveningen, is presented.

2.2 Model description

SWAN (Simulating WAves Nearshore) is a 2D numerical wave model for obtaining realistic estimates of wave parameters in coastal areas from given wind- bottom- and current conditions.
The model is based on the wave action balance equation given in (2.1)

$$\frac{\partial N}{\partial t}+\frac{\partial c_x N}{\partial x}+\frac{\partial c_x N}{\partial y}+\frac{\partial c_\sigma N}{\partial \sigma}+\frac{\partial c_\theta N}{\partial \theta}=\frac{S}{\sigma} \qquad (2.1)$$

where:
$N(\sigma,\theta)$ = wave action density:
T = time [s]
x = distance in x direction [m]
y = distance in y direction [m]
σ = relative frequency [Hz] as observed in a frame of reference moving with current velocity
θ = wave direction [degrees]
$c_{x,y,\sigma,\theta}$ = propagations speeds [m/s] for respectively x, y, σ and θ
S = source/sink term in terms of energy density (generation by wind, dissipation and non-linear wave-interactions)

The action density $N(\sigma,\theta)$ is equal to the energy density divided by the relative frequency: $N(\sigma,\theta) = E(\sigma,\theta)/\sigma$.
The first term in equation (2.1) represents the local rate of change of action density in time, the second and third terms represent the

propagation of action density in space. The fourth term represents shifting of the relative frequency due to variations in depth and currents. The fifth term represents depth-induced and current-induced refraction. The expressions for all propagation speeds $c_{x,y,\sigma,\theta}$ are taken from linear wave theory.

The following wave propagation processes are represented in SWAN:
- Propagation through geographic space
- Refraction due to spatial variations in bottom and currents
- Shoaling due to spatial variations in bottom and currents

The following wave energy generation and dissipations processes are represent in SWAN:
- Generation by wind
- Dissipation by white capping
- Dissipation by depth-induced wave breaking
- Dissipation by bottom friction

Generation by wind
Transfer of wind energy to the waves is described in SWAN with a resonance mechanism (Phillips, 1957) and a feed-back mechanism (Miles, 1957).

Dissipation
The dissipation of wave energy is represented by the summation of the three different contributions: white capping, bottom friction and depth-induced breaking.
White capping is primarily controlled by the steepness of the waves and in SWAN it is based on a pulse-based model (Hasselmann, 1974). The process of bottom friction is described by the empirical model of Hasselmann et al. (JONSWAP, 1973) which gives an empirical constant value, typically different for swell and wind driven sea (Bouws and Komen, 1983). The energy dissipation in random waves due to depth induced breaking is modeled a spectral form (Elderberky and Battjes, 1995) of the bore-based model of Battjes and Janssen (1978).

SWAN is therefore capable of calculating the wave conditions in a grid point given the conditions in the up-wave grid points. This means the progression of wave conditions in space and time is known for given boundary conditions of the model, given the local water depth and the conditions in the up-wave grid points.

2.3 Boundary conditions

The model area is selected in such a way that two locations where the wave climate is measured are located at its boundaries which is

illustrated in Figure 7. The model area covers a large part of the Dutch coast from south of the Port of Rotterdam up to just south of the sluices of Ymuiden, with Scheveningen located more or less in the middle along the shoreline. One of the two wave buoys is 'Europlatform' the other is 'Munitie stortplaats Ymuiden'. At these two locations wave characteristics have been measured over the past 20 years and the boundary conditions are derived from these measurements. In Figure 7 it is illustrated how the boundary conditions are applied: To the blue line the boundary conditions derived from measurements from Europlatform are applied, and to the green line the boundary conditions derived from Ymuiden. For both lines the boundary conditions are applied up to 10 kilometers from the shoreline. The boundary condition applied to the yellow line is a linear interpolation between the boundary conditions for the blue and green line.

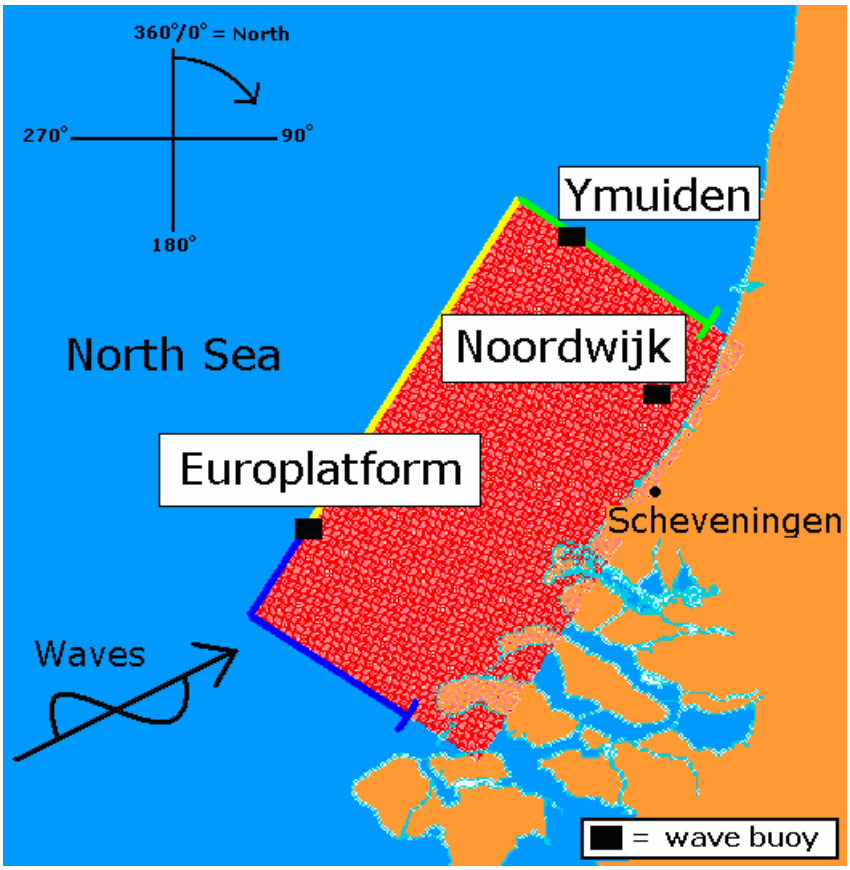


Figure 7: the model area (red surface) and the wave measure locations

The direction the waves come from is important. Waves coming from direction 30° to 210° (clockwise, see Figure 7 for definition of the directions) are of no interest because they travel away from the shore at Scheveningen. Therefore only waves from direction 210° to 360° (clockwise) are taken into account. Although waves approach the surf

reef from all these directions, the surf reef will be pointed in the direction where the most suitable waves come from. From statistical wave data[1] it is found that 20% of the time waves come from 210°-240° and from direction 240°-270° about 11.5 % of the time. It is found that the wave height of waves from direction 210°-240° is significantly reduced by refraction. This is shown in Figure 8 where the distribution of the significant wave height in grid 3 is given for waves at the boundaries with H_s = 1.1 meter from direction 210°-240°.

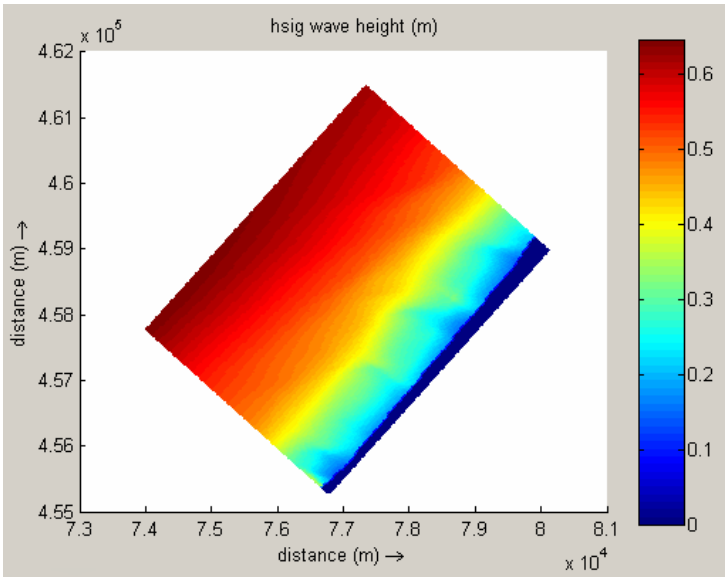


Figure 8: wave height in grid 3 for input with waves from direction 210°-240°

Therefore waves from direction 210°-240°are used for the model boundaries.

Intermezzo: Influence of MV2

A run is done in SWAN with waves with H_s = 1.1 m from direction 210°-240° as boundary conditions for when MV2, the future extension of the Port of Rotterdam into the North Sea, will have been constructed. The significant wave height distribution in grid 3 is shown in Figure 9. When compared to Figure 8 it shows that the wave height will be lower near Scheveningen when MV2 will have been constructed.

[1] www.golfklimaat.nl

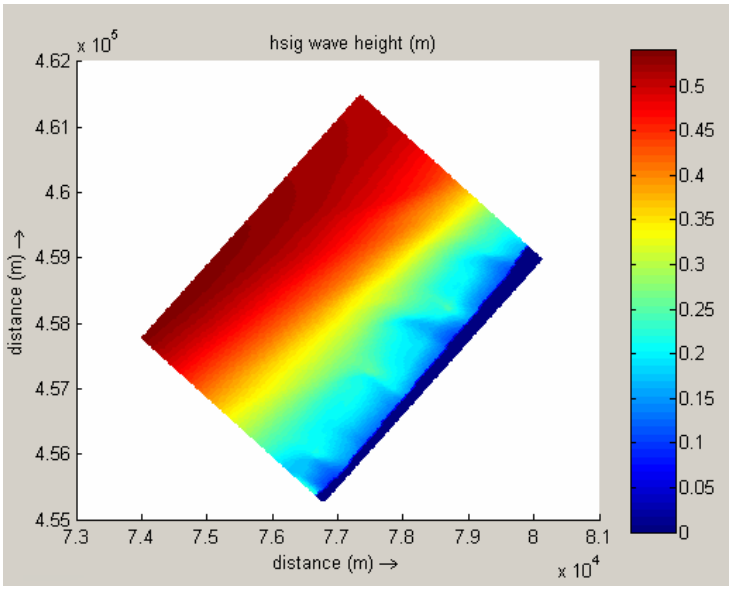


Figure 9: wave height distribution in grid 3 for the situation when MV2 will have been constructed

Wave data

As an example of how the wave statistics are presented at golfklimaat.nl, the statistics are given for Europlatform in Table 1 (for the direction 240°-270°):

Table 1: wave data for Europlatform (source: golfklimaat.nl)

eur: 3D directional dependent simultaneous ditribution H1_3, TH1_3 : 240.00 - 270.00, period year

TH1_3 (s)	3 to 4	4 to 5	5 to 6	6 to 7	7 to 8	8 to 9	9 to 10	all	
H1/3 (m)									
1.00 - 1.20	0.624	**6.593**	2.747	0.125	0	0	0	10.089	
1.20 - 1.40	0.125	**4.045**	3.646	0.212	0	0	0	8.028	
1.40 - 1.60	0.05	2.61	**4.994**	0.275	0	0	0	7.929	
1.60 - 1.80	0	0.724	**4.632**	0.537	0	0	0	5.893	
1.80 - 2.00	0	0.225	**3.958**	1.061	0.025	0.012	0	5.282	
2.00 - 2.20	0	0.062	**2.747**	1.561	0.025	0	0	4.395	
2.20 - 2.40	0	0	1.448	**1.81**	0.062	0	0	3.321	
2.40 - 2.60	0	0	0.562	**2.185**	0.075	0	0	2.822	
2.60 - 2.80	0	0	0.35	1.661	0.162	0	0	2.173	**occurence less than 24 hours /yr**
2.80 - 3.00	0	0	0.075	1.498	0.225	0	0	1.798	
alle	13.884	37.92	29.954	14.26	3.496	0.312	0.012	100	

The numbers in the table represent the chance of occurrence of the conditions given of a wave from direction 240°-270°. The wave height is given in the first column and the wave period in the first row of the table. The wave height is given in bins of 0.2 meter (first column) and the wave period in bins of 1 second (first row). No waves lower than 1.0 meter are taken into account because these waves are too low to be of any interest for surfers and therefore of no relevance to the ASR. For the wave heights and wave periods the bin averages are taken. For all wave periods in a certain wave height bin one wave period is selected, namely the period that occurs most often for that wave height. The chance of occurrence for a certain wave height is

determined by adding up the chances of occurrence for each wave period in that wave height bin: these chances are shown in the last column in Table 1. Only wave heights with a chance of occurrence of more than 24 hours a year are taken into account. The conditions selected this way are shown as the bold numbers in the table, with chance of occurrence found in the last column (total for all different wave periods in a wave height bin). This means in total eight runs for Scheveningen are done in SWAN.

The statistical data give values for $T_{1/3}$ where for the input of SWAN the peak period T_p is needed. The ratio between $T_{1/3}$ and T_p is found empirically by Goda (1978) for wind driven waves to be $T_{1/3}/T_p = 0.9$ and this is used to convert values of $T_{1/3}$ into T_p. The input for the eight runs in SWAN can be seen in Table 2 (all waves come from direction 240°-270°).

Table 2: input for Scheveningen model

	Europlatform		Ymuiden	
	H_s (m)	T_p (s)	H_s (m)	T_p (s)
Run				
1	1.1	5.56	1.1	5
2	1.3	6.11	1.3	5
3	1.5	6.11	1.5	6.11
4	1.7	6.11	1.7	6.11
5	1.9	6.11	1.9	6.11
6	2.1	7.22	2.1	6.11
7	2.3	7.22	2.3	7.22
8	2.5	7.22	2.5	7.22

In Table 3 the chance of occurrence for each of the boundary conditions a year is given:

Table 3: chance of occurrence of the test conditions

Run	**01**	**02**	**03**	**04**	**05**	**06**	**07**	**08**
Chance of occurrence a year from direction 240°-270° (%)	10.1	8.0	8.0	5.9	5.3	4.4	3.3	2.8
Chance of occurrence of the time (%)	1.16	0.92	0.92	0.68	0.61	0.51	0.38	0.32

2.4 Computational grids and topography

Computational grids are used to calculate the change of wave characteristics in the model area. The largest grid covers the entire model area and two smaller grids with higher resolution are applied closer to Scheveningen because the topography changes more rapidly towards the coast. Grid 2 is nested in grid 1 and grid 3 is nested in grid 2; all three grids are rectangular and shown in Figure 10.

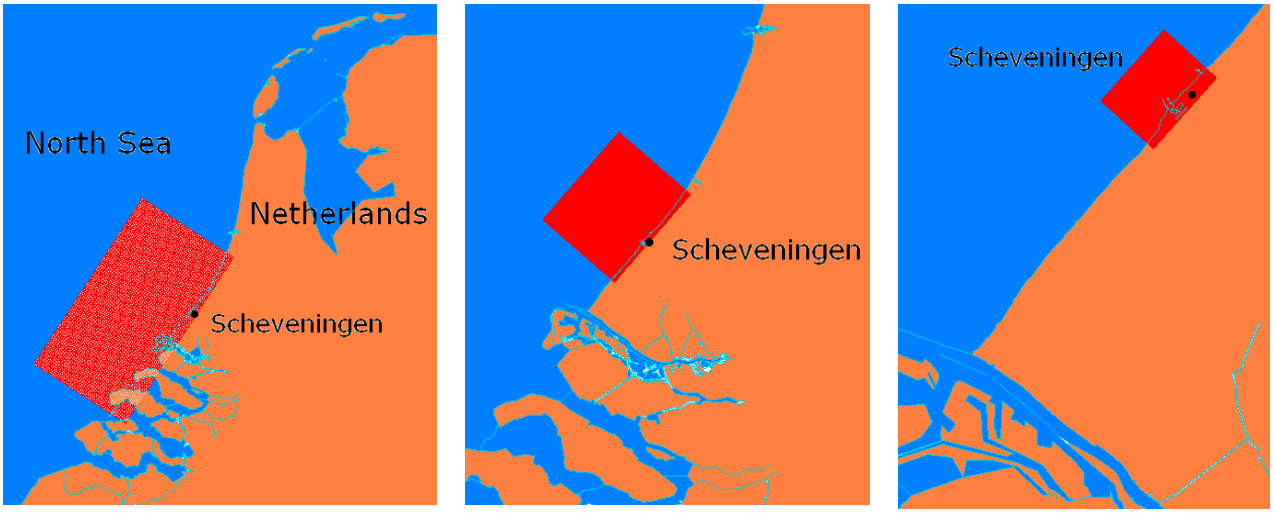


Figure 10: locations of the three computational grids

In Table 4 specifications can be found on all three grids.

Table 4: specifications of the three computational grids

	Size (km x km)	Grid cell spacing (m)
Grid 1	100 x 55 km^2	500
Grid 2	22 x 18 km^2	100
Grid 3	5 x 3,75 km^2	25

Each grid point in a computational grid is provided with a local water depth: these are found by interpolations of measurements that were taken every 20 meters by the Hydrographical Service of the Dutch Royal Navy. The interpolated topography for grid 1 can be seen in Figure 11.

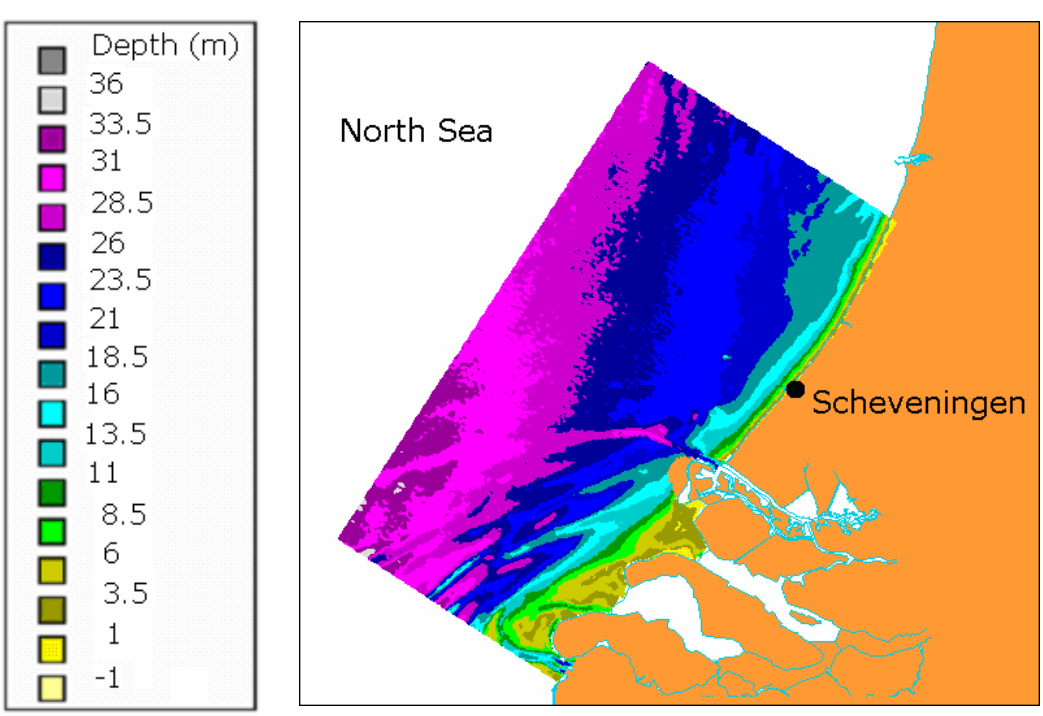


Figure 11: bathymetry of the model area

2.5 Parameter sensitivity and verification

Before using the model to calculate the wave characteristics for Scheveningen it has to be verified whether the model can be used for this situation. This is done by comparing the output of the model and actual wave records for a certain date. To show the validity of the model for this situation waves in the range H_s = 1-2 m are used from direction 240°-270°.

The output for the verification will come from a location called 'Meetpost Noordwijk' which is about 13 km of the coast of Noordwijk (see Figure 7). At this position an offshore structure is located (local water depth of MSL – 18m) where once radio was broadcast from; now it is used to measure the local wave climate. It is assumed here that when the results from the model for this point are comparable to the actual wave records, the model can be used to calculate the wave characteristics for Scheveningen as well.

This paragraph is also used to determine the sensitivity of parameters in SWAN and which functions can be turned off to reduce computation time. The parameters looked at are bottom friction, growth by wind, white capping and directional spreading.

Bottom friction, growth by wind and white capping

For the 14th of March 2001 (time: 1.00) the following wave[2] and wind[3] data are found:

Table 5: wave and wind input for test with SWAN with H_s = 1.5 m

	Waves			Wind	
Location	H_s (m)	Wave period T_{m01} (s)	Direction (degrees) nautical	Speed (m/s)	Direction (degrees) nautical
Europlatform	1.50	5.0	270	10.9	280
Ijmuiden	1.87	5.6	289	11.2	260
Noordwijk*	1.36	4.7	270		
* The Noordwijk measurements are the reference values: the results are compared to these values					

The model is run five times in SWAN where the effects of the growth by wind, white capping and bottom friction are investigated in the first four runs. The fifth run is done to examine the influence of the bottom friction. Functions as quadruplets and triads are turned off in all five runs. The results of the five scenarios can be seen in table 3:

Table 6: results of tests with SWAN for H_s = 1.5 m

Model	Bottom friction	Growth by wind	White capping		Depth at Noordwijk (m)	H_s (m)	Period (T_{m01}) (s)	Direction, nautical (degrees)
test								
1	✓	x	x		17.83	1.41	4.53	267.0
2	✓	x	✓		17.83	1.19	5.08	267.7
3	✓	✓	x		17.83	2.74	4.62	265.1
4	✓	✓	✓		17.83	1.49	4.46	266.8
5	x	x	x		17.83	1.49	4.58	266.9
Actual wave record at Noordwijk:					18.00	1.36	4.7	270.0

It can be seen that the wave height from run 1 is closest to the recorded wave height. Therefore the settings from run 1 will be used in the determination of wave conditions for Scheveningen. This means wind growth and white capping are not used in the model (which will reduce computing time significantly).

[2] www.golfklimaat.nl
[3] www.knmi.nl

Directional spreading

The influence of directional spreading on the results is determined by comparing the results for two tests: the first has a directional spreading of 20° and the second a directional spreading of 4° (which is the default in Delft3D). The input of the two tests and the output, taken from a depth contour at MSL -6 meter at Scheveningen are presented in Table 7:

Table 7: influence of directional spreading on results for the wave height at Scheveningen

	H_s (m)	T_{m01} (s)	T_p (s)	Directional spreading (°)
Input				
Test 1	0.92	3.84	4.99	20
Test 2	0.91	3.83	4.98	4

This means for these conditions the differences are negligible and the default value for the directional spreading will be used (= 4).

Verification of results for Scheveningen

The model is also verified for waves with wave height around 1.9 m, because the range of wave heights the model will be used for is 1-2.5 meter and the model has to be valid for all waves in this range. The conditions found for the 5th of April 2001 are:

Table 8: wave input for test with SWAN for H_s = 1.95 m

Location	H_s (m)	Wave period T_{m01} (s)	Direction (degrees) nautical
Europlatform	1.95	5.6	273
Ijmuiden	2.17	5.9	276
Noordwijk*	1.98	6.0	273
* The Noordwijk measurements are the reference values: the results are compared to these values			

The results from the run in SWAN are:

Table 9: results for test with SWAN for H_s = 1.95 m

		Depth at Noordwijk (m)	H_s (m)	Wave period T_{m01} (s)	Direction (degrees) nautical

Output SWAN Noordwijk	17.83	1.93	5.53	269
Measured at Noordwijk	18	1.98	6.0	273

From these results it is concluded the model can be used to calculate the wave characteristics at Scheveningen for this wave direction and for this range of wave heights.

The results are verified by using a simple hand calculation based on shoaling and refraction only (linear wave theory). This calculation can be found in Appendix I.

2.6 Typical wave conditions for Scheveningen

The output of SWAN is in H_s and T_{m01} where for the input of the physical model tests the peak period T_p is needed. The ratio between T_p and T_{m01} is T_p/T_{m01} = 1.30 for a JONSWAP spectrum and this is used to convert values of T_{m01} into T_p.

The input and output for a depth contour at MSL -6 m at Scheveningen is given in Table 10. For all parameters there was only a small variation along the depth contour and the mean values are given here.

Table 10: Input and output for the 8 runs of SWAN for Scheveningen

	Input					Output			
	Ymuiden		Europlatform			Scheveningen			
Run	Hs (m)	Tp (s)	Hs (m)	Tp (s)		Hs (m)	Tm01 (s)	Tp (s)	Direction*
1	1.1	5.56	1.1	5		0.91	3.83	4.98	260
2	1.3	6.11	1.3	5		1.08	3.83	4.98	261
3	1.5	6.11	1.5	6.11	→	1.09	4.49	5.84	263
4	1.7	6.11	1.7	6.11		1.23	4.49	5.84	263
5	1.9	6.11	1.9	6.11		1.37	4.49	5.84	264
6	2.1	7.22	2.1	6.11		1.51	4.488	5.83	264
7	2.3	7.22	2.3	7.22		1.5	5.198	6.76	267
8	2.5	7.22	2.5	7.22		1.63	5.184	6.74	267
* = the direction waves come from (degrees nautical convention)									

It is clear that wave heights are much lower near the shore of Scheveningen than at the boundaries and this decrease becomes larger as the waves at the boundaries get bigger. Furthermore run 7 shows a slightly lower wave height than run 6 although the wave input was higher at the boundaries. This is to be expected given the fact that the model is based on shoaling and refraction and the reduction of the wave height by refraction is larger due to the longer wave period (see Appendix I for an example calculation with linear wave theory).

3 Experimental study

3.1 Introduction

A physical scale model of the ASR was built by van Ettinger (2005) in the large 2D wave basin in the Laboratory for Fluid Mechanics at the Faculty of Civil Engineering and Geosciences of the Delft University of Technology. Because the subject of this thesis is to determine the performance of the existing design of the ASR by van Ettinger (2005) on the surfability under irregular waves the same physical scale model will be used for these experiments. The setup of the experiment is the subject of paragraph 3.2. The test conditions and the instruments used are discussed in paragraphs 3.3 and 0 respectively. The procedure followed before, during and after each test is given in paragraph 3.5.

3.2 Experimental setup

The setup of the experiment is illustrated in Figure 12: the basin has an effective length of 28 m and an effective width of 15 m. The limited height of the wave board results in a maximum water depth of h = 0.40 m. The walls of the basin serve as wave guides. Opposite to the wave makers a plane 1:20 concrete slope over the whole width of the wave basin acts as a beach. The smooth bottom of the wave basin ensures minimal frictional dissipation in the part between the wave makers and the slope.

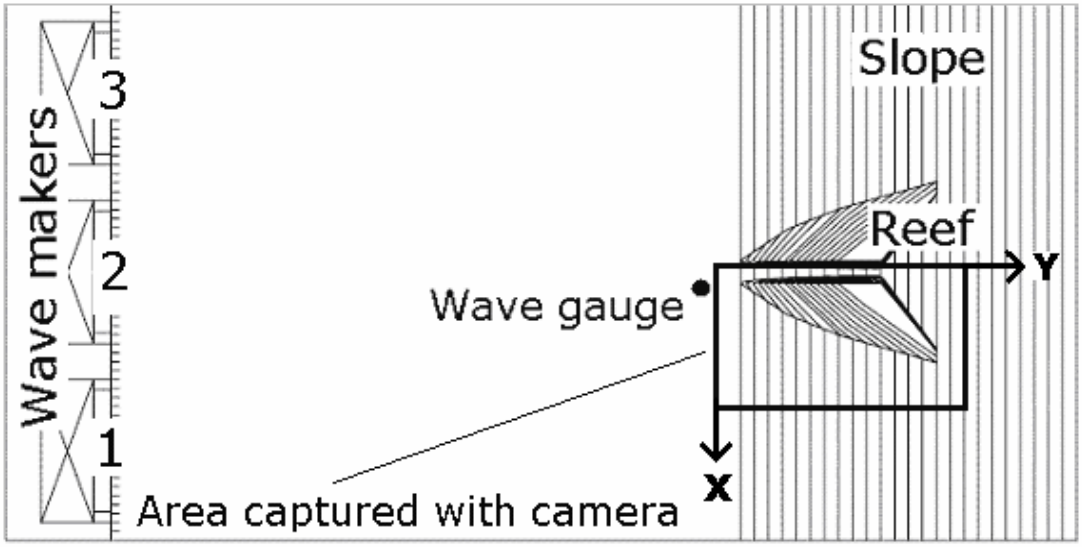


Figure 12: lay out of the physical model

The reef itself is shaped as is illustrated in Figure 13. The reef was built for the research by van Ettinger (2005) at geometric scale 1:15 in

the basin. The crest of the reef lies 0.30 meter above the floor of the basin.

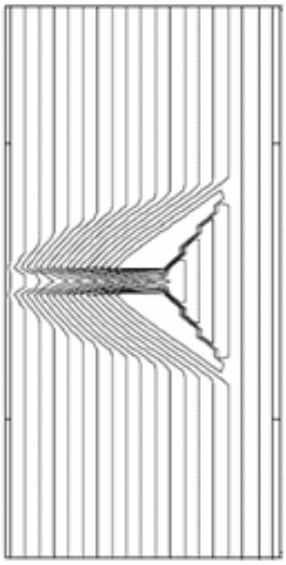


Figure 13: shape of the reef

On one side of the basin three hydraulic piston wave makers are positioned, 5 meters wide each. The wave makers are not equipped with reflection wave compensation and can produce regular, multi-chromatic and irregular waves, unidirectional only. The wave makers receive a signal from a single computer which uses a wave file that contains the wave steering signal. A software program called Delft-AUKE is used to make the wave files and it checks the limitations of the wave makers and the Ursell number to see whether it is possible to make a certain wave in the basin given the water depth. The Ursell number is given by:

$$U = \frac{H * L^2}{h^3} \tag{3.1}$$

where h is the water depth, *H* the wave height and *L* the wave length at the wave maker. If *U* > 25 second order wave board control is not longer valid.

The behavior of waves going over the reef is monitored with a camera and their wave height is measured 1 meter in front of the toe of the reef with a wave gauge as shown in Figure 12. An example image captured with the camera and the coordinates system used in the images is illustrated in Figure 14.

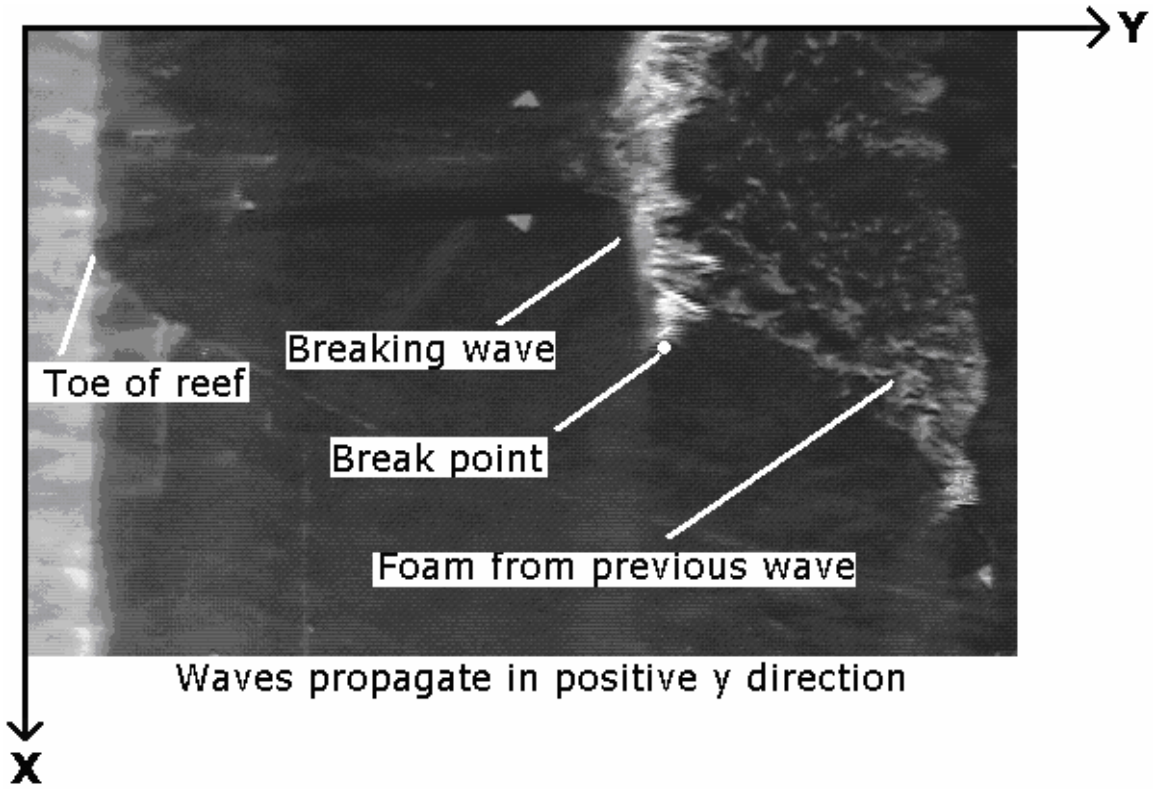


Figure 14: example image captured with digital camera

3.3 Tests conditions

Reproducing a three dimensional sea state where directional spreading is present by a two dimensional process with unidirectional waves is fundamentally incorrect. It provides however a way to gain better understanding of the processes involved.

The irregular waves in the basin will be of the synthesized nondeterministic kind which means that no constraints have been placed on one or more variables, but that it is attempted to match the random characteristics of the natural sea state only within the bounds of probability: only the peak period T_p, the significant wave height H_s and the shape (Jonswap) of the wave spectrum are used to construct the wave field.

Scaling

For a physical model test the object of interest and its surroundings have to be scaled. For a short wave near shore model the physical model should be Froude scaled (Hughes, 1993). The Froude number is:

- The Froude number $V / \sqrt{g * L}$

Where

V = Velocity
g = Gravitational attraction
L = Length
This comes down to the requirement that the scale model is geometrically undistorted and the time scale is equal to the Froude time scale which is the square root of the geometric scale = $1:\sqrt{15}$.

The effect of tidal water level fluctuations on the surfability of the ASR will be determined by tests with different water levels. Because the tidal range near Scheveningen is 2.30 meters a range of 2.30/15 ≈ 0.15 m water difference should be considered in the scale model.

The water level in the basin during the first eight tests will be 40 cm at the toe of the reef and three more tests are done to determine the influence of the water level on the surfability. For each of these three tests the water level will be lowered 4 cm: tests will be done with 36, 32 and 28 cm water depth with respect to the bottom of the basin. This means the influence on the surfability of a tidal range of 0.12*15 = 1.80 meter is considered.

The tests with water depths 36 and 32 cm will have the same wave spectrum as test 5 and the test with water depth 28 cm will have the same wave spectrum as test 4 due the limitations of the wave maker. All the wave files have a cycle time of 20 minutes. The wave fields of tests 1-6 have second-order wave board control whereas tests 7 and 8 have first-order wave board control due to the limitations of the wave makers and the Ursell number. The 11 tests that are performed in the wave basin are shown in Table 11:

Table 11: test conditions

Reference	H_s (cm) model	T_p (s) model	Wave board control	Water depth h (m)	Remarks
Test 1	6.1	1.28	Second-order	0.40	
Test 2	7.2	1.28	Second-order	0.40	
Test 3	7.2	1.51	Second-order	0.40	
Test 4	8.2	1.51	Second-order	0.40	
Test 5	9.1	1.51	Second-order	0.40	
Test 6	10.1	1.51	Second-order	0.40	
Test 7	10.0	1.75	First-order	0.40	
Test 8	10.35*	1.75	First-order	0.40	*This is the maximum value of H_s possible in the basin for this spectrum where H_s = 10.9 was wanted

Test 36	9.1	1.51	Second-order	0.36	Same wave spectrum as test 5
Test 32	9.1	1.51	Second-order	0.32	Same wave spectrum as test 5
Test 28	8.2	1.51	Second-order	0.28	Same wave spectrum as test 4; the spectrum of test 5 was not possible for this water depth

The Ursell number for test 8 is 19.4, for test 32 it is 19.83 and for test 28 it is 23.34 which are all smaller than 25. The fact that the Ursell number for test 8 is 19.4 suggests that the fact that test 7 and 8 need to have first-order wave board control (limited by Delft-AUKE) is due to the limitations of the wave makers and not the need for the Ursell number to be smaller than 25.
The consequences of the lack of second-order wave board control for test 7 and 8 are that it will create spurious waves in the basin which are originally not present in the wave signal. The tests are not sensitive to long waves because the focus lies on the breaker type and the location of the break point in time which is not influenced by these long waves. Therefore the effect of the spurious long waves can be neglected.
First order wave board control will also cause unwanted high frequency waves in the basin. To what extent these occur will be analyzed later in chapter 4 from the recordings of the water surface in time.

3.4 Instruments

Digital camera

The waves on the reef are monitored with a camera from an elevated position, approximately 10 meters above the water level. The camera is a conventional Panasonic digital camera equipped with a fish eye lens to get as much of the reef as possible. The resolution of the camera is 576x720 pixels and the frame rate of recording is 25 Hz. It is not possible to record non-interlaced images with the camera.

Wave gauge

One resistant type wave gauge with an accuracy of 1 millimeter is used to measure the water surface elevation 1 meter in front of the toe of the reef as is illustrated in Figure 12.

3.5 Test procedure

The following steps are taken before, during and after each test

- All artificial lighting is turned off before the test to eliminate reflections on the water surface.
- A spin up time for every test of 2 minutes is taken to give currents in the basin time to develop.

- The tests with water depth 40 cm are recorded during 40 minutes which means that actually two times the same test is repeated. The tests with variable water depth are recorded for one cycle time, 20 minutes.
- After the test the recording is converted into a digital movie (.AVI) using Adobe Premiere. The same program is used to extract bitmap images from the AVI-movie (5 images per second recording). From these images the change of the surfability parameters in time will be estimated.
- Another software program called Jasc Image Robot is used to crop these images so that only the reef is still completely visible and the images are changed to grey scale images, which is done to reduce the size of the images.

4 Results of experimental study

4.1 Introduction

The behavior of irregular waves on the ASR is monitored with a camera and the wave heights with a wave gauge. The video data from the camera are used to track the break points of waves in time and from this the peel angle, the speed of a surfer and the length of a ride can be estimated. This is the subject op paragraph 4.2.1 and 4.2.2 respectively. Furthermore a method is developed which is used to determine the breaker type from the video data which is discussed in paragraph 4.2.3. In paragraphs 4.3 and 4.4 the data of the experimental study are evaluated. In paragraph 4.3 the results of the analysis of the surface elevation are presented. In paragraph 4.4 the number of surfable waves found from the analysis of the video data is estimated. This is followed by analyzing the influence of tidal water level fluctuations in paragraph 4.4.2.

4.2 Method of analysis of video data

The objective of the analysis of the video data is to determine the surfability of irregular waves typical found at Scheveningen. Therefore it is necessary to determine the following surfability parameters for all images in a recording:

- The breaker type
- The peel angle
- The length of a ride

The peel angle and length of ride can be estimated by tracking the break point of a wave in time. This is done by locating the break point in each image (with interval 0.2 seconds) that is extracted from the video recording and is discussed in paragraph 4.2.1. The determination of the breaker type is estimated by comparing the brightness of the foam between plunging and spilling waves and is discussed in paragraph 4.2.3.

The images are analyzed in Matlab, by utilizing the Imaging Toolbox. With this toolbox it is possible to read images into the workspace which can be manipulated by a wide variety of mathematical operations. The script for the algorithms in this paragraph is written for Matlab but the developed algorithms can be used independently from Matlab.

4.2.1 Locating the break point

The breakpoint of a wave is defined by the transition between the broken and unbroken wave crest. The broken wave crest consists of turbulent water mixed with air and is usually referred to as foam. The foam is very bright and at its brightest where the wave most recently has broken. This feature is used to estimate the location of the break point.

The algorithm to find the location of a break point is:

1. Read an image into Matlab. This means the grey scale image is turned into matrix in which every pixel in the image is an entry in the matrix and the value of the entry represents the intensity of the pixel. This intensity can be seen as the brightness of the pixels and lies in the range 0 to 255.
2. Crop the image so that only the reef is depicted.
3. Subtract a background image from the current image to remove non-changing pixels. This way only changing pixels remain in the image representing the breaking wave(s).
4. Convert the image into a binary image using a brightness threshold. The only thing still visible in the image is the parts where foam was created by a breaking wave. The value of the brightness threshold has to be determined.
5. Apply a spatial filter to remove noise: small pieces of foam which might be left in the image by the last wave. The value of this spatial filter has to be determined.

The pixel with the largest value for the x-coordinate (see Figure 14) of the remaining pixels represents the break point. The method is described in detail in Appendix II with an example. The script used in Matlab can be found in Appendix IV.

The algorithm was calibrated and tested by comparing locations of break points found with the algorithm with locations of break points found by visually determining in the same series of images. A series of images (2834 images) was extracted from a recording of a test of almost 10 minutes with a JONSWAP spectrum in the basin (H_s = 10 cm and T_p = 2 s). During this recording the breaker type was visually determined for every breaking wave. A distinction was made between spilling waves, plunging waves and something in between. This 'in between' waves means waves started breaking plunging but turning into spilling along the way (about halfway). This type of wave will be called intermediate from here on.

A series of 90 subsequent images which featured three spilling, one intermediate and one plunging wave, is taken from the series of 2834 images for the calibration and testing of the algorithm. The calibration means optimizing the brightness threshold and the spatial filter.

In Figure 15 the locations of the break point found with the algorithm and by visual means are presented.

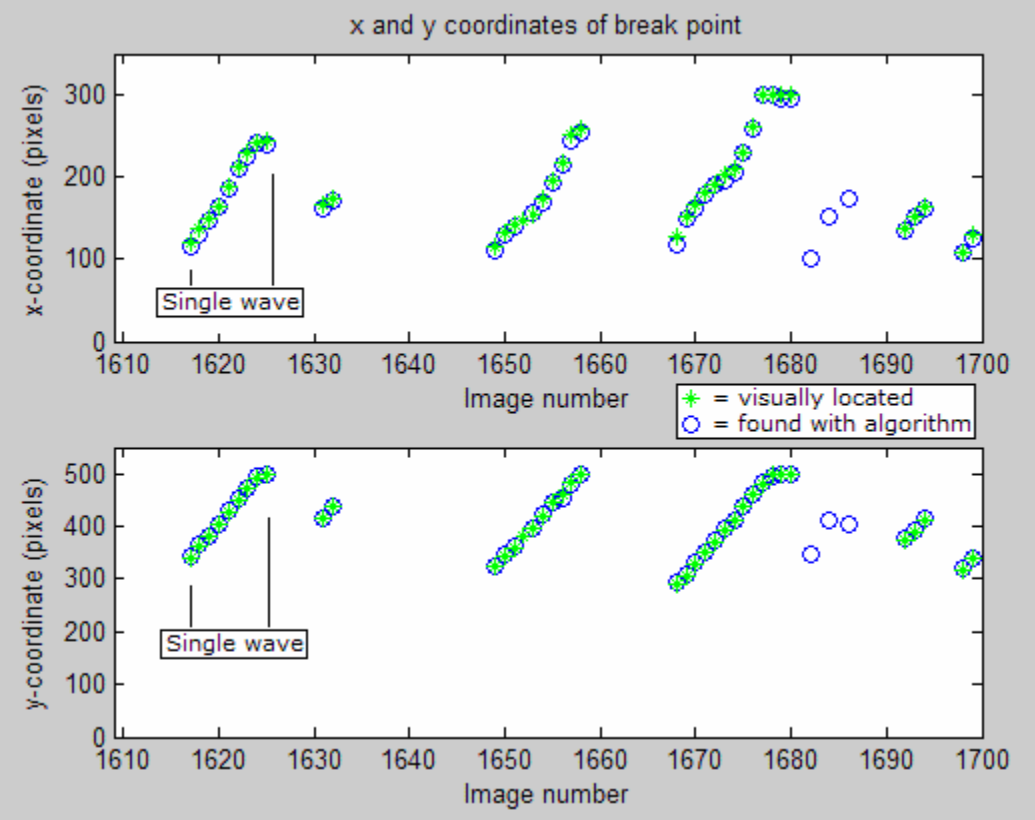


Figure 15: the coordinates of break points found with the algorithm and by visual locating of in total 5 separate waves is followed in time: the time interval in between two images is 0.2 seconds.

From the figure it can be concluded that the algorithm performs very well. Errors can occur when remnants of foam from a previous wave are mistakenly marked as break points. The points found by the algorithm in images 1682, 1685 and 1688 are examples of these errors. Another error that can occur is when a break point is not located by the algorithm which is the case for image 1652. These errors however do not interfere with the estimation of the surfability parameters. Namely, the surfability parameters are only determined if the wave consists of more than 3 images and the length of a ride is determined for an entire wave. Images such as image 1652 are simply skipped and the peel angle is than determined from the locations of the break point in image 1651 and 1653.

4.2.2 Estimating the peel angle and length of a ride

The length of a ride and the peel angle can be estimated by following the position of the break point in time: in two consecutive images. Knowing the coordinates of the break point in the consecutive images and the time interval in between those images, the length two concerning surfability parameters can be estimated. Figure 16 shows two images from different time frames of the same wave and in Figure 17 the area in the white rectangle in Figure 16 is enlarged to show how the two concerning surfability parameters are derived.

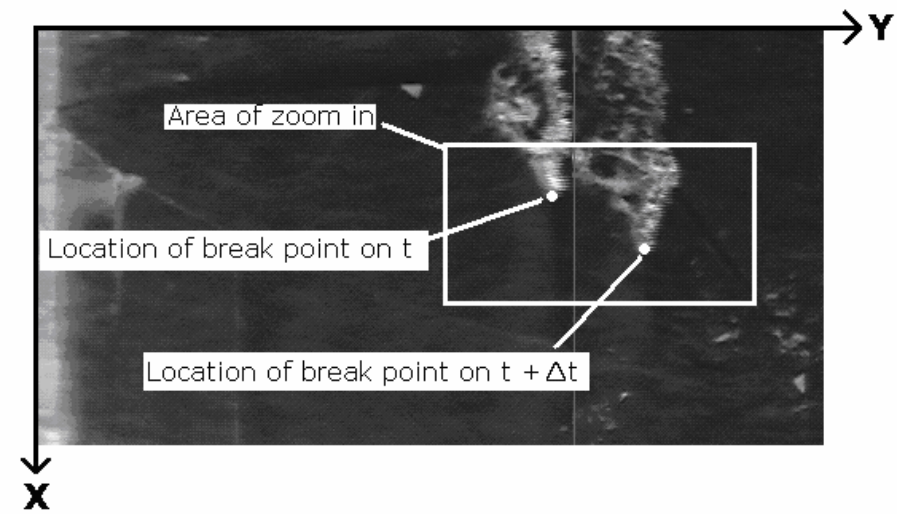


Figure 16: movement of a break point in time

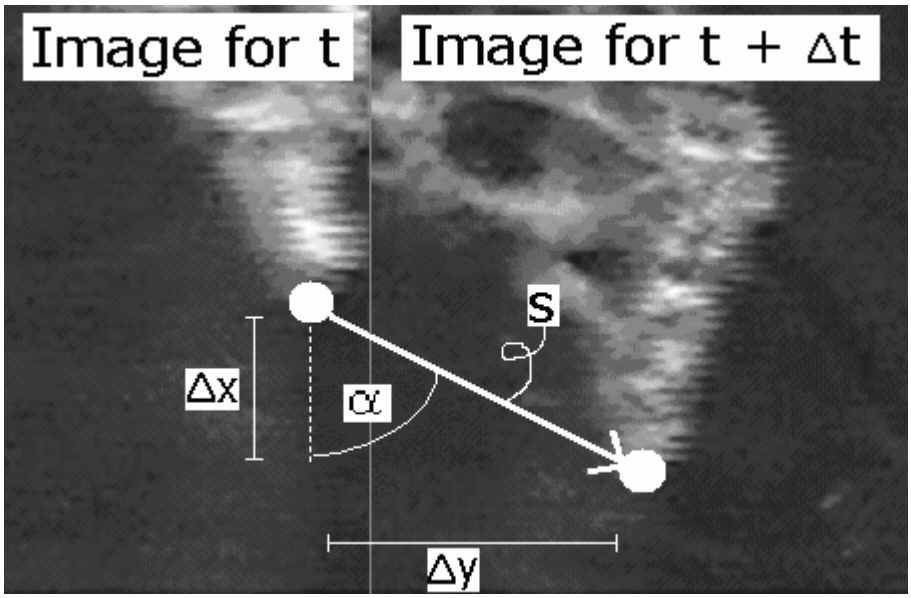


Figure 17: peel angle, length of ride s and speed of a surfer from the movement of a break point in images in time (zoom in area of Figure 16)

It is illustrated in Figure 17 that the change of location of a break point consists of a change in X and Y direction, Δx and Δy respectively (according to the axis shown in Figure 12). The two surfability parameters are estimated by:

- The peel angle α:
  $\tan(\alpha) = \Delta y / \Delta x$
- The length of a ride s:
  $s = \sqrt{(\Delta x^2 + \Delta y^2)}$

It has to be noted that the expression given for the peel angle is an estimation of the real peel angle. The peel angle is defined as the angle between the tangent of the wave front at the pocket of the wave and the direction of the breaker line. In the estimation the wave front is considered to be parallel to the depth contours, by which the effect of refraction is neglected. The actual peel angle will be smaller than found with the estimation given.

Scaling of distances and velocities in the model to prototype

All the distances and thus also velocities are estimated in the images in pixels. The conversion to actual meters and meters/second in prototype is shown in equations (4.1) and (4.2) respectively:

$$s_{prototype} = s_m * f_{sc} * sc_{geo} \tag{4.1}$$

$$v_{prototype} = \frac{s_m * f_{sc} * sc_{geo}}{t_{interval} * sc_{Froude}} \tag{4.2}$$

where:

$s_{prototype}$ = the down-line distance in prototype
$v_{prototype}$ = the down-line velocity in prototype
s_m = distance in the model (pixels)
f_{sc} = factor for scaling from pixels to meters
sc_{geo} = geometric scale
$t_{interval}$ = time interval between two images
sc_{Froude} = Froude time scale (=√geometric scale)

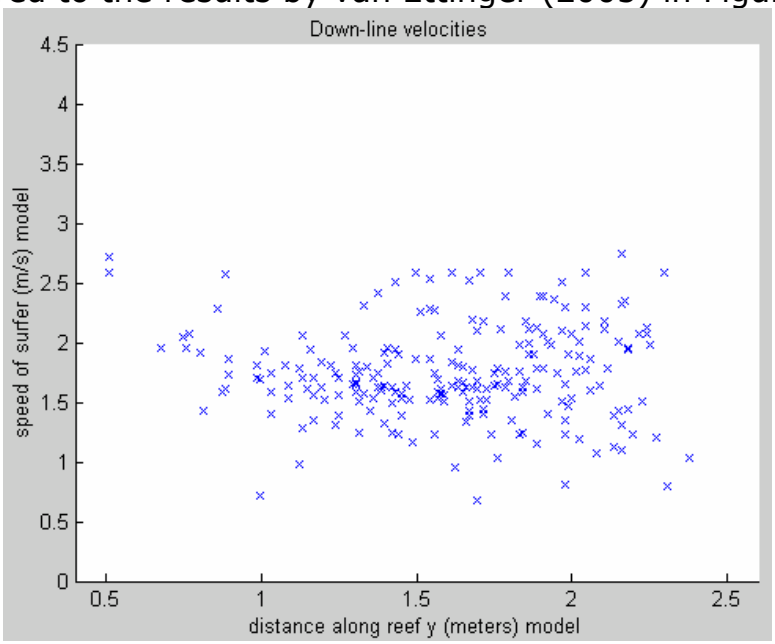
The scaling factor $f_{scaling}$ was found to be 0.0112 meter/pixel for all recordings because they are taken from the same location with the same camera (settings).

The algorithm is tested again, now against the down-line velocities found manually by van Ettinger (2005) for bichromatic waves (H = 0.10 m, f_1=0.518 Hz and f_2 =0.448 Hz). The down-line velocity was

expressed by van Ettinger in m/s model scale (v_m) which is given in the algorithm with:

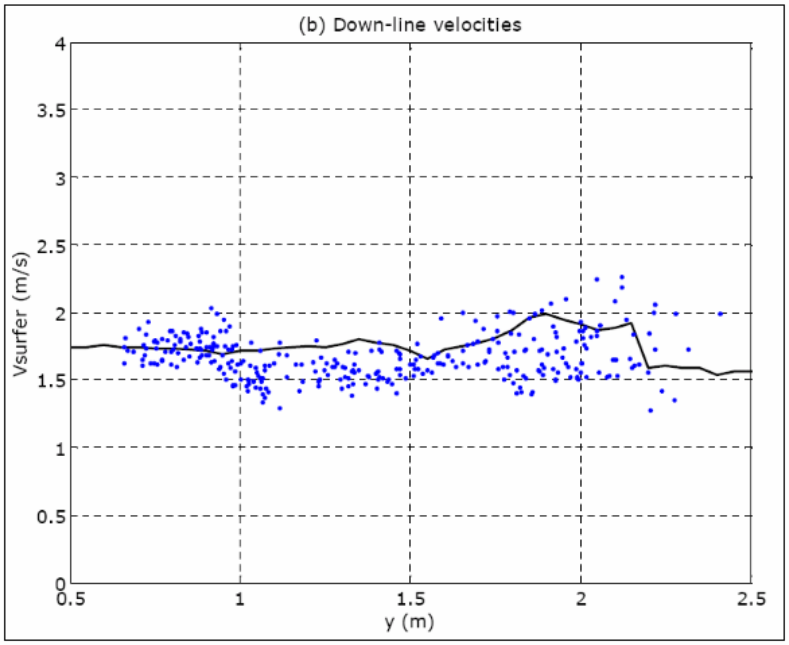
$$v_m = \frac{s_m * f_{sc}}{t_{interval}} \tag{4.3}$$

The results found with the algorithm can be found in Figure 18 which are compared to the results by van Ettinger (2005) in Figure 19.



Resulting figure method described

Figure 18: the down-line velocities along the reef for a test with bichromatic waves as found with the method developed



Resulting figure van Ettinger (2005)

Figure 19: the change of the down-line velocity along the reef for a test with bichromatic waves as found by van Ettinger (2005)

It is clear that the results are very comparable. There is more scatter in the values found with the algorithm; this is explained by the fact that van Ettinger (2005) determined the down-line velocity for the highest wave in the set only whereas the algorithm determines the down-line velocity for all waves in a set.

4.2.3 Determining the breaker type

Besides the peel angle, down-line velocity and length of a ride, the surfability is determined by the breaker shape. In paragraph 4.2.1 a distinction is made between three breaker types: spilling, intermediate and plunging. Plunging waves are preferred by most surfers but intermediate waves are attractive for surfers as well: the first part of the wave breaks plunging which is perfect for surfing. The first requirement of a surfable wave given in paragraph 1.1 is therefore adjusted to:

The breaker shape is a plunging or intermediate.

Next a method is developed to distinguish between plunging, intermediate and spilling waves. From observations during physical model tests it is found that the breaker type is not only dependent on the wave height, but also on the wave history; the previous wave(s). During the same observations it seemed that the higher the Irribarren parameter ξ_b, the brighter the foam (for ξ_b <3). This is explained by the fact that more air is enclosed due to intense wave breaking. To

test this hypothesis the series of 2834 images is used (for which of every wave the breaker type was visually determined and recorded). The total number of plunging waves observed during the recording is 21.

Foam brightness in an image

To verify whether the foam brightness increases with the Irribarren number (for the range spilling-intermediate-plunging waves), histograms are made for pixel intensities in the range 150-250 for an image of a random spilling and a plunging wave. The histogram for the spilling wave is presented in Figure 20 and for the plunging wave in Figure 21.

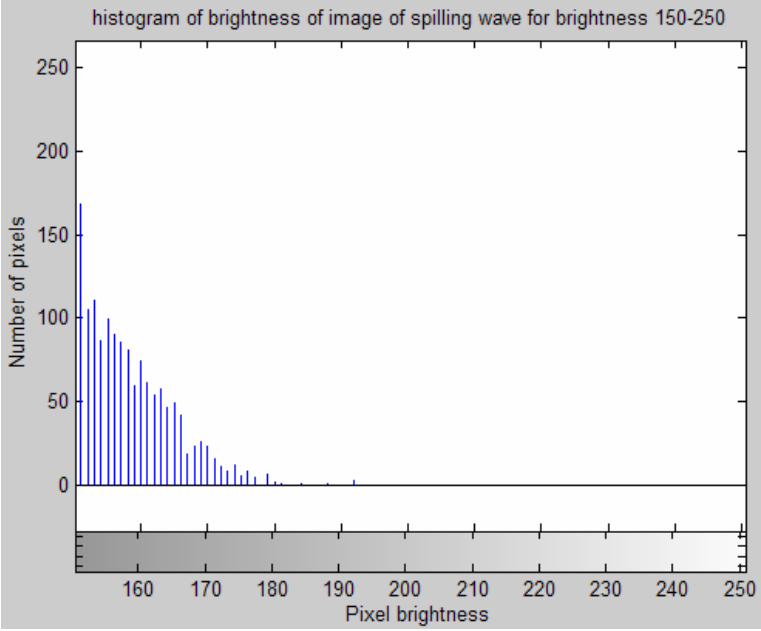


Figure 20: histogram of the pixel brightness in the range 150-250 for an image of a spilling wave

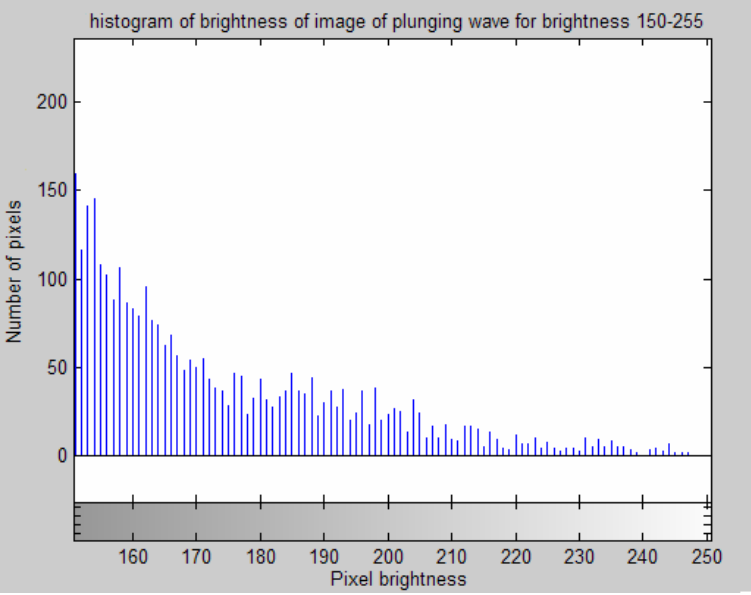
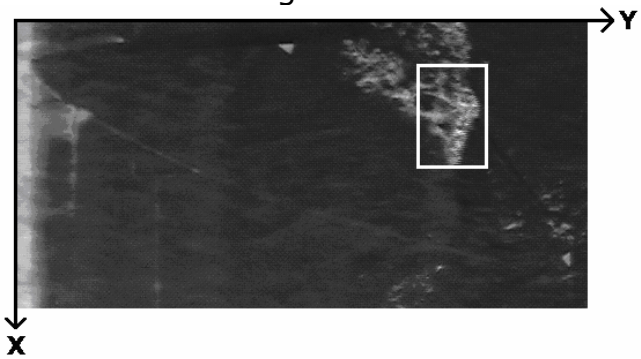


Figure 21: histogram of the pixel brightness in the range 150-250 for an image of a plunging wave

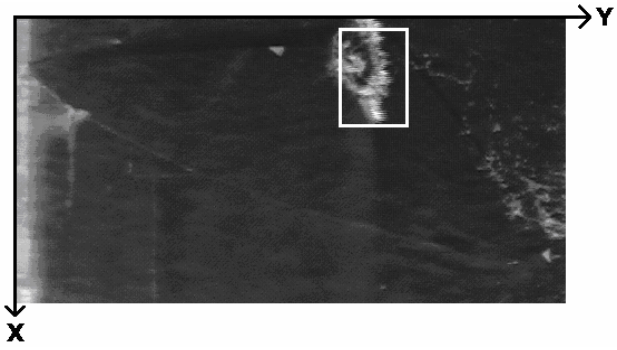
It is clear that in the image of this particular spilling wave hardly any pixels brighter than 180 are present, whereas the plunging wave shows lots of pixels higher than 180; up to 250 even. This feature can be used to estimate the breaker type from an image. This is done with the following method:

1. Select an area around the break point of a wave.
2. Take a number of pixels with the highest intensities (range 0-255) from the selected area around the break point. The number of pixels still has to be determined.
3. Take the average of the brightness of the selected pixels.

The area is a rectangle stretching from the break point -30 pixels and +30 in y direction and -90 pixels in x direction. The area includes always that part of the breaking wave where the foam was just created, no matter the location of the break point to the wave front as is illustrated in Figure 22.



break point "left" of the wave front



break point "in middle" of the wave front

Figure 22: area used for selection of highest intensity pixels

The number of highest intensity pixels that should be selected in the area around the break point is determined by looking at the amount of 'false positives' found with the method as a function of the number of highest intensity pixels selected. The false positives are determined as follows: the light intensity filter is lowered to the point that all 21 plunging waves in the series are detected. The numbers of non-plunging waves detected this way are considered false positives because these waves are marked as plunging waves whereas in reality they are not.

The amount of false positives is determined for the number of pixels selected in the following range: 10, 20, 50, 100, 200 and 400 pixels and their relation is shown in Figure 23.

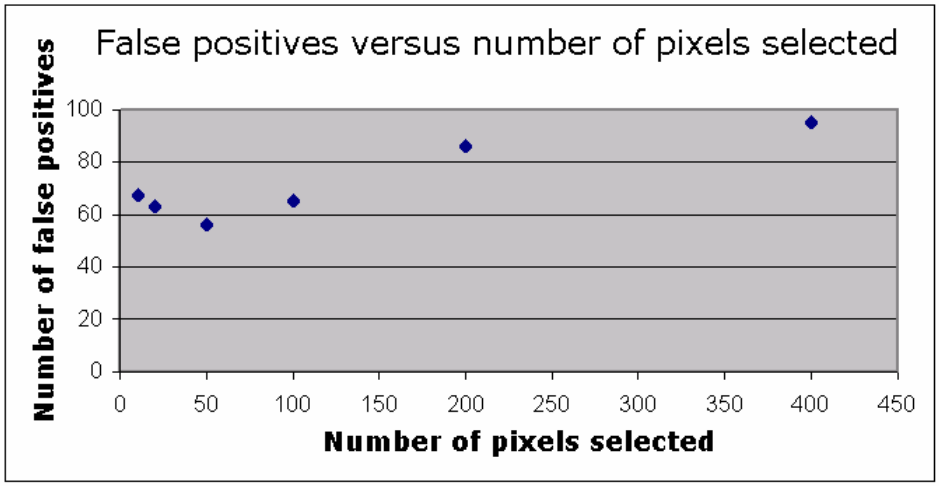


Figure 23: number of false positives versus the number of pixels selected

For the number of pixels between 20 and 100 the number of false positives is minimal. These values can be explained by:

- If the number of pixels is less than 20 more false positives are found, e.g. intermediate waves with some bright pixels.
- If the number of pixels is higher than 100 more false positives are found because the brightness threshold has to be lowered to be able to detect all 21 plungers. This is because of the fact that some images of plunging waves have less than 400 pixels above brightness of 200.

Based on Figure 23 it is chosen to select 50 pixels for the determination of the foam brightness of a wave in one image. It is noted that all false positives were of the intermediate breaker type.

External lighting adjustment

It is found that the natural light coming in through the windows influences the foam brightness in an image. It is found that the

brightness of all images can be adjusted to a certain reference level after recording. This was found by comparing several tests which were recorded with different amounts of light coming through the windows. The setup of these tests and the results can be found in Appendix III.

The method used to adjust the brightness to a reference is as follows:

1. Selecting an area in an image from the current recording and an image from the reference test determine the average brightness (for the whole area) fro both. The area is located in a bright part of the image because the brightest pixels have to be scaled: those also represent the foam of the wave.
2. The difference in brightness of the selected areas is used to adjust the brightness of the entire image from the current recording. This adjustment is done linearly because a factorial adjustment would alter the shape of the brightness histogram of an image. The change is therefore a simple subtracting or adding of the difference found to all pixels in the image.

The adjustment takes place just after reading the image into the workspace: after the light intensity compensation the method of determining the location of the break point and the breaker type remains the same. The brightness of all tests is scaled to the test with 2834 images (reference).

For each test the difference in overall brightness compared to the reference test is determined, see Table 12.

Table 12: difference in brightness for each test compared to reference test

Test	1	2	3	4	5	6	7	8		36	32	28
Difference in brightness	34	-30	0	51	18	15	20	15		2	8	51

Foam brightness of a wave

It was found that even with the optimal number of pixels selected false positives are found with the method. This is because only the foam brightness of one image is determined, which represents the foam brightness of a wave at a certain time. The consequence is that a spilling wave with one (or more) image(s) with high average foam brightness could be marked as plunging. The problem is clarified in Figure 24 where the change of foam brightness in time (along the breaker line) is shown for a random spilling, intermediate and plunging wave.

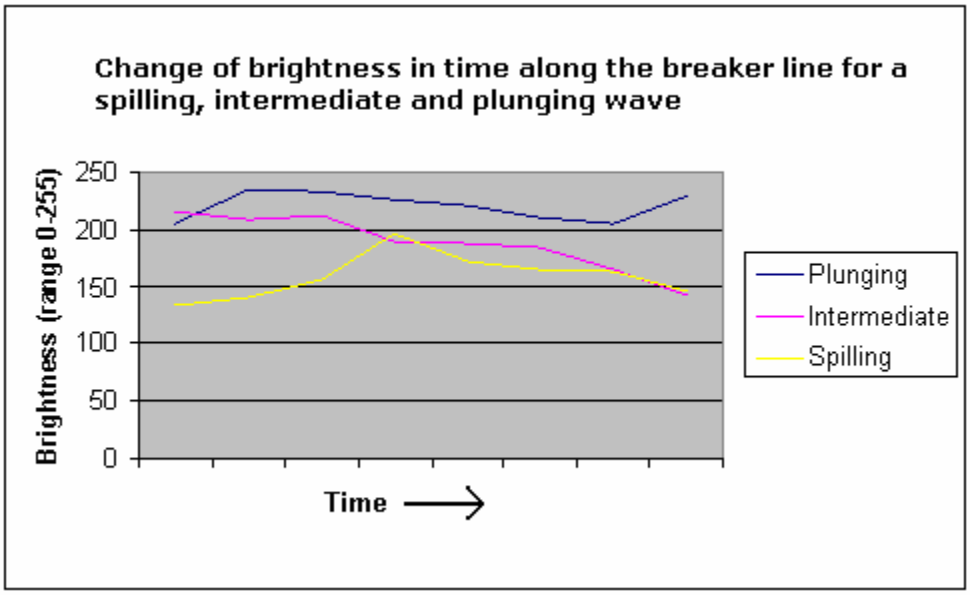


Figure 24: change of foam brightness in time (along the breaker line) for a spilling, intermediate and plunging wave

It is clear that a spilling wave can have high foam brightness in one image whereas the other images of the same wave show low intensities. For the intermediate wave it can be seen that the wave starts with high foam brightness but in time foam brightness becomes lower. This complies with the observations made during the test. The plunging wave shows constant high foam brightness along the breaker line. This is used to make the distinction between spilling, intermediate and plunging waves by determining the foam brightness of an entire wave by taking the average of the foam brightness in all images of the same wave.

Foam brightness per breaker type

The foam brightness for an entire wave is determined for all waves in the test with 2834 images and the results are plotted in histograms divided in spilling, intermediate and plunging waves in Figure 25.

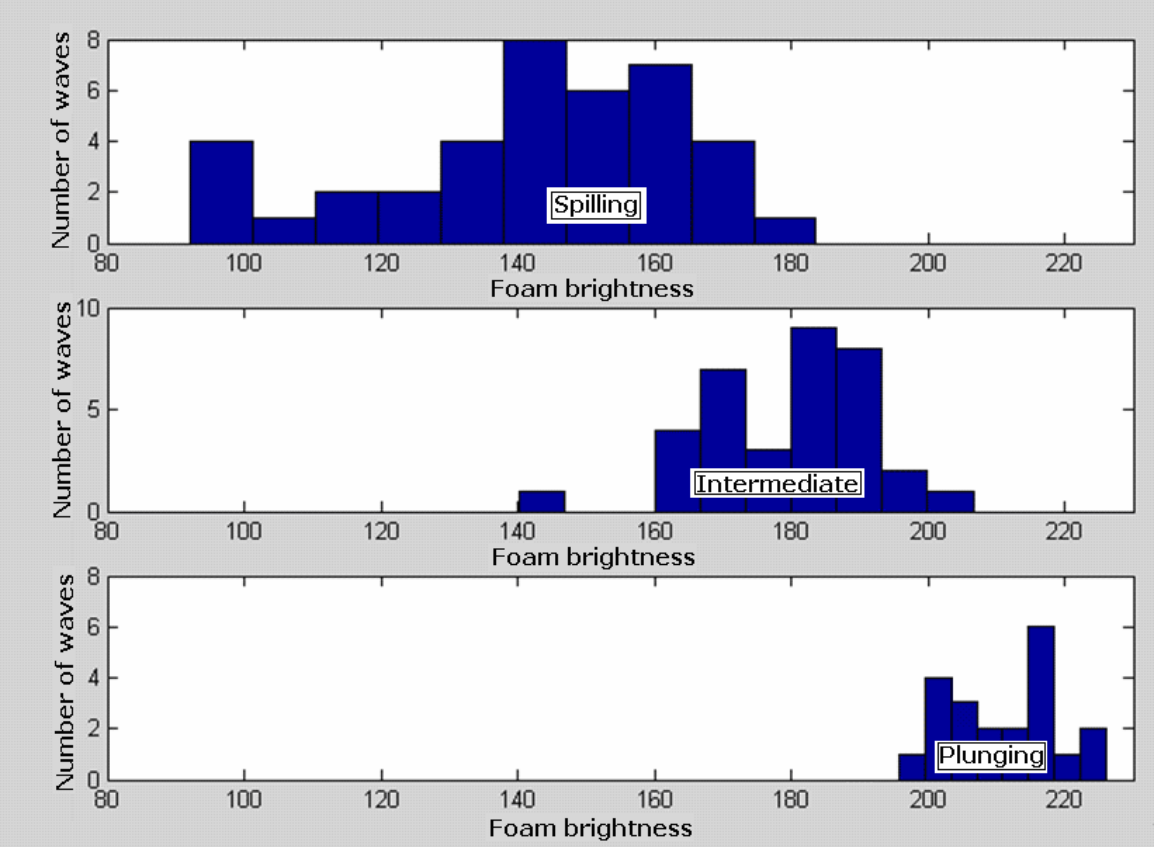


Figure 25: the number of waves given for the foam brightness for all waves of the recording with 2834 images, for each of the three breaker types.

Now the distinction between spilling and plunging waves is very clear: no spilling waves show foam brightness above 180. Intermediate waves with foam brightness above 200 are rare and so are plunging waves with foam brightness under 200. As said before both plunging and intermediate waves are attractive from a surfer's point of view. Therefore the surfability is determined for waves with foam brightness higher than 200 (representing plunging waves) and for waves with foam brightness in between 180 and 200 (representing about 60% of the intermediate waves). If about 95 % of the intermediate waves would be selected, meaning brightness in between 160 and 200, also spilling waves would be selected which is not desirable.

Summary

The conclusions of paragraph 4.2 are that the algorithms developed to track the break point in time perform very well and that the peel angle, the length of ride and the down-line velocity can be estimated from it. Furthermore a method has been developed to determine the breaker type of every breaking wave from the video data.

4.3 Analysis of the water surface elevation

The measurements if wave gauges contain the time series of the water surface elevation. The variance density spectrum of the water elevation at the toe of the reef is determined through a fast Fourier transfer. From these density spectra the significant wave height H_{m0} ($\approx H_s$) and peak period T_p are obtained. The relation between the significant wave height and the first moment of the density spectrum is given by:

$$Hm_0 = 4 * \sqrt{m_0} \tag{4.4}$$

where the zeroth moment of the density spectrum is given by:

$$m_0 = \int_0^\infty f^0 * E(f) df \tag{4.5}$$

The peak period is given by:

$$T_p = f_p^{-1} \tag{4.6}$$

where f_p is the frequency with the highest energy in the spectrum.

Table 13 shows the measured T_p and H_s, where the 95 % confidence interval is given for the fast Fourier transfer:

Table 13: the wave spectrum parameters H_s and T_p from the measurements compared to the input

Reference	From measurements			Input steering computer	
Test	T_p (s)	H_s (cm)	95 % confidence interval H_s (cm)	T_p (s)	H_s (cm)
1	1.27	5.48	5.03 - 6.03	1.28	6.1
2	1.28	6.60	6.05 – 7.25	1.28	7.2
3	1.47	6.56	6.02 – 7.20	1.51	7.2
4	1.49	7.47	6.86 – 8.20	1.51	8.2
5	1.52	8.06	7.40 – 8.86	1.51	9.1
6	1.49	9.10	8.36 – 10.00	1.51	10.1
7	1.69	9.24	8.48 – 10.15	1.75	10.0
8	1.72	9.82	9.02 – 10.77	1.75	10.35
36	1.49	8.08	7.15 – 9.28	1.51	9.1

32	1.49	8.00	7.11 – 9.14	1.51	9.1
28	1.52	7.11	6.31 – 8.14	1.51	8.2

The measured values for H_s are significantly lower than intended for all tests, about 9%. This is due to the calibration of the wave maker which was carried out with regular waves. It appears that this is not valid for irregular waves. The reduction in gain is comparable to the reduction in wave height. Unfortunately all tests were already recorded when this was discovered and therefore no adjustments are made. The spectral shape is verified by comparing the power density spectrum for the test to the standard Jonswap spectrum (Figure 26) where the measured values of H_s and T_p are used as input parameters.

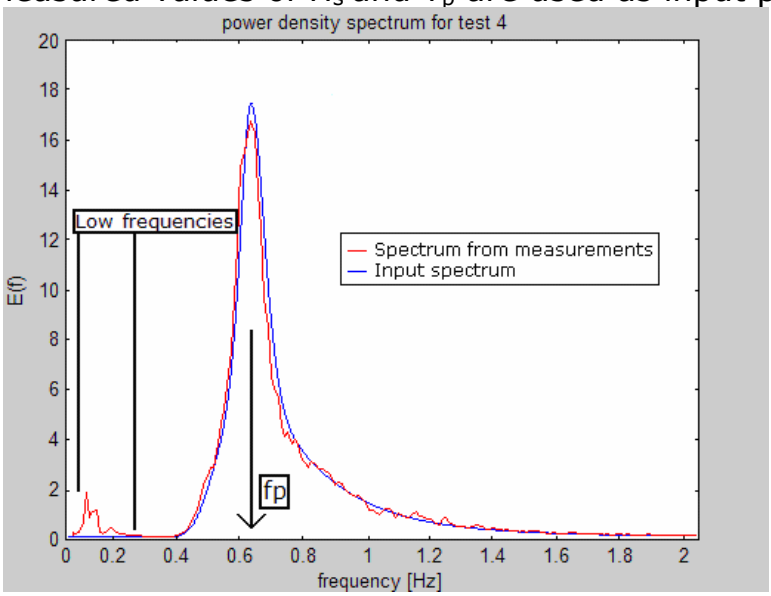


Figure 26: power density spectrum for test 4 from the measurements and the input spectrum

The spectrum shows a low-frequency peak around f= 0.09 and 1.9 Hz which represent standing waves in the basin. Furthermore there are no significant unwanted high-frequency waves (see paragraph 3.3) present (<1 % of the total wave energy).

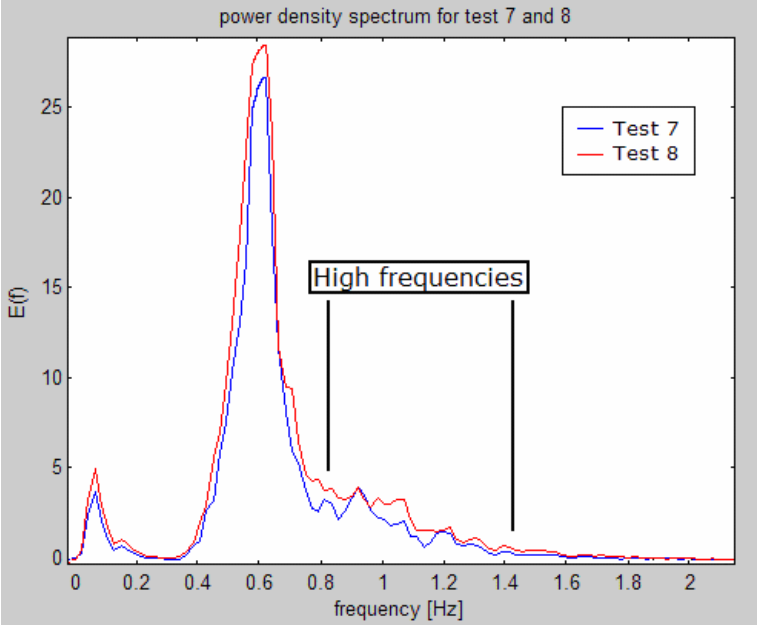


Figure 27: power density spectrum for test 7 and 8

In Figure 27 the power density spectra of test 7 and 8 are plotted and it can be seen that there is a significant amount of low-frequency and high-frequency waves in the spectrum. The amount of energy in the low-frequency waves in test 7 and 8 is much larger than found for test 4 (Figure 26) and is approximately 7 % of the total wave energy for tests 7 and 8.

4.4 Analysis of the video data

The objective in this paragraph is to estimate the number of surfable waves for a typical irregular Dutch wave field over an ASR. This is achieved by analyzing the video data recorded during the test 1 to 8 and the analysis is presented in paragraph 0. The influence of tidal water level fluctuations on the surfability and the number of surfable waves is presented in paragraph 4.4.2.

4.4.1 Number of surfable waves

The requirements for the parameters of a surfable wave were given in paragraphs 1.1 (the first requirement was adjusted in paragraph 4.2.3) and are:

- The breaker type is either plunging or intermediate.
- The peel angle is between 30 and 70 degrees.
- The length of ride is longer than 20 meters.

To estimate the number of surfable waves the number of plunging and intermediate waves is determined for test 1 to 8. This is achieved by using algorithm described in paragraph 4.2 where the foam brightness

of the waves is compared. The number of plunging and intermediate waves (during the time span of 40 minutes) in test 1 to 8 is given in Table 14:

Table 14: number of plunging and intermediate waves for tests 1-8 (in 40 minutes of recording)

Test	1	2	3	4	5	6	7	8
Number of plunging waves	2	2	10	16	19	87	99	164
Number of intermediate waves	2	13	36	56	73	123	163	166

The waves in Table 14 are plunging and intermediate waves which have desirable breaker shapes. The surfability of these waves is further determined by the peel angles and the possible length of ride. Therefore the length of ride *s* along the breaker line is determined for which the peel angle is in between 30 and 70 degrees. In addition, surfable waves are waves with possible length of ride longer than 20 meters. The code used in Matlab to determine these surfable waves can be found in Appendix V. Plots are made for the peel angle along the breaker line which are presented in Appendix VI together with the histograms of *s*. The numbers of surfable waves found for test 1 to 8 are given in Table 15:

Table 15: number of surfable waves for tests 1-8 (in 40 minutes of recording)

Test	1	2	3	4	5	6	7	8	Total
Number of surfable plunging waves	1	1	2	3	5	31	61	77	181
Number of surfable intermediate waves	0	0	18	23	34	48	90	88	301
Total	1	1	20	26	39	79	151	165	482

The conditions in each test represent a part of the wave climate coming from direction 240-270°. The wave climate selected in paragraph 2.3 from direction 240-270° is therefore represented by the total of the conditions for test 1 to 8. Therefore, results of test 1 to 8 can be presented together.

It is interesting to see what the differences for the possible length of ride *s* are for plunging and intermediate waves because for surfers it will matter what percentage of surfable waves are plunging what percentage intermediate. In Figure 28 the values of *s* are presented for all plunging and intermediate waves in test 1 to 8.

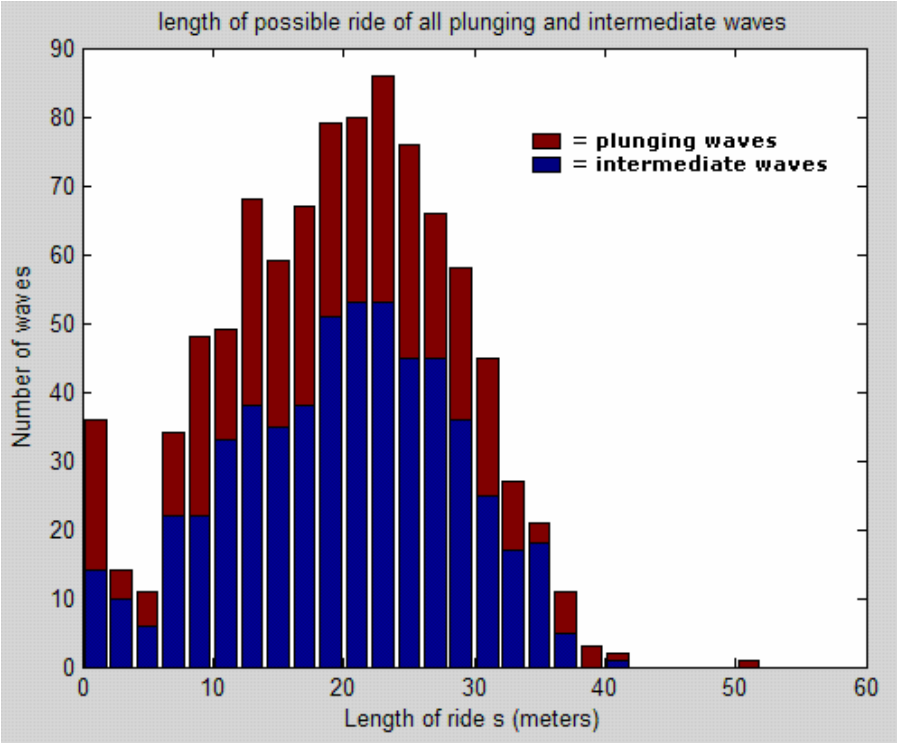


Figure 28: the possible length of ride *s* for all plunging and intermediate waves in test 1 to 8

It is interesting to analyze how peel angles change over the reef. To analyze this, the local peel angle is plotted on a Cartesian coordinate system. The area looked at on the reef is shown in Figure 29.

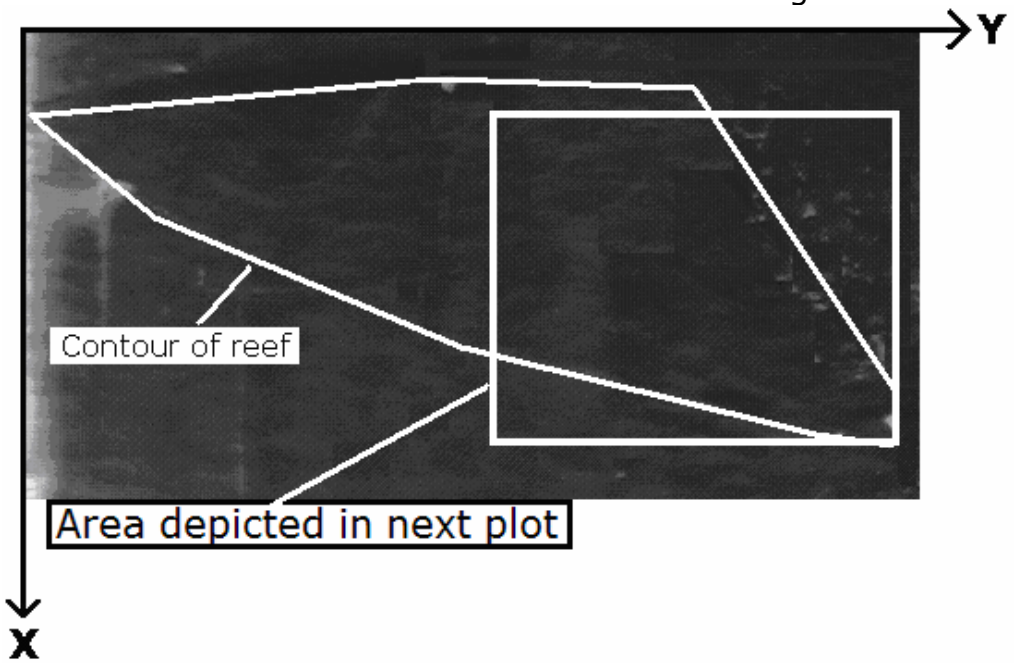


Figure 29: the white rectangle shows the area depicted in the next figure

The plot of local peel angles for break points of all plunging and intermediate waves in test 1 to 8 is given in Figure 30.

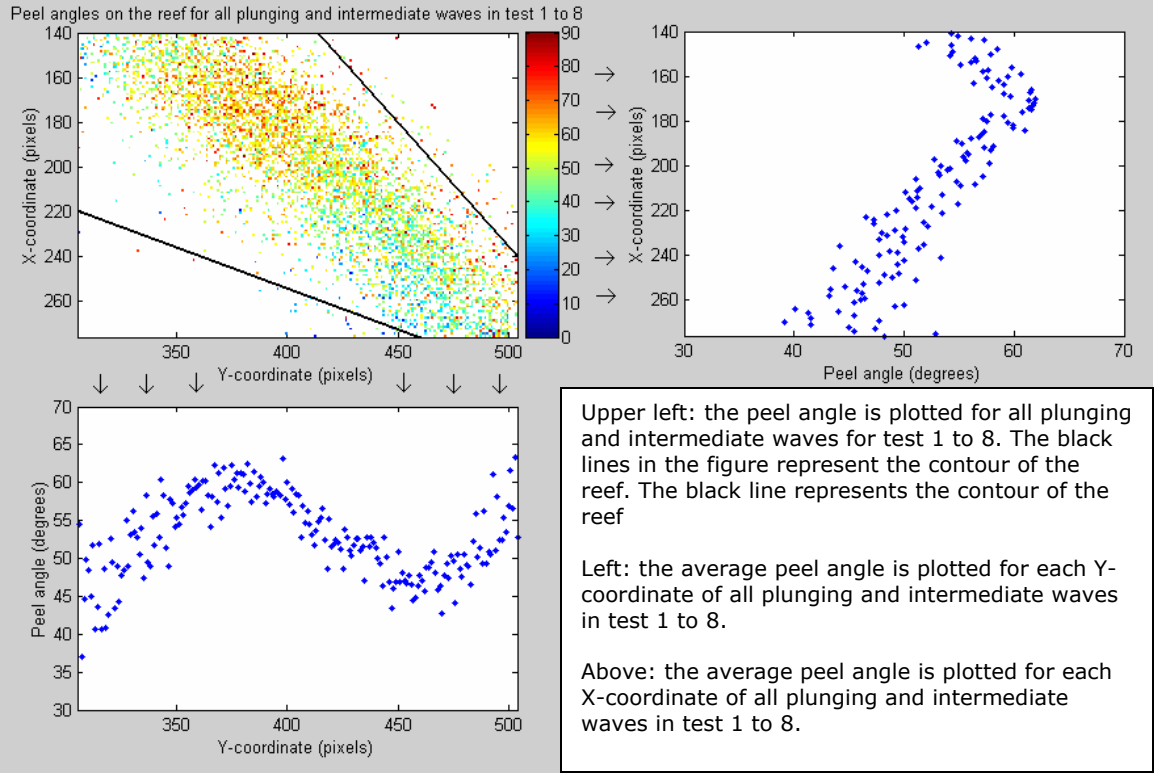


Figure 30: local peel angles for break point of all plunging and intermediate waves in test 1 to 8. In the two subfigures the average peel angle over the x- and y-axis is plotted. This is done by taking the average of the peel angle of all break points with a certain x- or y-coordinate.

Number of surfable waves in prototype

To make an estimate of the total number of surfable waves in Scheveningen due to the ASR, the model results have to be scaled to prototype. With the values in Table 3: chance of occurrence of the test conditions in prototype scale, an estimate can be made for the total amount of surfable waves a year in real scale. The number of surfable waves that can be expected a year in Scheveningen from direction 240-270° is presented in Table 16 for each test condition:

Table 16: number of surfable waves to be expected for each test a year

Test	1	2	3	4	5	6	7	8
Number of surfable waves a year	40	31	624	577	807	1367	1947	1791

The total of surfable waves to be expected is the sum of all surfable waves of all tests:

N_{total} = 7180 waves a year from the direction 240-270°.

This number of waves would occur ideally, however the following notes have to be made: these waves occur not evenly spread through out the year; during the winter months more often and higher waves are present. Furthermore these waves can occur any time during a day, which means also a night when it is not possible to surf. Roughly one can say that about one third of all waves will occur during day time because day time in winter is also shorter than in summer. As found in paragraph 4.3, the wave heights during the tests were about 9% lower than intended. Finally, only 60% of the intermediate waves are taken into account as seen in paragraph 4.2.3.

4.4.2 Influence of tidal water level fluctuations on surfability

The situation above would apply to a sea without tidal water level fluctuations. In Scheveningen however is a significant vertical tide present and the influence is analyzed through lowering the water level in the basin. The number of plunging and intermediate waves in test 36, 32 and 28 are determined as well as the number of surfable waves, peel angles and lengths of ride.

For test 36, 32 and 28 the number of plunging and intermediate waves is determined with the algorithm described in paragraph 4.2 and given in Table 17:

Table 17: number of plunging and intermediate waves for tests 36, 32 and 28

Test	**36**	**32**	**28**
Number of plunging waves	17	18	20
Number of intermediate waves	53	58	47
Total	70	76	67

It has to be noted these tests were recorded for 20 minutes, whereas test 1 to 8 for 40 minutes. This is compensated for to be able to compare the results by multiplying the number of waves in test 36, 32 and 28 by two. Test 36 and 32 are compared to test 5, and test 28 to test 4 because these test were performed with the same wave spectra. It appears that the total of plunging and intermediate waves for test 36 and 32 is almost twice as high as for test 5, and for test 28 approximately two and a halve times higher than for test 4.

The differences in distribution of the possible length of ride s between test 5 and tests 32 and 36, and between test 4 and test 28 are looked

at by showing the histogram of *s* for these tests. In Figure 31 the histograms of *s* for test 5, 32 and 36 is presented:

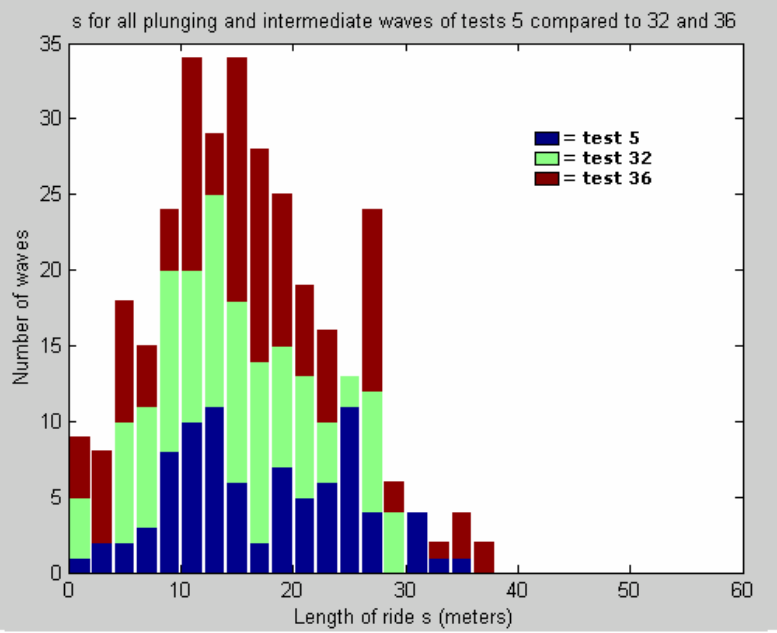


Figure 31: histogram for s for test 5 compared to tests 36 and 32

The conclusion from Figure 31 is that though the number of plunging and intermediate waves might be higher than for test 5, the weighted mean for those tests if below 20 meters. The weighted mean for test 5 is approximately 20 meters. In Figure 32 the histograms for test 4 and 28 are presented.

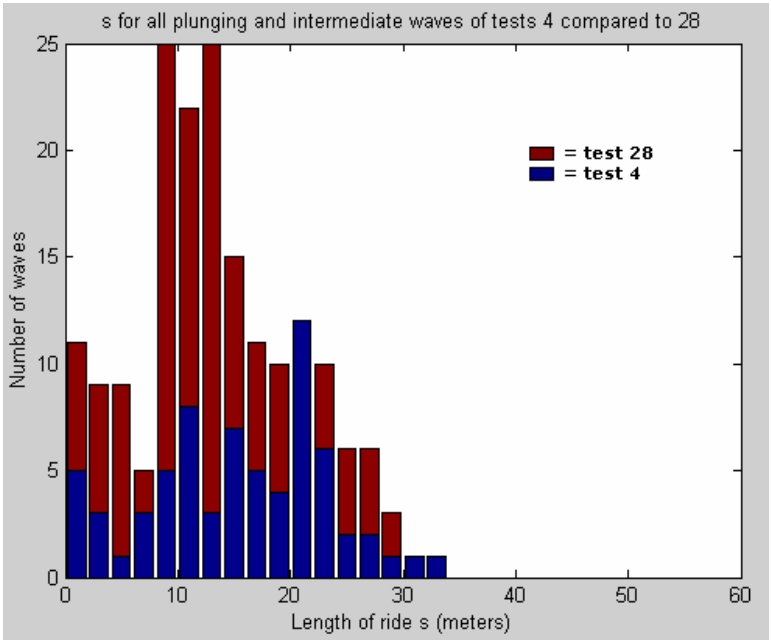


Figure 32: histogram for s for test 4 compared to tests 28

In Figure 32 it is also clear that although the number of plunging and intermediate waves is higher for test 28, the number of surfable waves is around the same for test 4 and 28.

The conclusion drawn from Figure 31 and Figure 32 is that when the water level is lowered, more waves have desirable a breaker shape but the distances of the ride possible become shorter. This can be explained by looking at the locations of the break points: in Figure 33 the break points of all plunging and intermediate waves are plotted in a Cartesian coordinate system for test 36, 32 and 28.

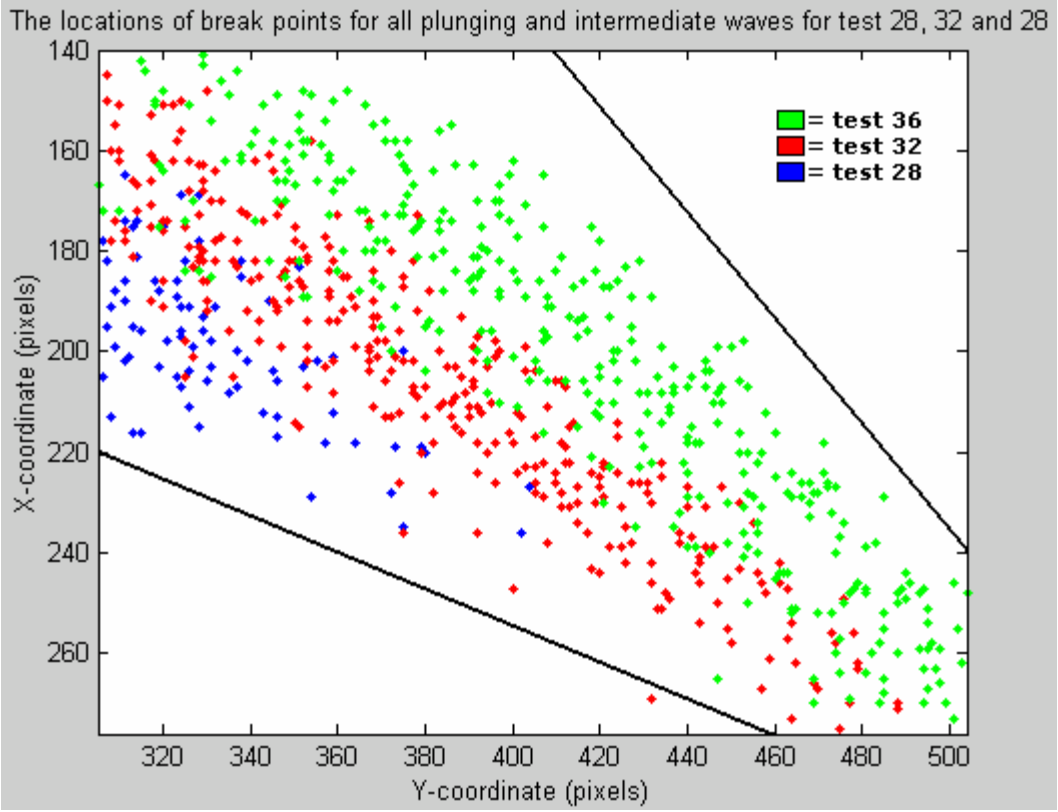


Figure 33: locations of all break points of plunging and intermediate waves for test 36, 32 and 28

It is clear that if the water level is lower, the breaker line shifts seaward (lower x-coordinate). This causes the possible length of ride to be shorter as is illustrated in Figure 33.
A note is made that it is the question whether the reef is surfable with lower water levels from a safety point of view: less water depth means the water depth on the crest becomes less and that if a surfer falls, injuries are more likely to happen.

Number of surfable waves

The numbers of surfable waves for tests 36, 32 and 28 are determined with the same procedure as used for tests 1 to 8. The plots and histograms can be found in Appendix VII and the numbers of surfable waves are given in Table 18.

Table 18: number of surfable waves for tests 36, 32 and 28

Test	36	32	28
Number of surfable plunging waves	5	4	2
Number of surfable intermediate waves	9	10	5
Total:	14	14	7

The number of surfable waves found for the model test are scaled to prototype and the results are given in Table 19 together with the results of test 4 and 5 where to the results are compared.

Table 19: number of surfable waves for test 36, 32 and 28 in prototype

Test	36	32	5		28	4
Number of surfable waves a year	579	579	807		290	577

The number of surfable waves for test 36 and 32 is approximately 70% of test 5, and for test 28 approximately 50% of test 4. It should be noted that low water lasts longer at Scheveningen than high water and that a tidal range of 1.80 meter is analyzed in the present study whereas the tidal range at Scheveningen is approximately 2.30.

The conclusion drawn is that the number of surfable waves will decrease due to tidal water level fluctuations. Based on the results in this chapter, the decrease in surfable waves will be in between 30 and 50 %. On average 40% decrease is to be expected, bringing the number of surfable waves per year from the direction 240-270° to 4300 at Scheveningen.

5 Conclusions and recommendations

Conclusions

The main objective of the study is to determine the number of surfable waves a year on an existing surf reef design under irregular waves typically found at Scheveningen, the Netherlands. The main objective was divided into sub-objectives which are discussed here.

The wave conditions typically found at Scheveningen were determined with the numerical near-shore wave model SWAN. The numerical model built for Scheveningen was verified and calibrated with actual wave records. The wave conditions were determined for waves coming from the direction 240°-270°.

The surfability of typical Dutch irregular waves was analyzed in an experimental study. The boundary conditions were the wave climate typically found at Scheveningen from the direction 240°-270° with SWAN. The behavior of the irregular waves in the model was monitored with a camera, of which the recordings were processed into images.

Algorithms were developed to determine the surfability of irregular waves which determined the peel angle, length of ride and breaker type. One algorithm estimates the peel angle and length of ride from tracking the break point of waves in the images from the recording. The breaker shape is determined by looking at the foam brightness around the break point of a wave in the images.

With the algorithms developed to determine the surfability of individual waves, the recordings of the experimental study were analyzed. From the results an estimate is made for the total number of surfable waves for waves coming from direction 240°-270°, which is 7180 a year if no tides would be present.

The influence of tidal water level fluctuations in the Netherlands on the surfability is analyzed by tests with different water levels and is found two be twofold: more waves have desirable breaker shapes, but the possible lengths of ride are shorter. Tides will reduce the number of surfable waves with approximately 40%, which brings the number of surfable waves to 4300 a year with tides present.

Recommendations

The following recommendations are given for future studies:

- The camera used to monitor the behavior of the waves on the reef should be able to produce non-interlaced images, which makes the process of locating the break point more accurate, and thus the estimation of the peel angle and length of ride.
- Waves from a sector of 30° wide are treated unidirectional which is not conform reality. Therefore the influence of waves approaching the ASR already under an angle on the surfability has to be analyzed.
- Waves from more north-northwestern sectors should be looked at. More suitable waves come from this direction, but they are spread over a slightly larger sector: around 40 degrees wide.
- The experimental study should be recorded with equal light conditions to make the determination of the breaker type of breaking waves more accurate.
- Because in the estimation of the peel angle the refraction over the reef is not taken into account, a more accurate measure to determine the surfability is to look at the down-line velocity.
- The rip currents around the ASR have to be determined for different water levels and different channel widths and their influences on the surfability.
- More wave conditions from direction 240°-270° have to be taken into account: from the number of surfable waves a year in prototype it is clear that the tests with the highest waves produce the most surfable waves, although the chance of occurrence is smaller for those conditions.
- It has to be determined if there is a relation and if so, what the relation is between the Irribarren parameter and the slope of an ASR. This should be done for different water depths on the crest, and for different values for the slope. With this relation it will be easier to design ASRs and predict the shape of breaking waves.

6 Bibliography

Battjes, J.A. 1974. Surf Similarity. *Proc 14th International Conference on Coastal Engineering*, 466-479.

Dally, W.R. 1990, Stochastic Modeling of Surfing climate. Proc. 22nd International Conference on Coastal Engineering, Delft, The Netherlands. ASCE New York, 516-529.

Ettinger van, E. 2005. *Artificial surf reef design.* MSc. Thesis, Faculty of Civil Engineering and Geosciences, Delft University of Technology.

Galvin, C.J. 1968. Breaker Type Classification on Three Laboratory Beaches. *Journal of Geophysical Research*, **73**(12), 3651–3659.

Henriquez M. 2004. *Artificial Surf Reefs*. MSc. Thesis, Faculty of Civil Engineering and Geosciences, Delft University of Technology.

Holthuijsen, L.H., Booij, N. Ris, R.C., Haagsma, IJ.G. Kieftenburg, A.T.M.M., Kriezi, E.E., Zijlema, M., van der Westhuyzen, A.J. 2004, SWAN user manual, SWAN cycle III version 40.31. Delft University of Technology, Faulty of Civil Engineering and Geosciences, Environmental Fluid Mechanics Section.

Hughes, S. A. 1993. Physical models and laboratory techniques in coastal engineering, advanced series on Ocean Engineering.

Hutt, J.A., Black, K.P., & Mead, S.T. 2001. Classification of Surf Breaks in Relation to Surfing Skill. *Journal of Coastal Research*, 66–81. Special Issue.

KNMI, 2006. Wind data files Meetpost Noordwijk, Ymuiden and Europlatform, www.knmi.nl.

Ministry of Transport, Public Works and Water Management 2006. Wave data files Meetpost Noordwijk, Ymuiden and Europlatform, http://www.golfklimaat.nl.

Walker, J.R. 1974. *Recreational Surf Parameters*. Tech. rept. 30. University of Hawaii, James K.K. Look Laboratory of Oceanographic Engineering.

Appendices

Contents

Appendix I
Hand calculation based on shoaling and refraction to verify results SWAN for Scheveningen

Appendix II
Procedure followed to determine the location of the break point of a wave in detail

Appendix III
Adjustment brightness for external light

Appendix IV
The script used in Matlab to estimate the location of the break point and the breaker type

Appendix V
Script used to plot smoothed lines for each plunging and intermediate wave for the peel angle along the reef. The possible length of ride is determined for which the peel angle α falls within the limits set: $30<\alpha<70$.

Appendix VI
Plots of the change of peel angle along a wave for plunging and intermediate waves of test 1 to 8.

Appendix VII
Plots of peel angles and speed of a surfer versus the distance along the reef for tests 28, 32 and 36.

Appendix I

Hand calculation based on shoaling and refraction to verify results SWAN for Scheveningen

Three runs are done in SWAN for Scheveningen and a simple calculation based on shoaling and refraction is done manually to verify the results from SWAN.

The conditions tested are:

	Input tests				Output SWAN	
	H_s (m)	T_p (s)	θ_0 (degrees Cartesian)		H_s (m)	T_p (s)
Test 1	1.1	5	55		0.91	4.98
Test 2	2.1	6.11	55		1.51	5.84
Test 3	2.3	7.22	55		1.50	6.76

It is checked whether it is deep water for these conditions which means the water depth is relatively large to the wave length: k*h > π

The water depth is around 25 meter for the measure locations and L is determined for the most unfavorable condition: the wave with period 7.22 s. This gives:

$L = g*T^2/2*\pi = 81$ m and $k = 2*\pi/L = 0.0806$ m^{-1} which gives

k*h=2.52 < π and therefore it is intermediate water for this (unfavorable) condition.

The wave height for given depth can be determined as follows:

$L_0 = g*T^2/2*\pi \quad \rightarrow$

For h/L_0 the values of K_s (shoaling coefficient) and $\tanh(kh)$ can be found.

The refraction coefficient K_r is determined with $K_r = \sqrt{(\cos\theta_0/\cos\theta)}$

The wave height then follows from: $H_x = H_0 * K_r * K_s$

The conditions in for test 1 are:

$H_s = 1.1m$

$T = 5s$

$\theta_0 = 55^\circ$

Where H_{MSL-6} is needed (dissipation is neglected):

$h/L_0 = 0.154$ which gives $K_s = 0.913$ and $\tanh(kh) = 0.824 \quad \rightarrow$

$\sin\theta = \tanh(kh)*\sin\theta_0$: and $\cos\theta = 0.738 \rightarrow$

This gives for the refraction coefficient $K_r = \sqrt{(\cos\theta_0/\cos\theta)} = 0.88 \rightarrow$

$H_{MSL-6} = H_0*K_r*K_s = 1.1*0.913*0.88 = 0.89$ m.

From the SWAN model a wave height of 0.91 m is found which means the results are comparable in magnitude.

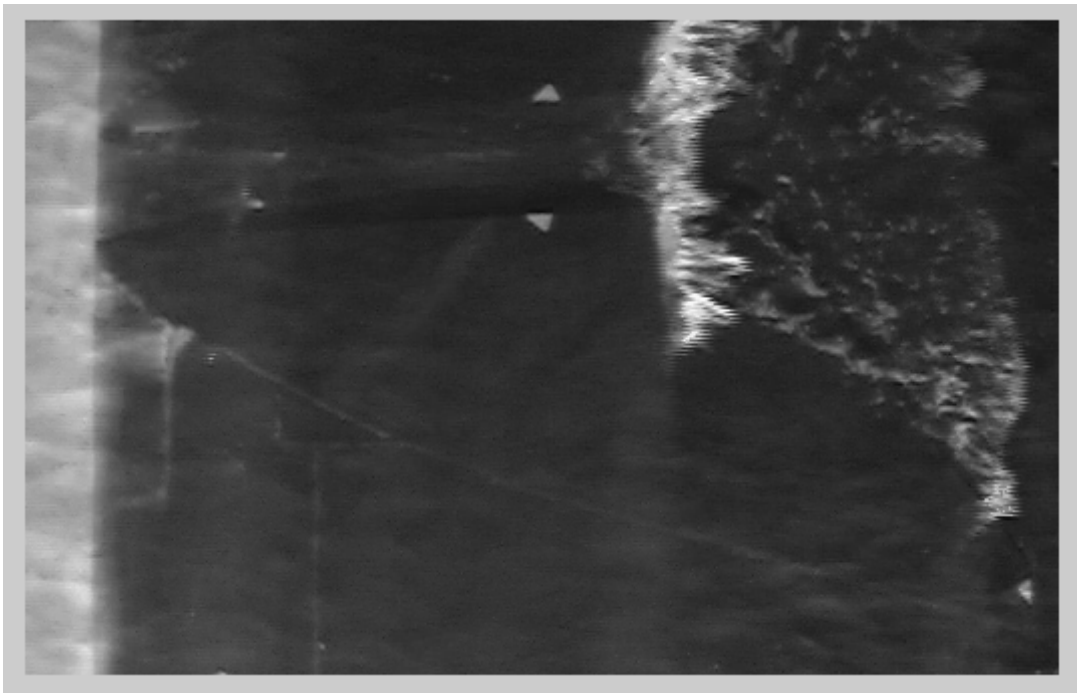
If the same is done for test 2 and 3, we get:
Test 2: hand calculation, with T_0 = 6.11 s and H_s = 2.1 m: $H_{MSL-6} = H_0 * K_s * K_r = 2.1 * 0.93 * 0.85 = 1.66$ m
Test 3: hand calculation, with T_0 = 7.11 s and H_s = 2.3 m: $H_{MSL-6} = H_0 * K_s * K_r = 2.3 * 0.95 * 0.81 = 1.76$ m

K_r becomes smaller because the wave period becomes longer. This makes the difference in wave height between run 6 and 7 at the shore two times smaller than at he boundaries: only 0.1 m where the wave heights in deep water differ 0.2 m. This gives an explanation for the difference observed between run 6 and 7, although the difference in the results of SWAN is even larger.

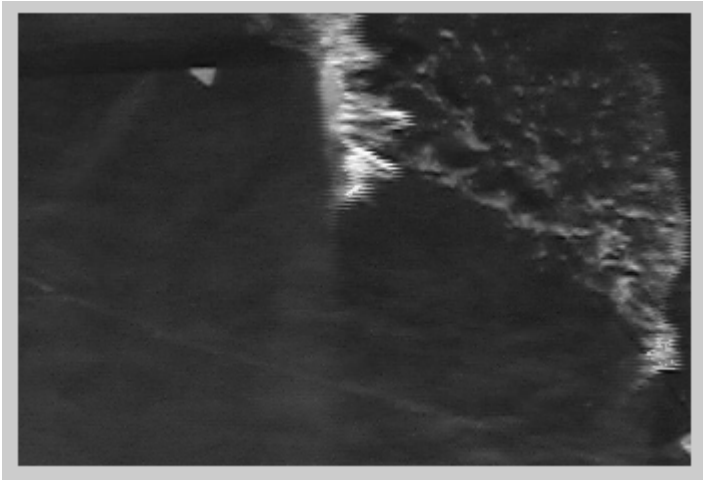
Appendix II

Procedure followed to determine the location of the break point of a wave in detail

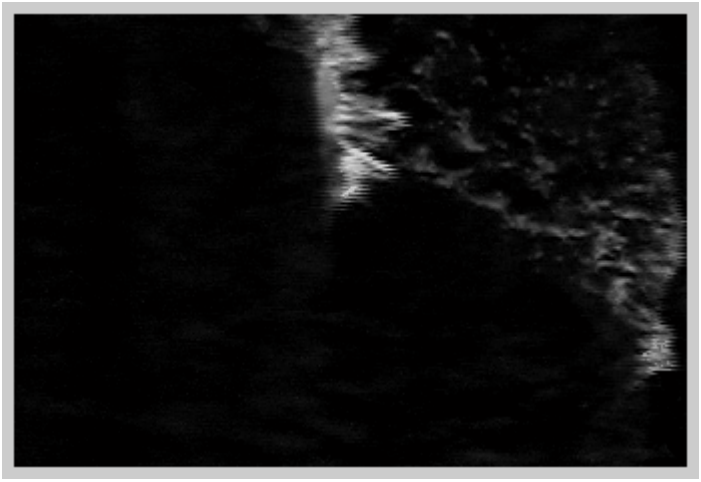
Step 1
An image is read into Matlab:



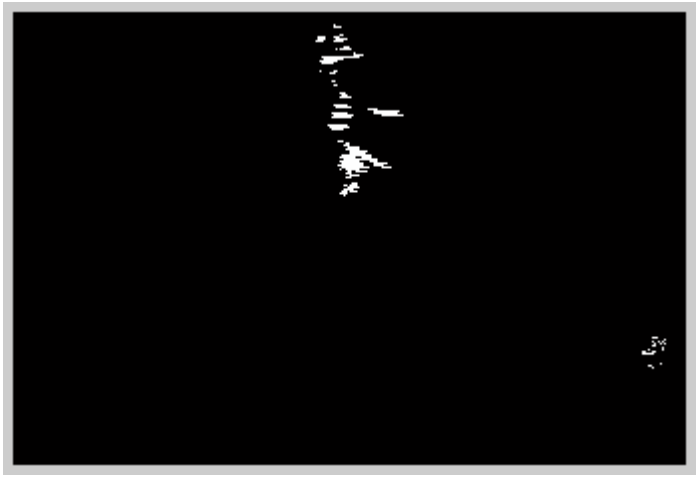
Step 2
Crop the image so only that part of the reef where the wave breaks is visible



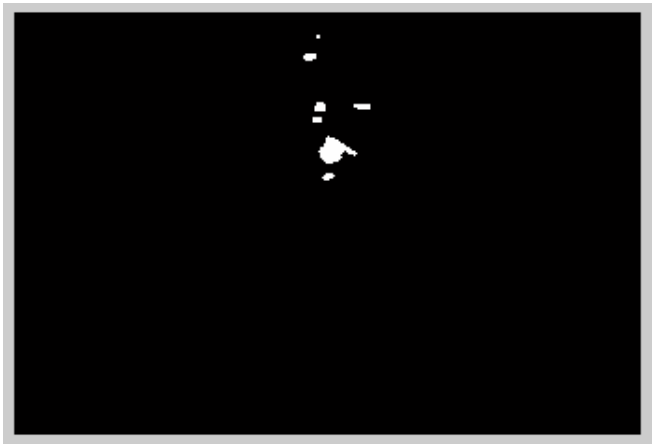
Step 3
Subtract the background picture leaving only the changing pixels in the image. Foam from the previous wave is still present in the image in the right lower corner.



Step 4
The image is turned into a binary image: instead of a grey scale image there are only white and black pixels now. The foam of the previous wave is still visible in the right lower corner of the picture. Because the wave has passed in between 1.5 to 2 seconds ago there is only a little left.



Step 5
The spatial filter is used to remove the remaining pixels of the foam of the previous wave.



The white pixels with the highest value for the x-coordinate in the remaining image correspond to the location of the break point of the wave.

Appendix III
Adjustment brightness for external light

It is determined if it is possible to adjust the brightness of images of recordings afterwards without losing the capacity to distinguish between spilling, intermediate and plunging waves. The method followed is given by:

3. Selecting an area in an image from the current recording and an image from the reference test determine the average brightness (for the whole area) fro both. The area is located in a bright part of the image because the brightest pixels have to be scaled: those also represent the foam of the wave.
4. The difference in brightness of the selected areas is used to adjust the brightness of the entire image from the current recording. This adjustment is done linearly because a factorial adjustment would alter the shape of the brightness histogram of an image. The change is therefore a simple subtracting or adding of the difference found to all pixels in the image.

The adjustment takes place just after reading the image into the workspace: after the light intensity compensation the method of determining the location of the break point and the breaker type remains the same.

The area that is selected to determine the difference in lighting intensity between the current recording and the reference will be a rectangle in the image where a small part of the (bright) concrete floor of the wave basin is visible. The dimensions of the rectangle selected in the image are 15 pixels from the tip of the reef towards the left and 100 pixels down.

To determine if the procedure is applicable, two tests are done with normal lighting and two tests with closed curtains to reduce the light coming in through the windows. These recordings will be referred to as the light and dark recordings. Tests are performed for both regular and irregular waves and recorded during 1 minute. In between each test enough time is taken to let the water level settle and currents die out.

For each test the mean and the highest value of the foam brightness of all waves in the test is determined and these values are used to compare the results. The reason the mean and maximum of the foam brightness of all waves are used to compare the results is that the mean gives an impression on the correctness of the entire series while

the highest values are the values used to make the distinction between spilling and plunging waves.

The results for the dark, light and adjusted light recording are shown in Table 20 for regular waves and in Table 21 for irregular waves.

Table 20: results for regular wave tests with different lighting

	Regular Waves					
	Dark recording	Light recording		Adjusted light recording		Lighting difference
Brightness		Test 1	Test 2	Test 1	Test 2	
Mean	134	243	241	139	147	86.9
Highest	141	251	248	145	155	87.5

Table 21: results for irregular wave tests with different lighting

	Irregular Waves					
	Dark recording	Light recording		Adjusted light recording		Lighting difference
Brightness		Test 1	Test 2	Test 1	Test 2	
Mean	143	183	181	151	150	74.5
Highest	188	244	255	181	179	80.4

It is clear that the results are much better after the adjustment than before. The values found do not match perfectly but for detecting the intermediate and plunging waves it is good enough. In this context two things have to be noted:

- First of all these tests were done at extreme conditions: the dark recording was done with all curtains closed in the laboratory where in reality it does not get that dark with the curtains open ever during the day.
- Two tests were done of with the curtain closed with regular and irregular waves. In the tables above the result of only one test is shown because that is the test the light recordings were scaled to. When the results of two dark recordings are compared to each other it shows that there is some distribution in the results for two tests with the same conditions: this means a test can not be reproduced completely (see Table 22 below).

Table 22: differences in results of similar tests

	Dark recordings			
	Regular		Irregular	
Brightness	Test 1	Test 2	Test 1	Test 2
Mean	134	140	143	152
Highest	141	146	188	186

From the results in Table 20 and Table 21 it is concluded that this procedure should be carried out for all images of all experiments. The resulting script used in Matlab for the analysis of the video data can be found in Appendix II. The background image used to remove the non-changing pixels from each image (see paragraph 4.2.1) is also used to determine the difference in external lighting.

Appendix IV
The script used in Matlab to estimate the location of the break point and the breaker type

```
%============================================================
% Procedure that determines the location of he break point of a wave in an
% image made by filming the wave from above.
% The second feature determines the intensity of the foam of each wave
% through which a distinction can be made between spilling waves and
% (semi-) plunging waves. Nov 2005 - Apr 2006 Rutger Over
%============================================================
```

% the variables below are used in determining the location of the break point

```
Ibackground = imread('achtergrond.bmp'); % background picture used to subtract background from current picture
reference_current_series = imread('reference_current_series.bmp'); % image from current series to compare light intensity to the reference pic
reference_pic = imread('reference_pic.bmp'); % reference pic used to compare light intensity to

str2 = 'test1_'; % Strings are used to compose filenames
str3 = '.bmp';
str4 = '0';
begin = 1; % index number of first image
last = 12002; % index number of last image
delta = 1; % can be used to skip images (not used at the moment)
Xvar = 90; % number of pixels around the break point where is looked for high intensity pixels in x direction
Yvar = 60; % number of pixels around the break point where is looked for high intensity pixels in y direction
Xmin = 195;
Ymin = 95;
Width = 305;
Height = 200;
Width2 = 150;
Height2 = 110;
Rect = [Xmin Ymin Width Height]; % rectangle used for cropping the image
Rect2 = [0 0 Width2 Height2];% area used to crop a smaller area within the first crop
Rect3 =[18 109 15 100]; % area selected in the reference_current_series image to compare to same area in the reference_pic image
numb_pix = 50; % number of pixels selected around the break point to determine the breaker type
M = 5; % value for MEDFILT2 function; a spatial filter
endtime = (last-begin)/5;
```

```
teller2 = 0; % index of all pictures: it is shown in matlab during calculation to estimate the remaining calculation time

% the variables below are used in determining the intensity of the foam of every wave

Xborder_reef = 280; % beyond this x coordinate there is no reef
teller6 = 0;
teller7 = 0;
Int_aver = 0; % holds the foam intensity for every image
Vsurf_tot = 0;
Dist_surf_tot = 0; % holds the distance travelled by the surfer/break point between two images
aver_serie(begin:last) = NaN; % holds the average foam intensity for every wave (more than 3 pictures)
Vsurf(begin:last) = NaN; % holds the speed of the surfer/break point for every image
Vsurf_serie(begin:last) = NaN; % holds the speed of the surfer/break point for every wave
Dist_serie(begin:last) = NaN; % holds the distance travelled of the surfer/break point for every image
peel_angle(begin:last) = NaN; % holds the peel angle for every image
dist_pic(1:eind)=NaN; % holds the distance traveled between two images
teller8=0; % is used to count the number of images for a certain wave
aantal_images(1:eind)=NaN; % holds the number of images there are for every wave

% now the difference in lighting intensity is determined: the difference between the current series of images
% and the reference series on which this script was built

I_ref_current = imcrop(reference_current_series, Rect3);
I_ref_reference = imcrop(reference_pic, [13 109 15 100]);
Mean_reference = mean(mean(I_ref_reference));
Mean_reference_current_series = mean(mean(I_ref_reference_current_series));
diff = Mean_reference_current_series - Mean_reference

% the filename is constructed and read into the workspace
for teller = begin:delta:last
   tijd = [0:0.2:endtime];
   teller2 = teller2+1;
   str1 = num2str(teller);
   if teller < 10
      fname = [str2,str4,str4,str4,str4,str1,str3];
   elseif teller < 100
      fname = [str2,str4,str4,str4,str1,str3];
   elseif teller <1000
      fname = [str2,str4,str4,str1,str3];
```

```
   elseif teller <10000
      fname = [str2,str4,str1,str3];
   else
      fname = [str2,str1,str3];
   end

   I = imread(fname);
% the image is compensated for the difference in lighting with the reference series
         I=double(I);
         I=I-diff;
         I=uint8(I);
   I2 = imcrop(I,Rect);
   Ibackgroundcrop = imcrop(Ibackground,Rect);
% the background is subtracted from the current image
   I2 = imsubtract(I2,Ibackgroundcrop);
% the image is converted into a binary image using the optimal level as it was
determined
   level = graythresh(I2)+0.21;
   I3 = im2bw(I2,level);
% the spatial filter is applied and the image rotated
   I4 = medfilt2(I3,[M M]);
   I5 = rot90(I4,-1);
% now the actual location of the break point is looked for
   if  find(I5>0)
      Points = find(I5>0);
      siz = size(I5);
      ind = Points(1);
      [x,y] = ind2sub(siz,ind);

      Xbreak = Ymin+Height-y; % x-coordinate of the break point in the original
uncropped image
      Ybreak = Xmin+x; % y-coordinate of the break point in the original uncropped
image
   else Xbreak = NaN;
       Ybreak = NaN;
   end
   Xplot(:,teller2)=Xbreak;
   Yplot(:,teller2)=Ybreak;

% now the intensity of the foam is determined for a pre-selected area
   if Xbreak>0
      Xbegin = Xbreak-Xvar;
      Xlast = Xbreak + 10;
      if Xbegin<90
         Xbegin=90;
      end
```

```
      Ybegin = Ybreak-(Yvar/2);
      Ylast = Ybreak+(Yvar/2);
      if Ylast>512
      Ylast=512;
      end
      int=0;
      teller3=0;
      for Ycoor = Ybegin:1:Ylast
         for Xcoor = Xbegin:1:Xlast
            teller3 = teller3+1;
            Intmax(:,teller3) = I(Xcoor,Ycoor);
            Intmax=double(Intmax);
         end
      end
% the 50 (=numb_pix) highest intensity pixels are looked for
      Intmax = sort(-Intmax);
      Intmax = Intmax * -1;
      Int_aver = 0;
      for n = 1:1:numb_pix
         Int_aver = Int_aver + Intmax(n);
      end
      Int_aver = Int_aver/numb_pix;
   else
      Int_aver = NaN;
   end
```

% the same procedure for that part of the reef where waves start breaking: if a wave with high % brightness starts breaking in the same image it would not be noted. However, if % the brightness is higher than the brightness of the wave that almost leaves the
% reef, the new wave is taken into account, replacing the first break point found

```
   if Ybreak>400 & Xbreak>250
         I7 = imcrop(I3,Rect2);
         I8 = medfilt2(I7,[M M]);
         if  find(I8>0)
            I9 = rot90(I8,-1);
            Points = find(I9>0);
            siz = size(I7);
            ind = Points(1);
            [x,y] = ind2sub(siz,ind);
            Xbreak2 = Ymin+Height2-y;
            Ybreak2 = Xmin+x;
            Xbegin = Xbreak2-Xvar;
            if Xbegin<90
               Xbegin=90;
```

```
            end
            Ybegin = Ybreak2-(Yvar/2);
            Ylast = Ybreak2+(Yvar/2);
            teller3 = 0;
            for Ycoor = Ybegin:1:Ylast
                  for Xcoor = Xbegin:1:Xbreak2
                     teller3 = teller3+1;
                     Intmax(:,teller3) = I(Xcoor,Ycoor);
                     Intmax=double(Intmax);
                  end
            end
            Intmax = sort(-Intmax);
            Intmax = Intmax * -1;
            Int_aver = 0;
            for n = 1:1:numb_pix
               Int_aver = Int_aver + Intmax(n);
            end
            Int_aver = Int_aver/numb_pix;
         else Int_aver2 = NaN;
             Xbreak2 = NaN;
             Ybreak2 = NaN;
         end
   else Int_aver2 = NaN;
       Xbreak2 = NaN;
       Ybreak2 = NaN;
   end
   Xplot2(:,teller2)=Xbreak2;
   Yplot2(:,teller2)=Ybreak2;
   if Int_aver2 > Int_aver
      Int_aver = Int_aver2; % this to make sure the beginning of an high intensity wave is
always captured
      Xplot=Xplot2;
      Yplot=Yplot2;
   end
Intplot(:,teller2)=Int_aver;
teller2
end
```

% From here the foam brightness of an entire wave is determined, as well as the
% speed, distance travelled by the surfer and the peel angle.

```
for teller4 = begin+3:1:eind-3
   if ~isnan(Xplot(teller4))
      if Xplot(teller4) < Xgrens_% what happens beyond this point is of no interest
         if Xplot(teller4) >= Xplot(teller4-1)
```

```
            teller6 = teller6 + 1;
            teller8 = teller8 + 1;
            Int_gem = Int_gem + Intplot(teller4);
            dx = Xplot(teller4) - Xplot(teller4-1);
            dy = Yplot(teller4) - Yplot(teller4-1);
% determination of the distance travelled by the surfer, the peel angle and the speed
developed
            dist_surf = sqrt(dx^2 + dy^2)*0.168;
            dist_pic(teller4)=dist_surf;
            peel_angle(teller4) = atan(dy/dx)*180/pi;
            if peel_angle(teller4) < 0
               peel_angle(teller4) = NaN;
            end
            Dist_surf_tot = Dist_surf_tot + dist_surf;
            Vsurf(teller4) = (dist_surf/0.2)/sqrt(15);
% this is in pixels/second: later the conversion into m/s prototype is done
            if Vsurf(teller4) < 1.25 * Vsurf(teller4-1) & Vsurf(teller4) > 0.8 *
Vsurf(teller4-1)
               Vsurf_tot = Vsurf_tot + Vsurf(teller4);
               teller7 = teller7 + 1;
            end
% the same is done for two image back: there is a small chance the break point in the
previous image was not detected
         elseif isnan(Xplot(teller4-1))
            if Xplot(teller4) >= Xplot(teller4-2)
               teller6 = teller6 + 1;
               teller8 = teller8 + 2;
               Intgem = Intgem + Intplot(teller4);
               dx = Xplot(teller4) - Xplot(teller4-2);
               dy = Yplot(teller4) - Yplot(teller4-2);
               dist_surf = sqrt(dx^2 + dy^2)*0.168;
               dist_pic(teller4)=dist_surf;
               peel_angle(teller4) = atan(dy/dx)*180/pi;
               if peel_angle(teller4) < 0
                  peel_angle(teller4) = NaN;
               end
               Dist_surf_tot = Dist_surf_tot + dist_surf;
               Vsurf(teller4) = (dist_surf/0.4)/sqrt(15);
               if Vsurf(teller4) < 1.25 * Vsurf(teller4-2) & Vsurf(teller4) > 0.8 *
Vsurf(teller4-2)
                  Vsurf_tot = Vsurf_tot + Vsurf(teller4);
                  teller7 = teller7 + 1;
               end
% the same is done for three images back: there is a small chance the break point in the
two previous images was not detected
            elseif isnan(Xplot(teller4-2))
```

```
            if Xplot(teller4) >= Xplot(teller4-3)
               teller6 = teller6 + 1;
               teller8 = teller8 + 3;
               Int_gem = Int_gem + Intplot(teller4);
               % snelheids bepaling surfer
               dx = Xplot(teller4) - Xplot(teller4-3);
               dy = Yplot(teller4) - Yplot(teller4-3);
               dist_surf = sqrt(dx^2 + dy^2)*0.168;
               dist_pic(teller4) = dist_surf;
               peel_angle(teller4) = atan(dy/dx)*180/pi;
               if peel_angle(teller4) < 0
                  peel_angle(teller4) = NaN;
               end
               Dist_surf_tot = Dist_surf_tot + dist_surf;
               Vsurf(teller4) = (dist_surf/0.6)/sqrt(15);
               if Vsurf(teller4) < 1.25 * Vsurf(teller4-3)
                  if Vsurf(teller4) > 0.8 * Vsurf(teller4-3)
                     Vsurf_tot = Vsurf_tot + Vsurf(teller4);
                     teller7 = teller7 + 1;
                  end
               end
            end
         end

% this part is to detect the first image in a new series of images of a wave
      elseif Xplot(teller4) <= Xplot(teller4+1)
         teller6 = teller6 + 1;
         Int_gem = Int_gem + Intplot(teller4);
      elseif isnan(Xplot(teller4+1))
         if Xplot(teller4) <= Xplot(teller4+2)
            teller6 = teller6 + 1;
            Int_gem = Int_gem + Intplot(teller4);
         elseif isnan(Xplot(teller4+2))
            if Xplot(teller4) <= Xplot(teller4+3)
               teller6 = teller6 + 1;
                                          Int_gem = Int_gem + Intplot(teller4);
            end
         end
      end

% every time it is checked if the current image was the last of this wave: this is done
by comparing x coordinates of the break points
      if Xplot(teller4)>=Xplot(teller4+1) |
      isnan(Xplot(teller4+1))&Xplot(teller4)>=Xplot(teller4+2) |
      isnan(Xplot(teller4+1))&isnan(Xplot(teller4+2))&Xplot(teller4)>=Xplot(teller4+
      3) | isnan(Xplot(teller4+1))&isnan(Xplot(teller4+2))&isnan(Xplot(teller4+3))
```

```
            if teller6 > 3
               gem_serie(teller4) = Int_gem/teller6;
               Vsurf_serie(teller4) = Vsurf_tot/teller7;
               Dist_serie(teller4) = Dist_surf_tot;
               aantal_images(teller4)=teller8;
               Vsurf_tot = 0;
               Dist_surf_tot = 0;
               teller6 = 0;
               teller7 = 0;
               teller8 = 0;
               Int_gem = 0;
            else
               teller6 = 0;
               teller7 = 0;
               teller8 = 0;
               Vsurf_tot = 0;
               Dist_surf_tot = 0;
               Int_gem = 0;
            end
         end

% the following applies to images where the break point was located outside the
boundaries
      else
         if teller6 > 3
            gem_serie(teller4) = Int_gem / teller6;
            Vsurf_serie(teller4) = Vsurf_tot/teller7;
            Dist_serie(teller4) = Dist_surf_tot;
            aantal_images(teller4)=teller8;
            teller7 = 0;
            Vsurf_tot = 0;
            Dist_surf_tot = 0;
            teller6 = 0;
            Int_gem = 0;
            teller8 = 0;
         else
            teller6 = 0;
            teller7 = 0;
            teller8 = 0;
            Dist_surf_tot = 0;
            Vsurf_tot = 0;
            Int_gem = 0;
         end
       end
   end
end
```

Appendix V

Script used to plot smoothed lines for each plunging and intermediate wave for the peel angle along the reef. The possible length of ride is determined for which the peel angle α falls within the limits set: $30<\alpha<70$.

```
Xbeginpunt=95;  % the x coordinate of the upper right corner of the dropped image in
the uncropped image: fill in for every test
Ybeginpunt=250;  % the y coordinate of the upper right corner of the dropped image in
the uncropped image: fill in for every test
str2='test 1'; % name of the test
plung=1; % plung=1 means plunging waves are looked at, plung=0 means intermediates
max_peelangle=70;
min_peelangle=30;

if plung==1
   index=find(gem_serie>200);
   str1='plunging waves in ';
elseif plung==0
   index=find(180<gem_serie&gem_serie<200);
   str1='interm. waves in ';
end
laatste=length(index);
teller4=0;
teller6=0;

for teller=1:1:laatste
   nummer=index(teller);
   teller5=0;
   teller2=0;
   teller3=0;
   for teller3=nummer-aantal_images(nummer):1:nummer
      if ~isnan(peel_angle(teller3))
         teller2=teller2+1;
         teller5=teller5+1;
         OPSLAG(teller2,1,teller)=Xplot(teller3);
         OPSLAG(teller2,2,teller)=Yplot(teller3);
         OPSLAG(teller2,3,teller)=dist_pic(teller3);
         OPSLAG(teller2,4,teller)=peel_angle(teller3);
         OPSLAG(teller2,5,teller)=Vsurf(teller3);
         OPSLAG(1,6,teller)=teller5;
      end
   end
end

for teller4=1:1:laatste
```

```
   distan=0.168*sqrt(((OPSLAG(1,1,teller4)-Xbeginpunt)^2)+((OPSLAG(1,2,teller4)-
Ybeginpunt)^2));
   for teller3=1:1:OPSLAG(1,6,teller4)
      distan=distan+OPSLAG(teller3,3,teller4);
      peelangle(teller3)=OPSLAG(teller3,4,teller4);
      vsurf(teller3)=OPSLAG(teller3,5,teller4);
      distanc(teller3)=distan;
   end
   afstand(teller4)=distanc(end)-distanc(1);
```

% here the values for the peel angle are smoothed, and the length is determined that the peel angle falls in between the limits set

```
   peel_smooth=smooth(distanc,peelangle,'loess',4);
   distanci=[distanc(1):step:distanc(end)];
   peeli=interp1(distanc,peel_smooth,distanci,'linear');
   s_interval=(distan(end)-distanc(1))/length(distanci);

   drempel_1=find(peeli<min_peelangle);
         if isempty(drempel_1)
            bovengrens=distanci(end);
         else
             bovengrens=distanci(1)+((drempel_1(1))*s_interval);
         end

   drempel_2=find(peeli>max_peelangle);
         if isempty(drempel_2)
            ondergrens=distanci(1);
         else
            ondergrens=distanci(1)+((drempel_2(end))*s_interval);
         end

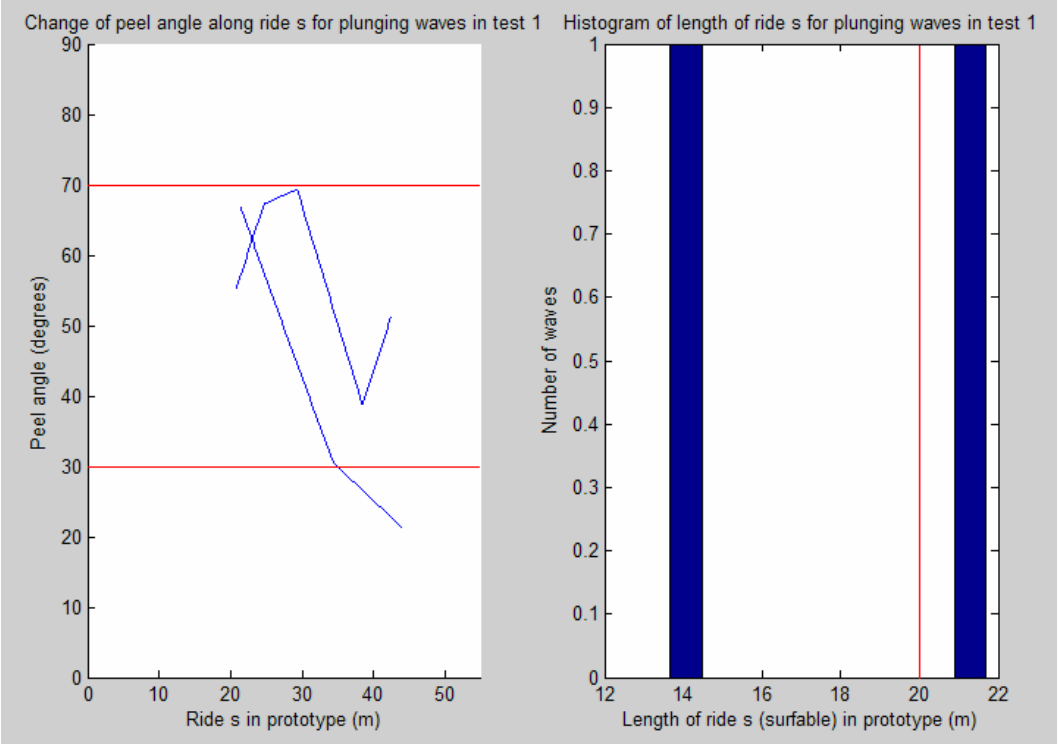
   clear drempel_1, clear drempel_2;
         y1=[min_peelangle min_peelangle];
         y2=[max_peelangle max_peelangle];
         xmax=55;
         xas=[0 xmax];
   subplot(121)
   hold on
   plot(distanci,peeli,'-',xas,y1,'r-',xas,y2,'r-');
   axis([0 xmax 0 90]);
   xlabel('Ride s in prototype (m)'), ylabel('Peel angle (degrees)'),title(['Change of peel
angle along ride s for ',str1,str2]);

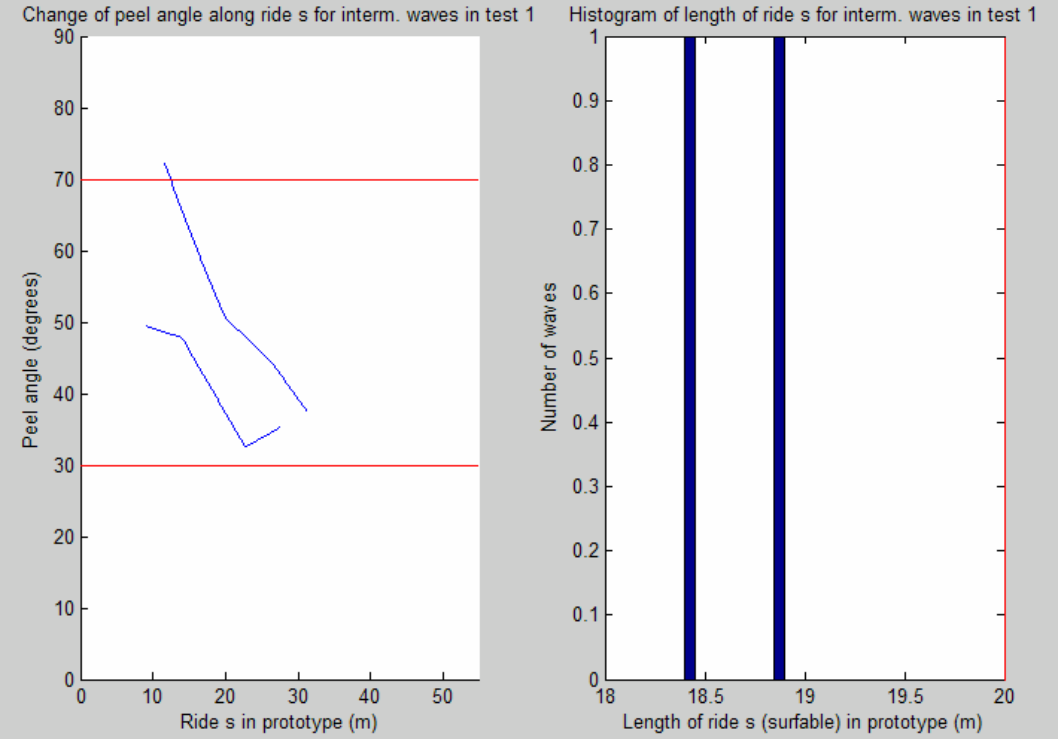
   s(teller4)=bovengrens-ondergrens;
```

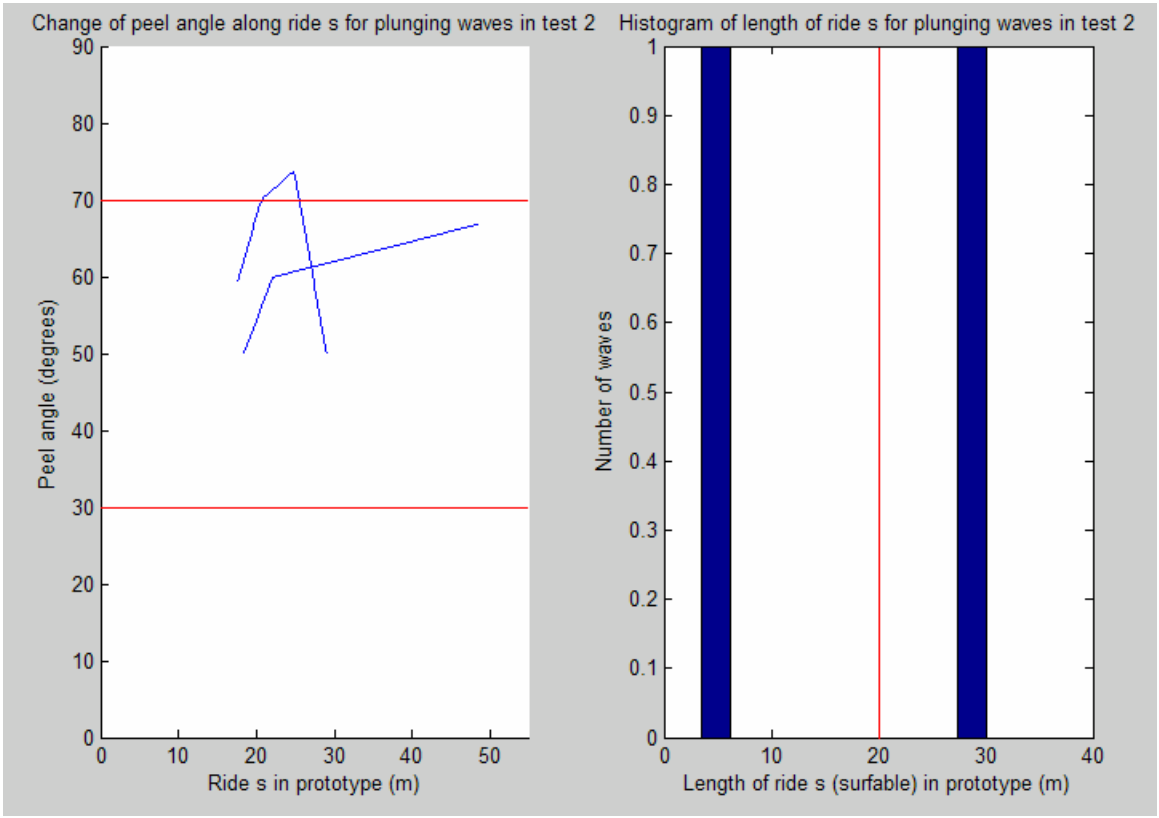
```
    clear drempel_1, clear drempel_2, clear distanc, clear peelangle, clear vsurf;
end
max_s=-sort(-(hist(s)));
ymax=max_s(1);
yas=[0 ymax];
x=[20 20];
subplot(122),hist(s),hold,plot(x,yas,'r-')
xlabel('Length of ride s (surfable) in prototype (m)'),ylabel('Number of waves');
title(['Histogram of length of ride s for ',str1,str2]);
number_of_surfable_waves=length(find(s>=20))
```

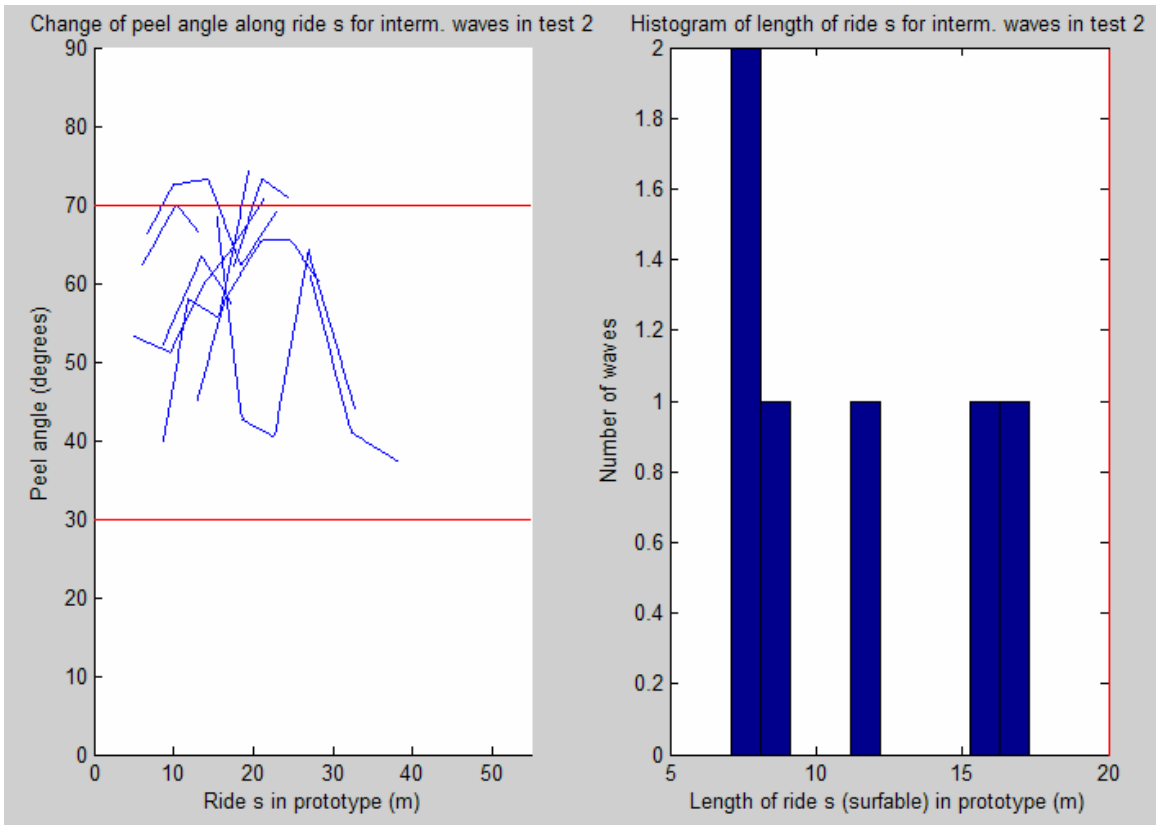
Appendix VI

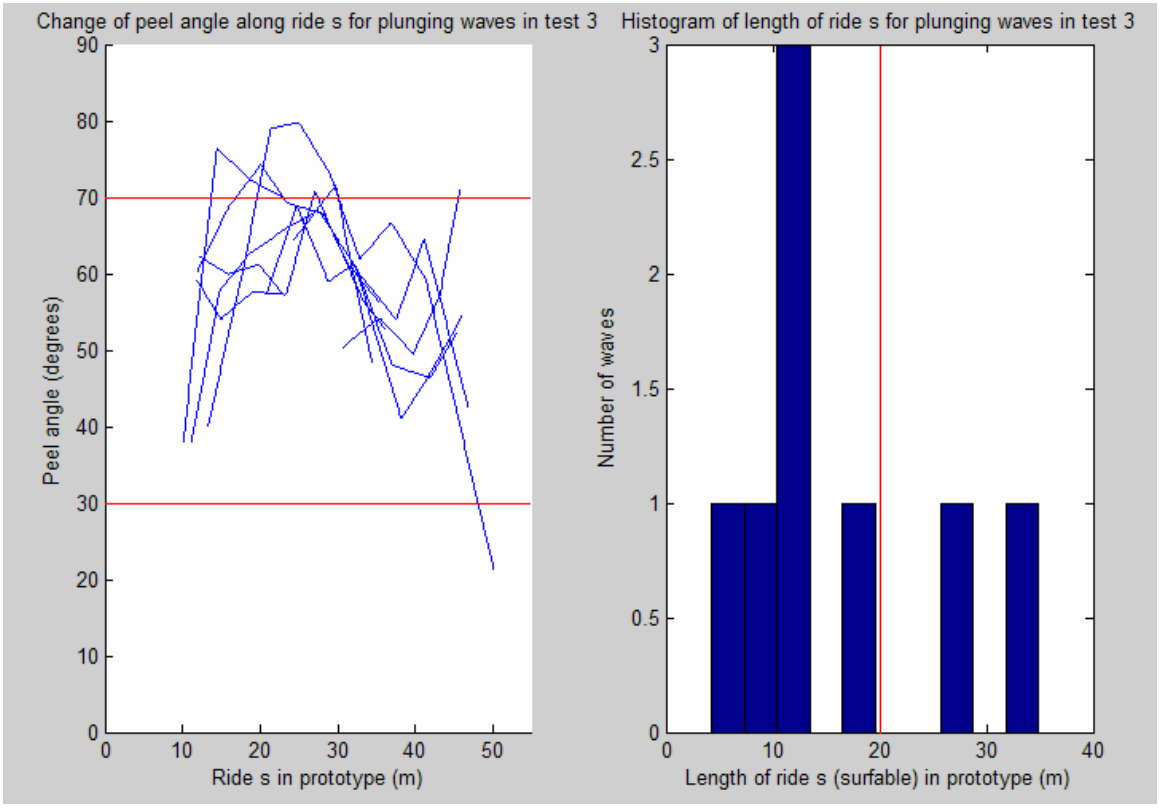
Plots of the change of peel angle along a wave for plunging and intermediate waves of test 1 to 8. See name above each figure for the scenario and the type of waves involved.

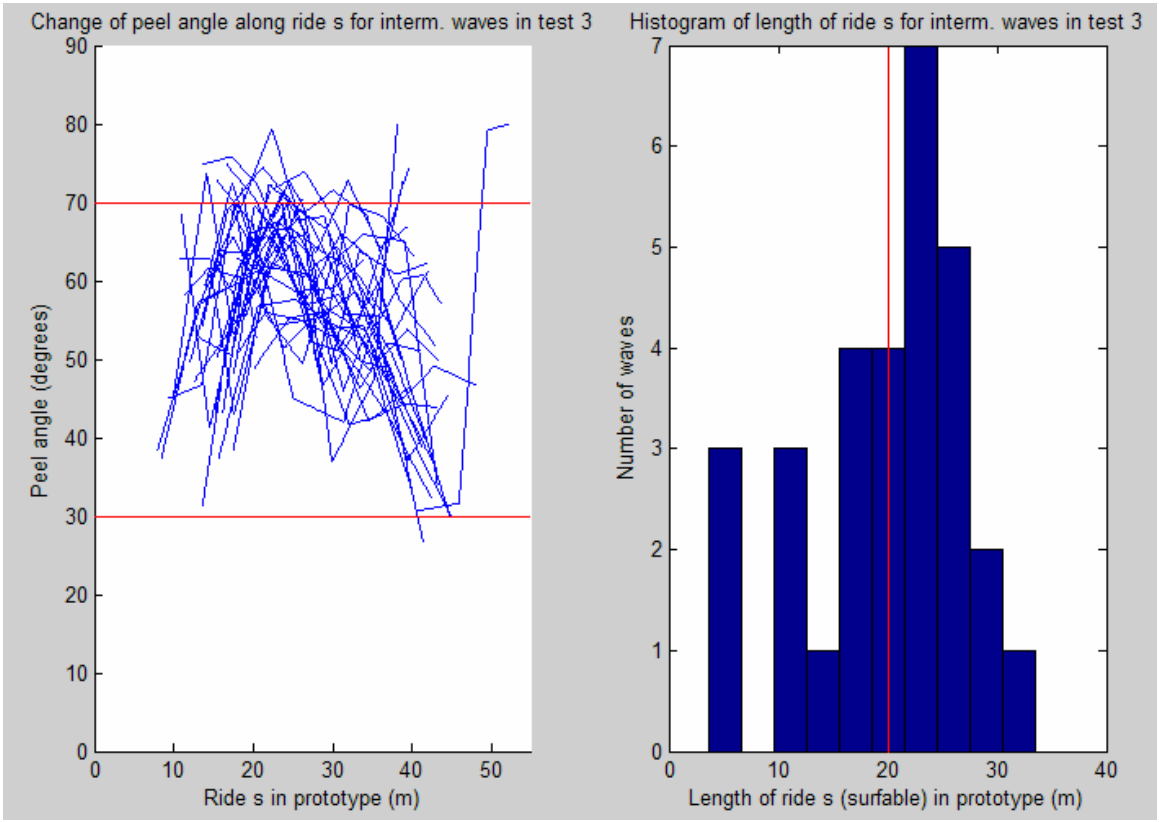


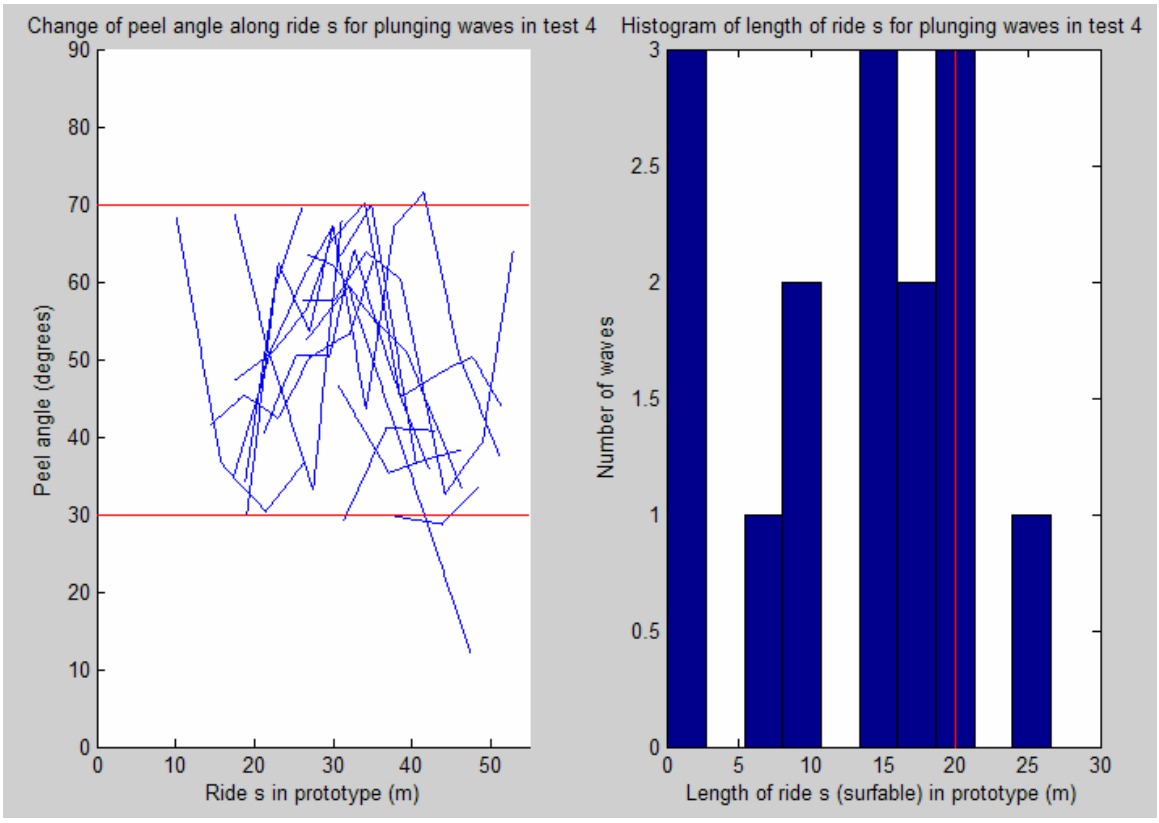


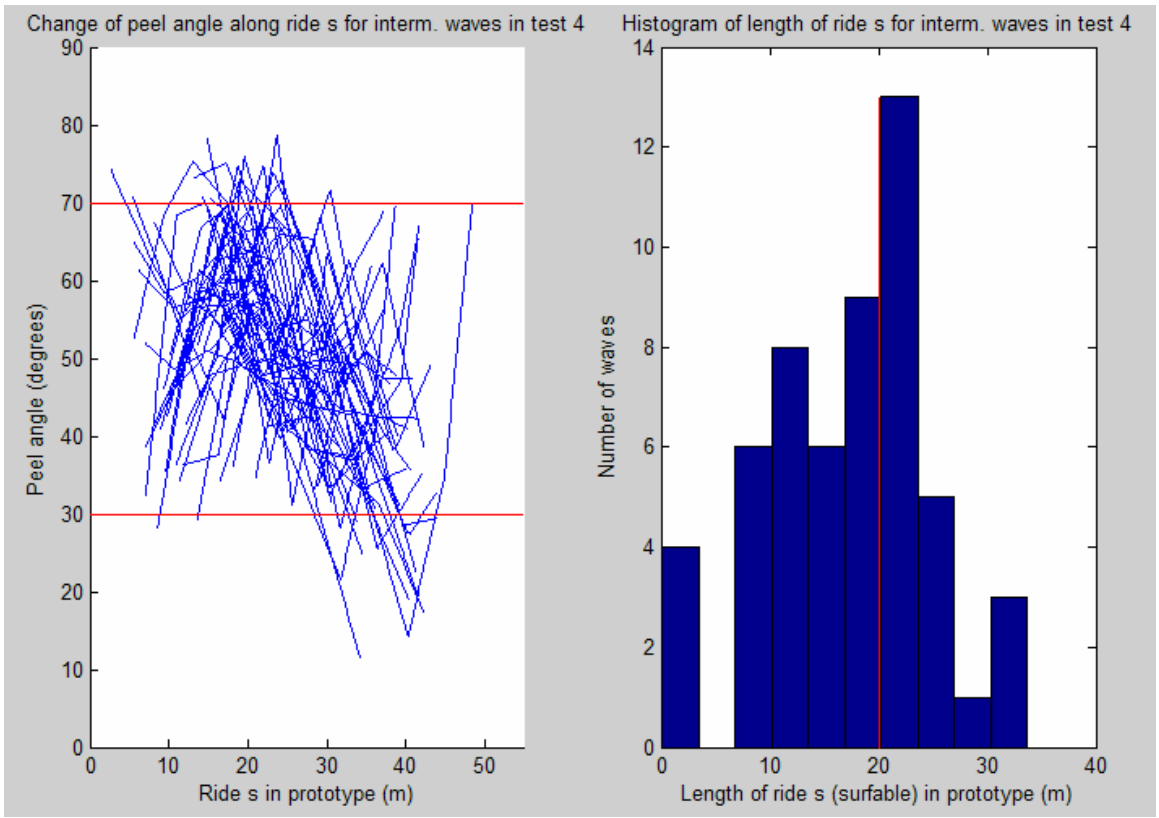

Change of peel angle along ride s for plunging waves in test 2
Peel angle (degrees)
Ride s in prototype (m)
Histogram of length of ride s for plunging waves in test 2
Number of waves
Length of ride s (surfable) in prototype (m)

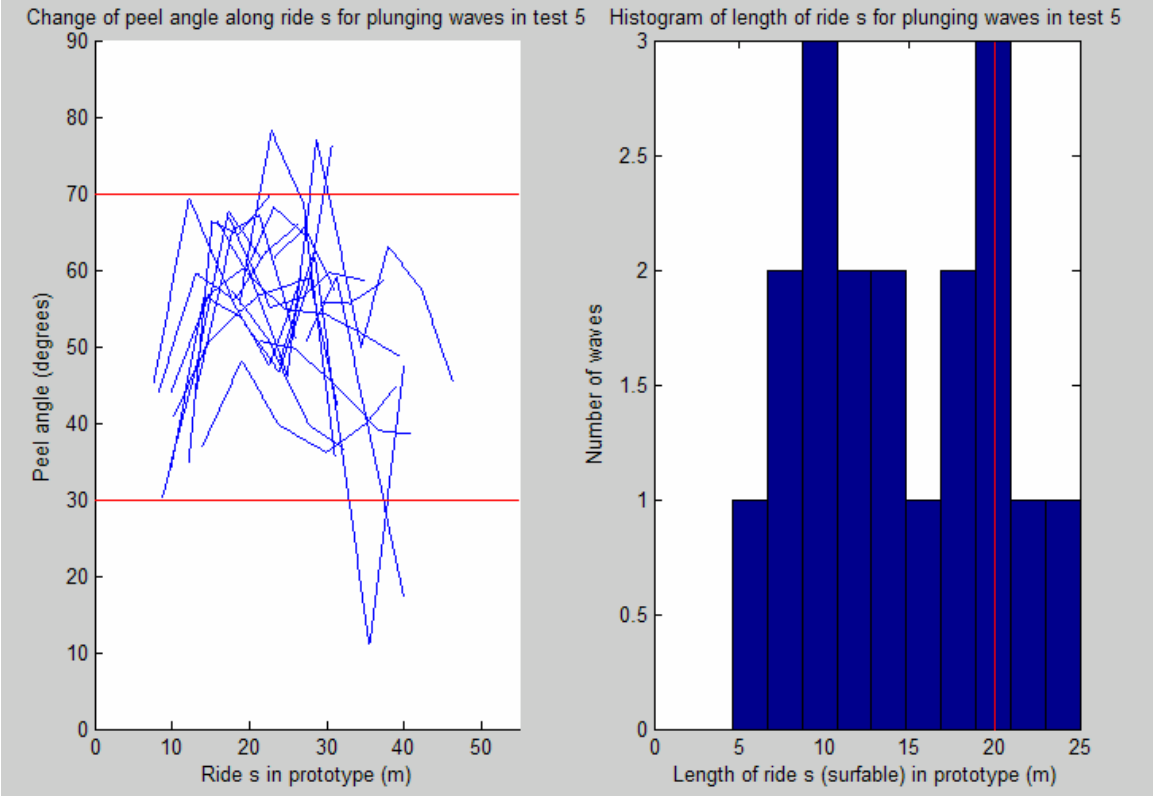

Change of peel angle along ride s for interm. waves in test 2
Peel angle (degrees)
Ride s in prototype (m)
Histogram of length of ride s for interm. waves in test 2
Number of waves
Length of ride s (surfable) in prototype (m)

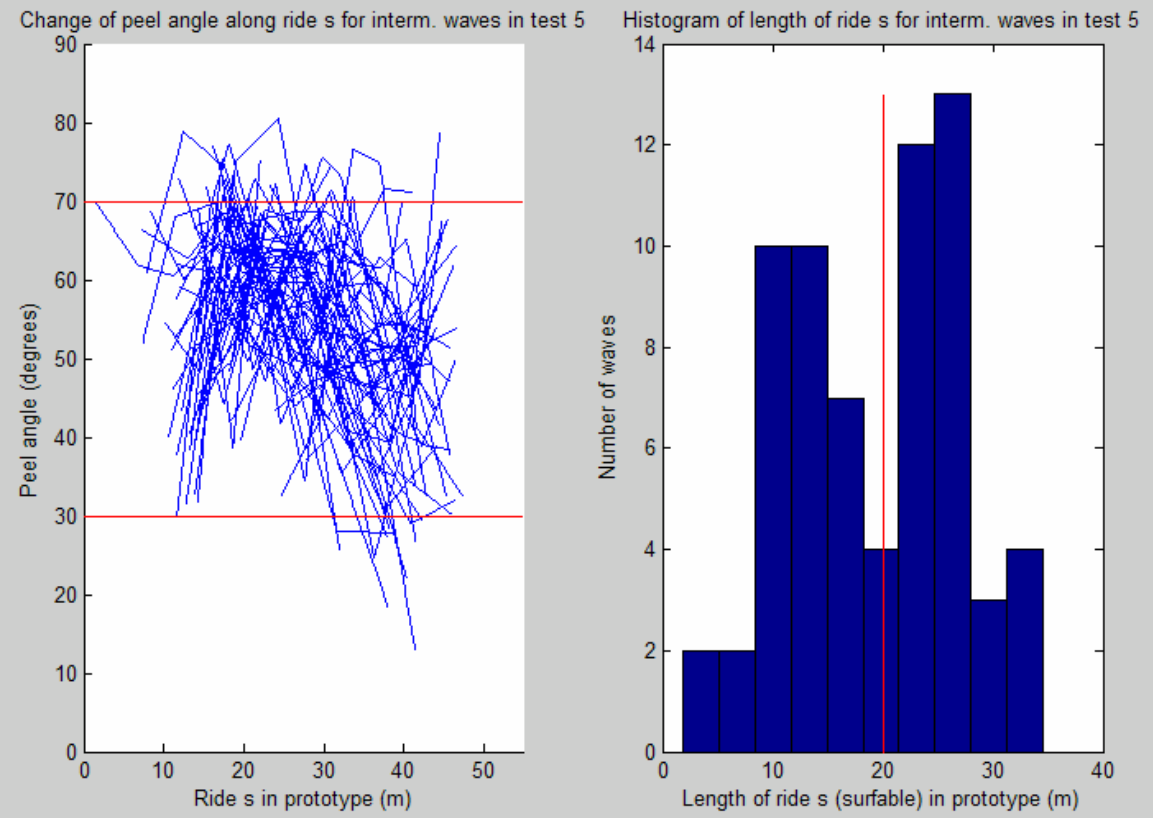

Change of peel angle along ride s for plunging waves in test 3
Peel angle (degrees)
Ride s in prototype (m)
Histogram of length of ride s for plunging waves in test 3
Number of waves
Length of ride s (surfable) in prototype (m)

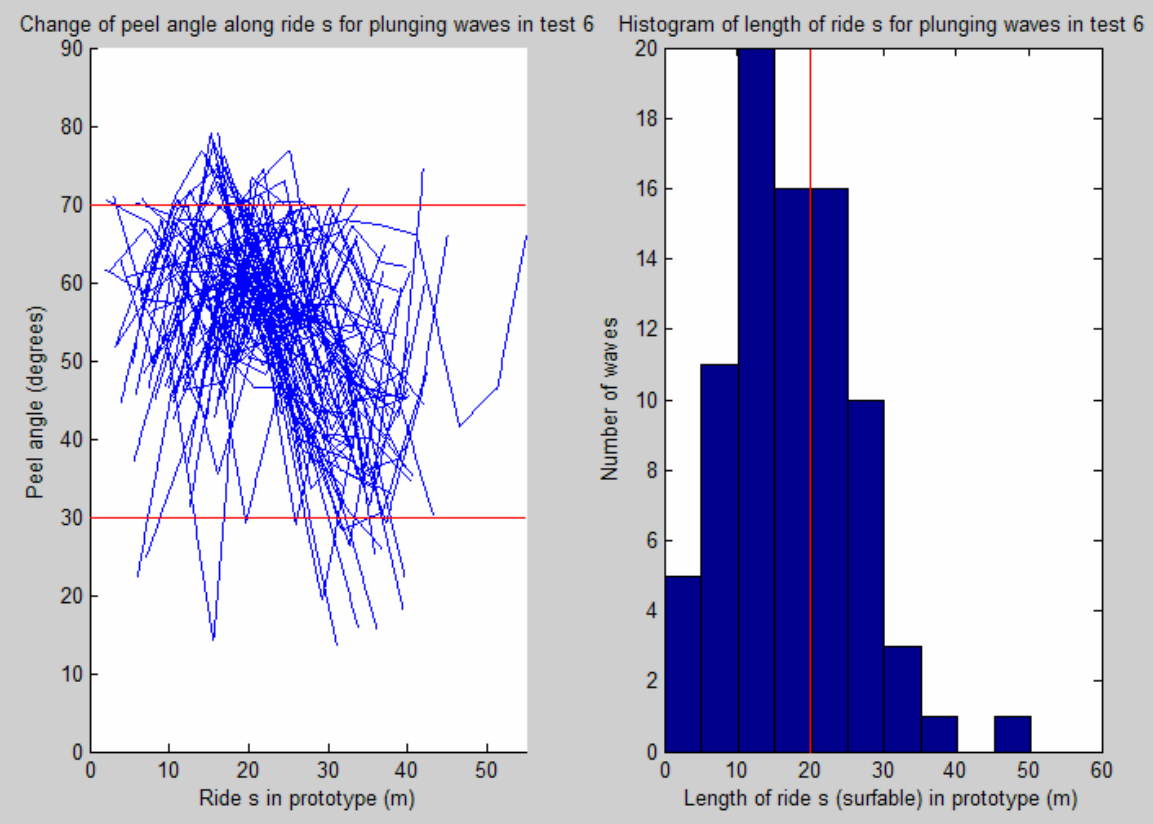

Change of peel angle along ride s for interm. waves in test 3
Peel angle (degrees)
Ride s in prototype (m)
Histogram of length of ride s for interm. waves in test 3
Number of waves
Length of ride s (surfable) in prototype (m)

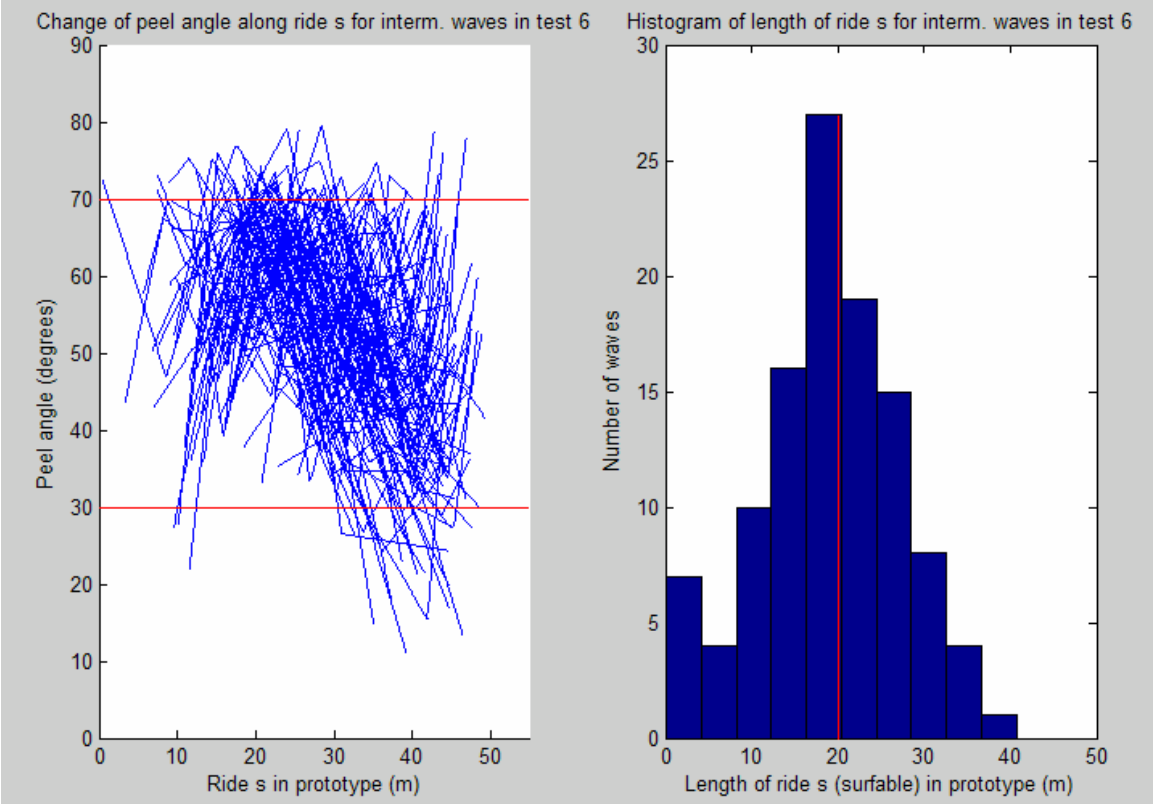

Change of peel angle along ride s for plunging waves in test 4
Peel angle (degrees)
Ride s in prototype (m)
Histogram of length of ride s for plunging waves in test 4
Number of waves
Length of ride s (surfable) in prototype (m)

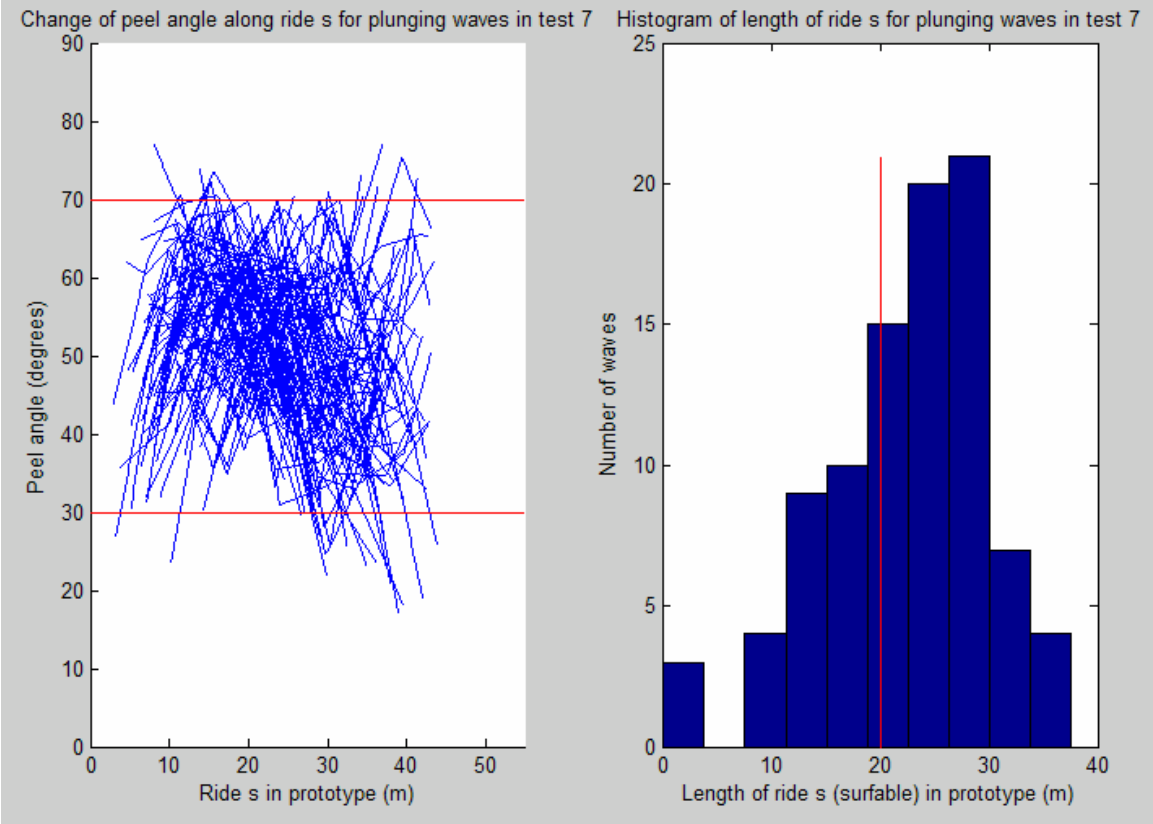

Change of peel angle along ride s for interm. waves in test 4
Peel angle (degrees)
Ride s in prototype (m)
Histogram of length of ride s for interm. waves in test 4
Number of waves
Length of ride s (surfable) in prototype (m)

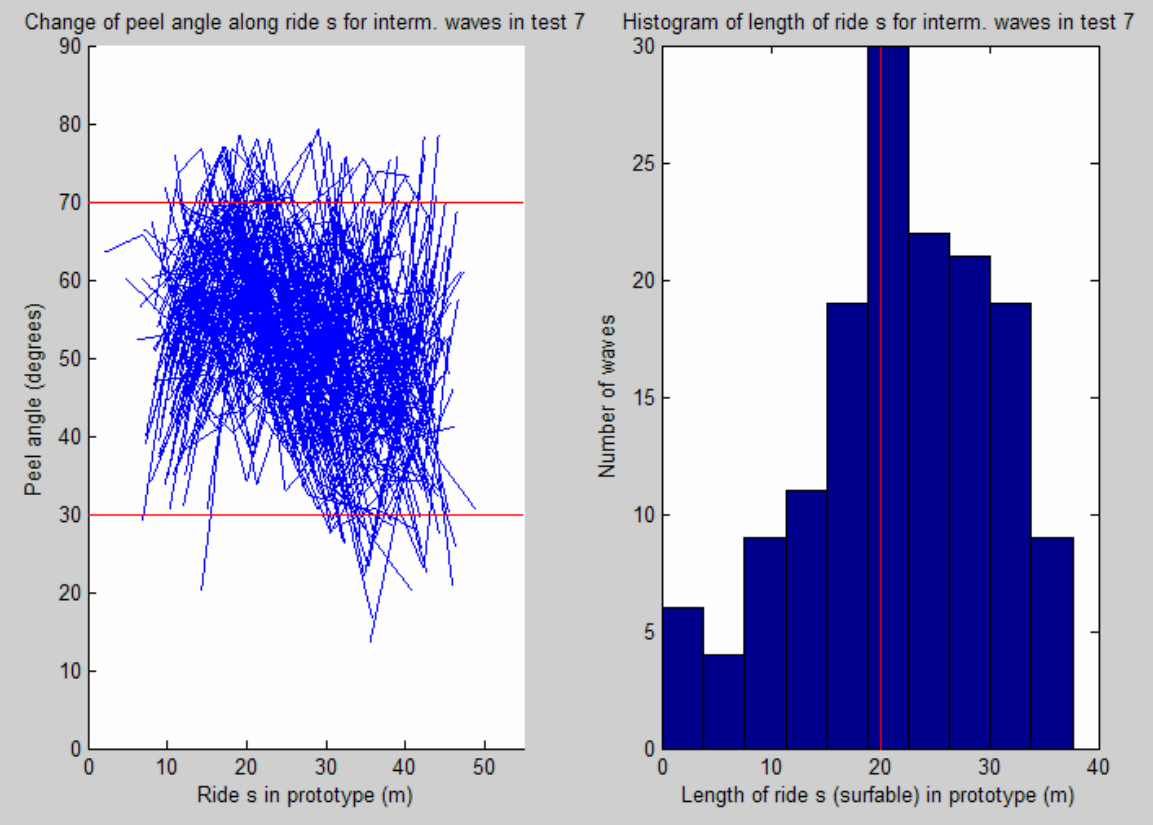

Change of peel angle along ride s for plunging waves in test 5
Peel angle (degrees)
Ride s in prototype (m)
Histogram of length of ride s for plunging waves in test 5
Number of waves
Length of ride s (surfable) in prototype (m)

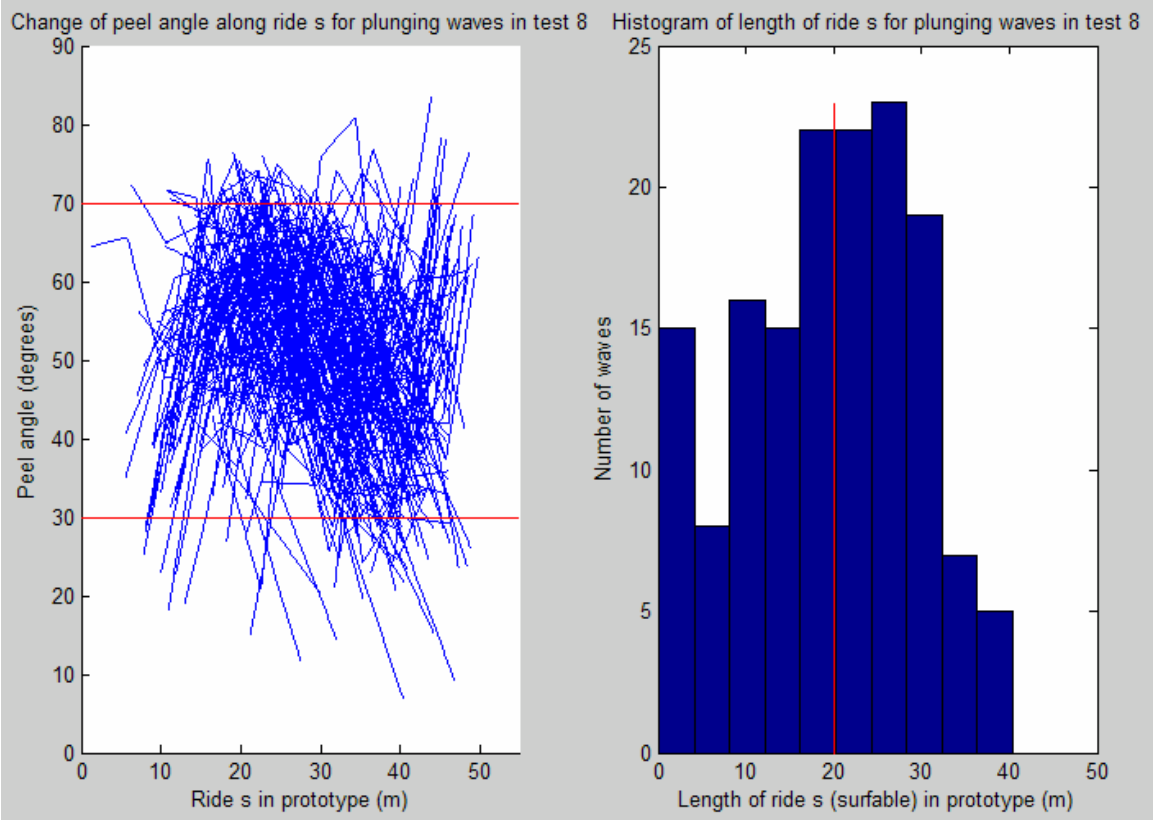

Change of peel angle along ride s for interm. waves in test 5
Peel angle (degrees)
Ride s in prototype (m)
Histogram of length of ride s for interm. waves in test 5
Number of waves
Length of ride s (surfable) in prototype (m)

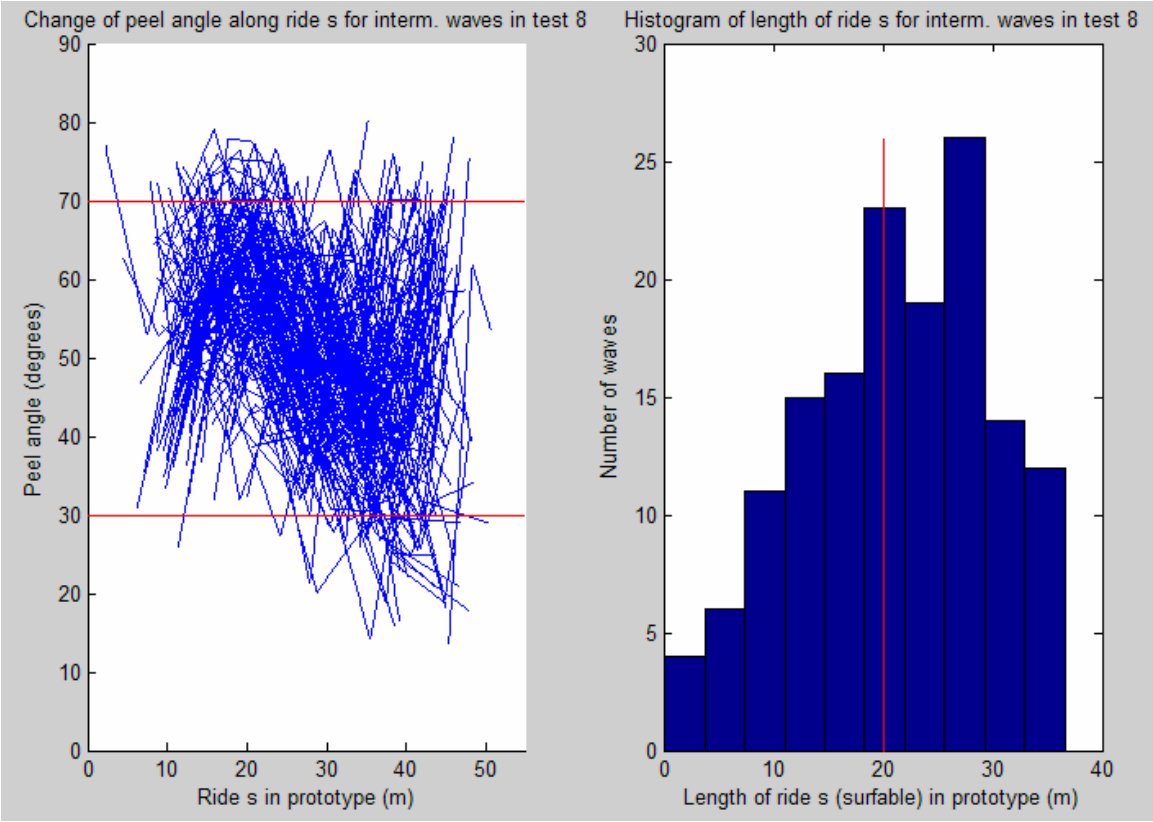

Change of peel angle along ride s for plunging waves in test 6
Peel angle (degrees)
Ride s in prototype (m)
Histogram of length of ride s for plunging waves in test 6
Number of waves
Length of ride s (surfable) in prototype (m)


Change of peel angle along ride s for interm. waves in test 6
Peel angle (degrees)
Ride s in prototype (m)
Histogram of length of ride s for interm. waves in test 6
Number of waves
Length of ride s (surfable) in prototype (m)


Change of peel angle along ride s for plunging waves in test 7
Peel angle (degrees)
Ride s in prototype (m)
Histogram of length of ride s for plunging waves in test 7
Number of waves
Length of ride s (surfable) in prototype (m)

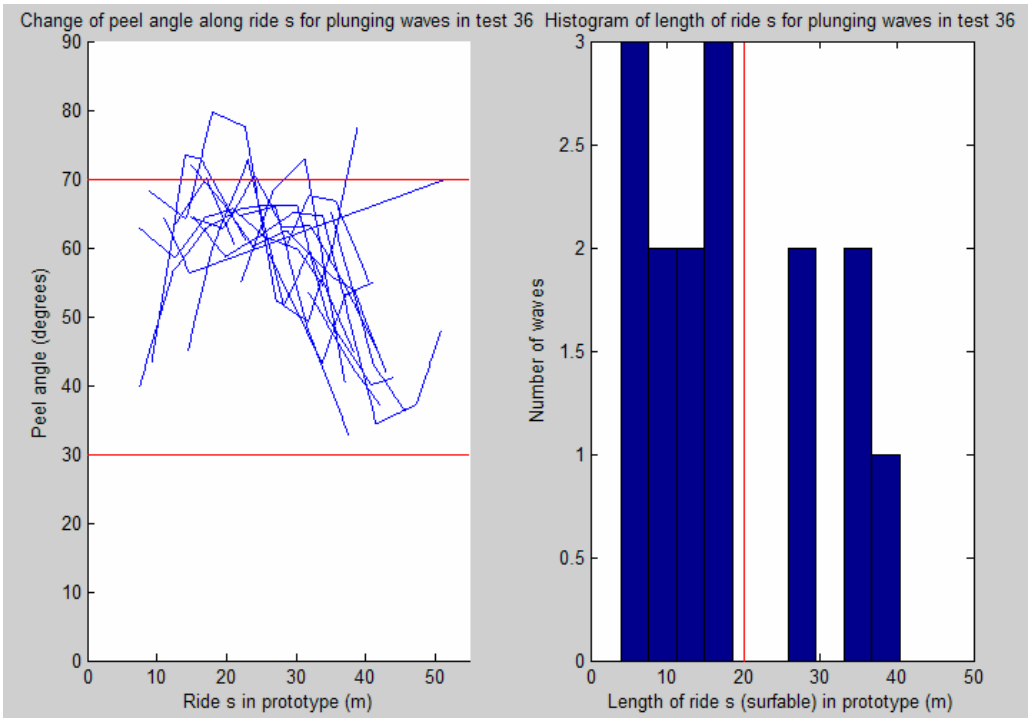

Change of peel angle along ride s for interm. waves in test 7
Peel angle (degrees)
Ride s in prototype (m)
Histogram of length of ride s for interm. waves in test 7
Number of waves
Length of ride s (surfable) in prototype (m)

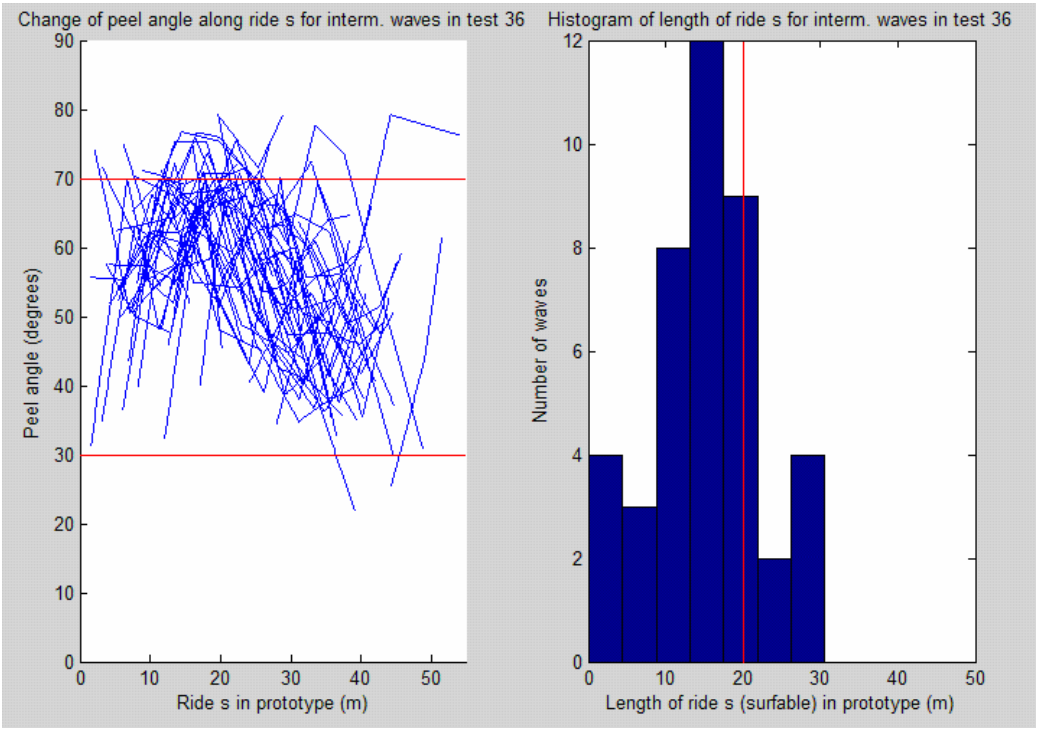

Change of peel angle along ride s for plunging waves in test 8
Peel angle (degrees)
Ride s in prototype (m)
Histogram of length of ride s for plunging waves in test 8
Number of waves
Length of ride s (surfable) in prototype (m)

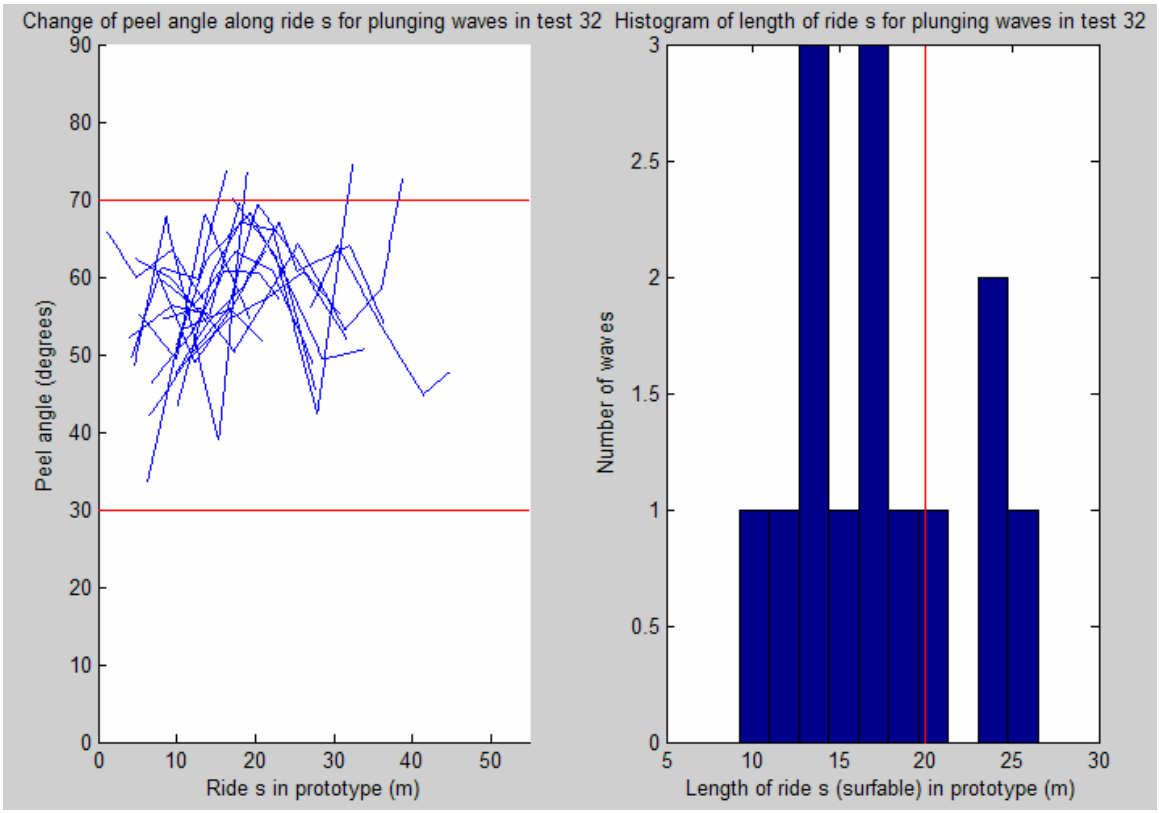

Change of peel angle along ride s for interm. waves in test 8
Peel angle (degrees)
Ride s in prototype (m)
Histogram of length of ride s for interm. waves in test 8
Number of waves
Length of ride s (surfable) in prototype (m)

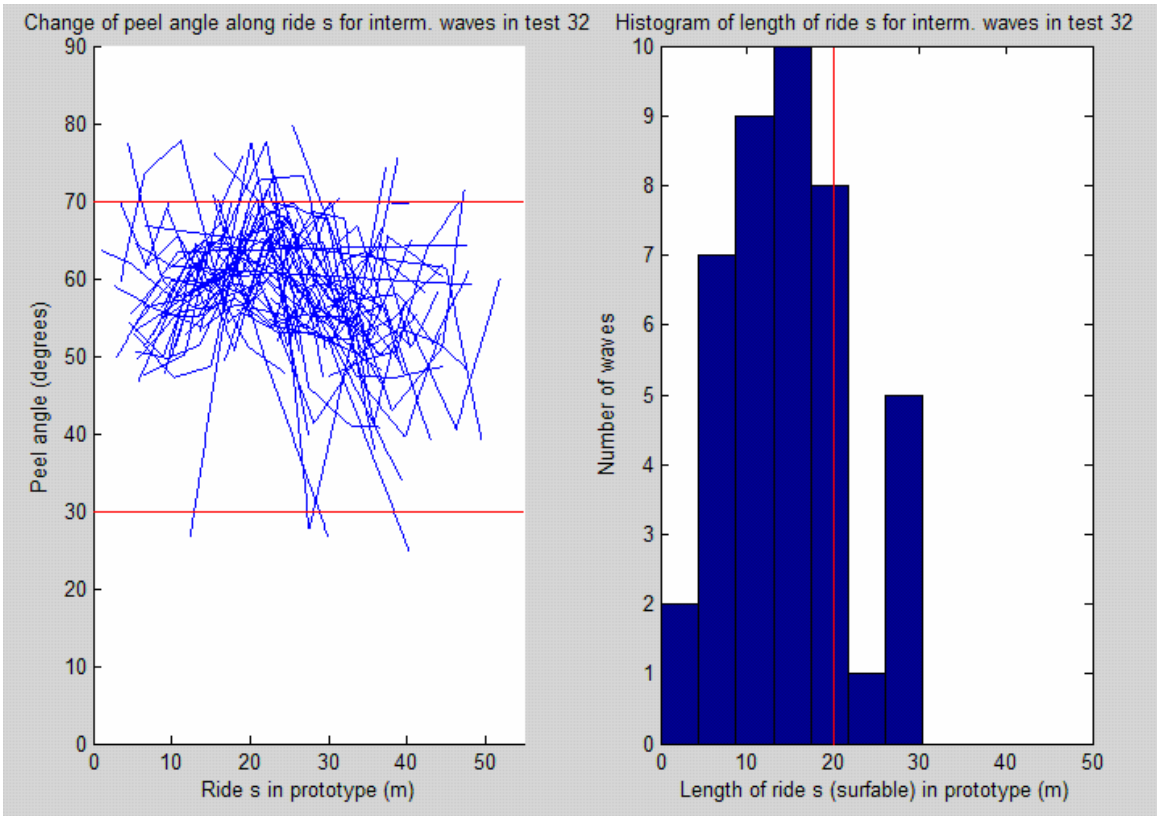
Appendix VII

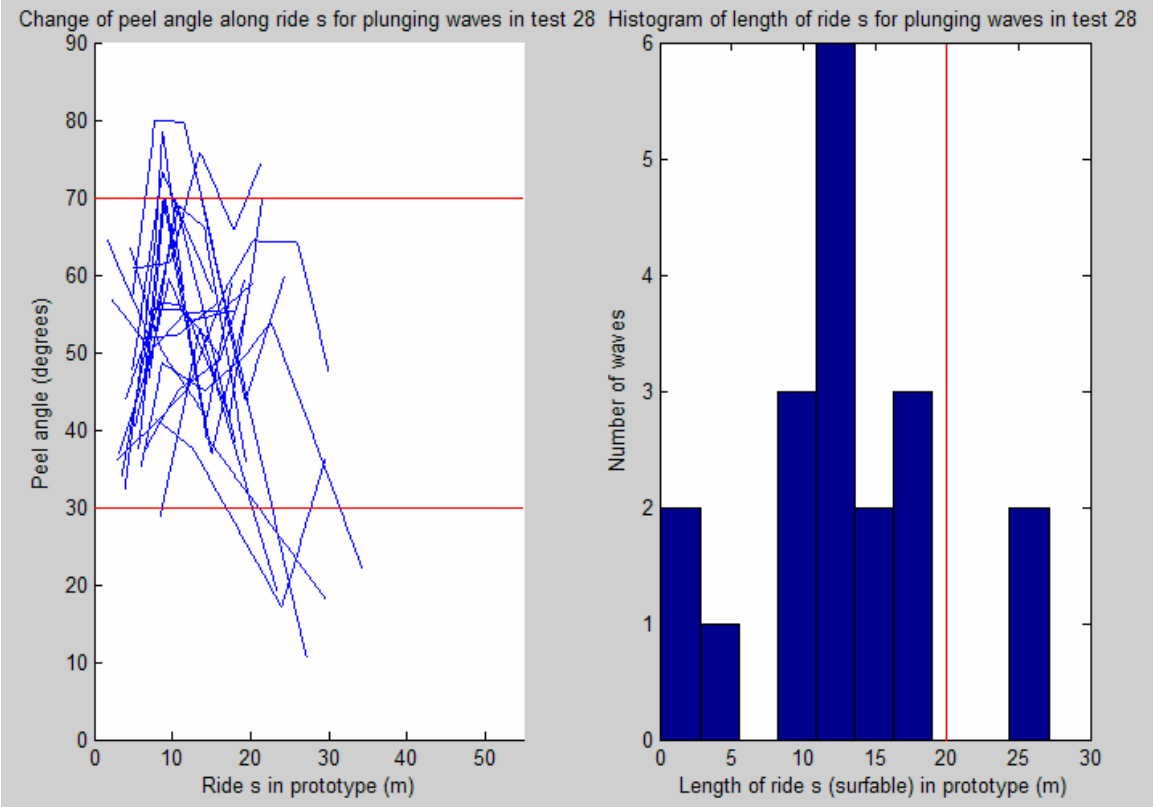
Plots of peel angles and speed of a surfer versus the distance along the reef for tests 28, 32 and 36. See name above each figure for the scenario involved and the type of waves.

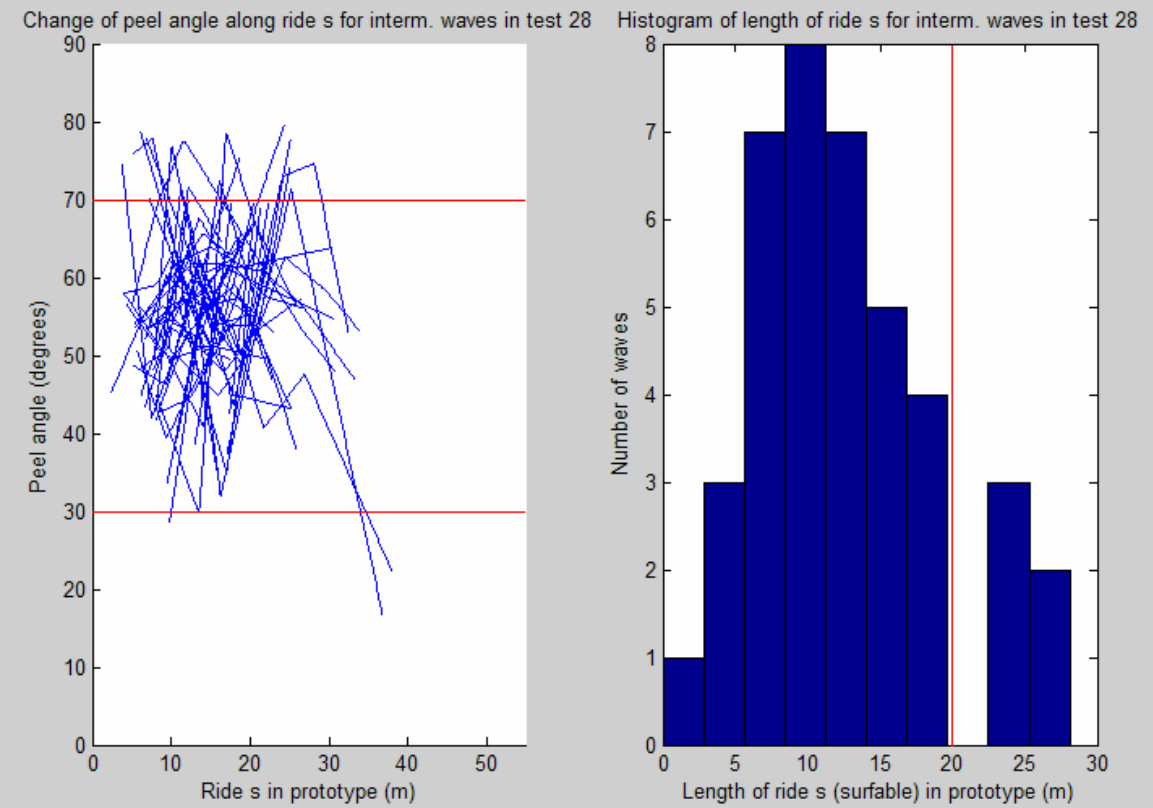





Change of peel angle along ride s for plunging waves in test 32
Peel angle (degrees)
Ride s in prototype (m)
Histogram of length of ride s for plunging waves in test 32
Number of waves
Length of ride s (surfable) in prototype (m)


Change of peel angle along ride s for interm. waves in test 32
Peel angle (degrees)
Ride s in prototype (m)
Histogram of length of ride s for interm. waves in test 32
Number of waves
Length of ride s (surfable) in prototype (m)


Change of peel angle along ride s for plunging waves in test 28
Peel angle (degrees)
Ride s in prototype (m)
Histogram of length of ride s for plunging waves in test 28
Number of waves
Length of ride s (surfable) in prototype (m)


Change of peel angle along ride s for interm. waves in test 28
Peel angle (degrees)
Ride s in prototype (m)
Histogram of length of ride s for interm. waves in test 28
Number of waves
Length of ride s (surfable) in prototype (m)